12-2022

Molecular Characterization of Nitrogenase Regulation in Methanosarcina acetivorans

Melissa Chanderban
University of Arkansas, Fayetteville

Molecular Characterization of Nitrogenase Regulation in *Methanosarcina acetivorans*

A dissertation submitted in partial fulfillment
of the requirements for the degree of
Doctor of Philosophy in Cell and Molecular Biology

by

Melissa Chanderban
University of Oklahoma
Bachelor of Science in Microbiology, 2017

December 2022
University of Arkansas

This dissertation is approved for recommendation to the Graduate Council.

_____
Daniel Lessner, Ph.D.
Dissertation Director

_____
Mack Ivey, Ph.D.
Committee Member

_____
Timothy Kral, Ph.D.
Committee Member

_____
Inés Pinto, Ph.D.
Committee Member

_____
Mary Savin, Ph.D.
Committee Member

ABSTRACT

Nitrogenase is the metalloenzyme only found in bacteria and archaea that is essential for biological nitrogen fixation (diazotrophy), but it can also serve as a catalyst in biofuel production. All diazotrophs contain a molybdenum (Mo) nitrogenase, while some species contain additional alternative nitrogenases where either vanadium (V) or iron (Fe) replace Mo in the active site cofactor. Nitrogen fixation by bacteria has been extensively studied. The limited investigation of nitrogen fixation in methanogenic archaea (methanogens) indicates production of nitrogenase is simpler than in bacteria and methanogen nitrogenase has different biochemical properties. Thus, methanogen nitrogenases provide a promising alternative for genetic engineering of nitrogen fixation in in heterologous hosts (e.g., crop plants) and in biofuel production. To exploit the use of methanogen nitrogenases in biotechnological applications, it is necessary to fully understand nitrogenase regulation, maturation, and catalysis. This dissertation investigates nitrogenase regulation in *Methanosarcina acetivorans*, a methanogen that contains all three nitrogenase isozymes. Expression studies demonstrate that nitrogenase regulation in *M. acetivorans* is unique; all three nitrogenases can be produced at once, whereas other diazotrophs typically produce one nitrogenase at a time based on metal availability. Results from mutational studies reveal that the production of Mo-nitrogenase is required for expression of V- and Fe-nitrogenases in the absence of Mo, despite Mo-nitrogenase unable to support nitrogen fixation without Mo. Additional mutational and expression studies identified ModE as the Mo-dependent repressor of *vnf* and *anf* operons encoding the V- and Fe-nitrogenases, respectively. Lastly, the physiological role of uncharacterized nitrogenase-like proteins MA2032-33 and MA1631-33 was examined, pointing to potential functions in nitrogen fixation and carbon specific

methanogenesis. Overall, these results provide substantial insight into the regulation of *M. acetivorans* nitrogenases, revealing previously unknown complexity.

ACKNOWLEDGMENTS

I have been so fortunate that my research career has been filled with support. First, from the Karr lab at the University of Oklahoma, where I learned what methanogens are and I decided I should research them for the next eight-plus years. There is no doubt I am where I am today because of the mentorship of Liz Karr, Cat Bishop, and Vy Trinh. Next, from my colleagues at the University of Arkansas: the Lessner lab, especially Ahmed Dhamad, Tom Deere, Jasleen Saini, Mack Mcintosh, and Chris Hill; members of my committee; fellow graduate students Brihget Sicairos, Crystal Crook, and Amanda Scholes; and Erik Pollock and Lindsey Conaway of the Stable Isotope Lab. Their support, advice, and methanol have been invaluable. Finally, this dissertation would not have been possible without Dan Lessner encouraging me to be a better scientist. I know I will always carry with me everything I've learned these last five years.

DEDICATION

For Miles—my proofreader, my one-man presentation audience, my biggest supporter.

TABLE OF CONTENTS

LIST OF PUBLISHED PAPERS

Chapter I – Chanderban M, Dhamad AE, Hill CA, Lessner DJ. *Methanosarcina acetivorans* simultaneously produces molybdenum, vanadium, and iron-only nitrogenases in response to fixed nitrogen and molybdenum depletion. Under revision.

Introduction

Nitrogen is crucial for life as a building block of essential biomolecules such as DNA and proteins. There is ample nitrogen in our atmosphere as dinitrogen (N_2), but the high activation energy to break the N_2 triple bond renders this gas relatively inert. However, in a process called nitrogen fixation, the nitrogenase enzyme complex converts N_2 into ammonia (NH_3), a form of nitrogen that can be assimilated into biological processes. For billions of years, nitrogenase was the primary source of fixed nitrogen entering the nitrogen cycle to support life on Earth.[1,2]

It has been proposed that the ancestor of modern nitrogenase first arose in methanogenic archaea (methanogens) and spread through bacteria via horizontal gene transfer.[2] To date, only bacteria and methanogens have been shown to fix nitrogen.[3,4] Fixed nitrogen was a substantial limiting factor in agriculture until the early 1900s, when the Haber-Bosch process allowed for large-scale production of synthetic fertilizer and an explosion of agricultural productivity.[5] Nonetheless, biological nitrogen fixation is still responsible for approximately 50% of current bioavailable nitrogen.[6] Of great interest are genetically engineered crop plants that express nitrogenase to mitigate high costs and pollution associated with synthetic fertilizer, a feat not yet realized despite extensive research on nitrogenase. Other avenues of research seek to use nitrogenase for production of biofuels. However, synthesizing nitrogenase is extremely complex, so a thorough understanding of nitrogenase regulation, assembly, and mechanism is necessary to fully take advantage of its abilities. Decades of research into nitrogenase regulation and assembly have yet to uncover the complete mechanism of nitrogenase maturation and catalysis. Most nitrogenase research thus far has been done using model bacteria that are relatively easy to grow and manipulate. In contrast, methanogens are slow-growing and require an anaerobic environment, so research into methanogen nitrogenase is particularly lacking. This introduction

will briefly cover the complexities of nitrogen fixation and highlight the importance of methanogen nitrogenases.

1. Nitrogen Fixation

Nitrogen fixation occurs using the enzyme complex comprising a dinitrogenase, where substrate is reduced to product, and a dinitrogenase reductase, which provides the electrons necessary for substrate reduction.[7,8] The overall mechanism of nitrogen fixation was first elucidated using the molybdenum nitrogenase (Mo-nitrogenase, or Nif), the most well-studied of the three nitrogenase isozymes.

1.1 Molybdenum Nitrogenase

The general scheme of nitrogen fixation begins with reduced carrier proteins—ferredoxin or flavodoxin—that provide electrons to the dinitrogenase reductase called NifH or the Fe protein since it contains a single [4Fe-4S] cluster (Fig. 1).[9,10] NifH transiently interacts with dinitrogenase NifDK (also called the MoFe protein) to donate electrons, hydrolyzing 2 ATP per electron.[11,12] NifDK contains unique, complex iron-sulfur (Fe-S) clusters: the [8Fe-7S] P-cluster and the [Fe_7MoS_9C-homocitrate] M-cluster, also called FeMo-co (Fig. 1). Electrons pass from the [4Fe-4S] cluster in NifH to the P-cluster, then to the catalytic FeMo-co in the active site (Fig. 2). 6 electrons are required to reduce N_2 to 2 NH_3, and an additional 2 protons must be reduced to H_2 as part of catalysis.[13,14] Thus, under ideal conditions, reducing one mol of N_2 uses the following stoichiometry:

$$N_2 + 8e^- + 8H^+ + 16ATP \rightarrow 2NH_3 + H_2 + 16ADP + 16P_i$$

Nitrogenase can account for 10% of total cellular protein, not counting the cellular machinery needed to form the active holoprotein.[15] Overall, nitrogen fixation requires an enormous amount of energy, and even more is necessary for the other two nitrogenase isozymes, or "alternative" nitrogenases.

1.2 Alternative Nitrogenases

Compared to the Mo-nitrogenase, catalytic clusters of the alternative nitrogenases contain either vanadium (FeV-co) or iron (FeFe-co) instead of Mo (Fig. 1).[16–18] FeV-co also differs from FeMo-co in the absence of one bridging sulfide which is replaced by a carbonate ligand.[19] The crystal structure of FeFe-co has yet to be determined, but spectroscopy supports a structure that resembles FeMo-co with Fe replacing Mo.[20]

V- and Fe-nitrogenases (Vnf and Anf) are considered secondary to the Mo-nitrogenase. Thus, far all characterized species that can fix nitrogen (diazotrophy) contain the Mo-nitrogenase. Diazotrophs can also encode one or both of the alternative nitrogenases.[3,21] The Mo-nitrogenase is preferentially expressed because the alternative nitrogenases represent an even greater energetic burden than the Mo-nitrogenase:

$$\text{V-nitrogenase: } N_2 + 12e^- + 12H^+ + 24ATP \rightarrow 2NH_3 + 3H_2 + 24ADP + 24P_i$$

$$\text{Fe-nitrogenase: } N_2 + 20e^- + 20H^+ + 40ATP \rightarrow 2NH_3 + 7H_2 + 40ADP + 40P_i$$

These differences in catalysis are due to properties of both the catalytic cluster and the protein environment. Thus, the alternative nitrogenases are primarily used by diazotrophs when both fixed nitrogen and Mo are limiting, which does not allow use of Mo-nitrogenase. Reducing energy expenditure by fixing nitrogen with FeMo-co is preferred to the extent that diazotrophs will insert FeMo-co into alternative nitrogenases when Mo becomes available again.[22–25]

However, the alternative nitrogenases are well-suited to produce hydrocarbons and hydrogen as biofuels and value-added compounds. The alternative nitrogenases contribute more electrons to proton reduction than the Mo-nitrogenase does; the V-nitrogenase allocates approximately 50% of its electrons to H_2 evolution, while the Fe-nitrogenase contributes most of its electrons to H_2, as shown in the equations above.[26–28]

While their primary biological role is the reduction of N_2 and protons, all three nitrogenases are promiscuous and will reduce numerous small molecules with multiple bonds. The alternative nitrogenases are more adept at this too.[29] While the Mo-nitrogenase is poor at reducing CO, the V-nitrogenase can reduce CO to hydrocarbons including ethane, ethylene, propane, and butane.[29,30] Both alternative nitrogenases can produce methane: the V-nitrogenase through CO reduction, and the Fe-nitrogenase through CO_2 reduction.[30,31] As mentioned before, these differences are partially dependent on the catalytic cluster. For example, the V-nitrogenase containing FeMo-co cannot produce methane like it can with FeV-co.[24] Therefore, understanding nitrogenase maturation and cluster biosynthesis is essential to take full advantage of nitrogenase and its modular properties.

2. Cofactors of Nitrogen Fixation

Fe-S clusters are at the heart of nitrogen fixation; nitrogenase could not function without simple [4Fe-4S] clusters and complex Fe-S clusters. [4Fe-4S] clusters are used by ferredoxin and NifH. Additionally, [4Fe-4S] clusters provide the backbone for the P-clusters and FeMo-co and are cofactors of the proteins that synthesize the complex Fe-S clusters. Most bacterial diazotrophs use dedicated systems to synthesize these clusters during nitrogen fixation.[32]

2.1 Simple Clusters

Prokaryotes use ISC, SUF, and NIF systems to synthesize simple [2Fe-2S] and [4Fe-4S] clusters. NIF (nitrogen fixation) specifically generates [4Fe-4S] clusters for nitrogenase and is only found in bacteria, though it is not limited to diazotrophs.[33,34] ISC (iron-sulfur cluster) and/or SUF (sulfur assimilation) systems are found in all domains of life. NIF, ISC, and SUF all comprise a cysteine desulfurase (NifS, IscS, SufSE) which donates a sulfur moiety from cysteine to a scaffold (NifU, IscU, SufBCD) where [2Fe-2S] and subsequent [4Fe-4S] clusters are formed.[34,35] Fe-S clusters can be transferred to target apo-proteins or to accessory proteins which then mediate transfer.[34]

Methanogens encode minimal versions of SUF and ISC systems: IscUS and SufBC. While all methanogens encode SufBC, only some encode IscUS. Methanogen SufBC is a minimal system, lacking a clear cysteine desulfurase but capable of binding and transferring Fe-S clusters.[36] How IscUS and SufBC contribute to nitrogenase Fe-S clusters in methanogens in unknown. Nitrogenase in bacteria that encode NifUS is largely dependent on that system, and other Fe-S cluster biogenesis systems such as IscUS are poor substitutes *in vivo*.[33,37,38] Methanogens and some bacteria do not encode NIF, instead encoding ISC and/or SUF systems—those which are present in the mitochondria and chloroplasts of crop plants.[39] Bacterial NifH can receive [4Fe-4S] from eukaryotic Fe-S machinery.[40] However, cluster-loaded NifDK has yet to be achieved. Nitrogenase proteins that naturally receive Fe-S clusters from ISC and SUF may prove more amenable to recombinant expression.

2.2 P-Cluster

Most of the research into Fe-S cluster biogenesis has focused on the Mo-nitrogenase. It is still unclear how the P-cluster is formed, but two [4Fe-4S] clusters are delivered to NifDK from NifU, and through some uncharacterized activity of NifH, the [8Fe-7S] cluster arises after reductive coupling.[41] While the P-cluster is formed directly within NifDK, FeMo-co is assembled on a separate scaffold and then the mature cluster is delivered to NifDK.[32]

2.3 FeMo-co

As characterized in bacterial diazotrophs, two [4Fe-4S] clusters from NifU are loaded onto NifB, a radical-SAM enzyme that converts the pair to an [8Fe-9S-C] cluster called NifB-co or the L-cluster (Fig. 3). NifB uses one catalytic and two permanent [4Fe-4S] clusters to accomplish this. NifB-co is loaded onto scaffold NifEN. Through another mechanism that is not yet fully understood, NifH helps incorporate Mo and homocitrate into the cluster to form FeMo-co, which is then delivered to NifDK. Homocitrate is produced by homocitrate synthase NifV.[32]

Incorporating FeV-co and FeFe-co into the dinitrogenase requires an accessory protein, the G subunit (VnfG and AnfG), which is part of the core structure of the dinitrogenase: the V- and Fe-nitrogenases comprise VnfDGK and AnfDGK, respectively.[42,43] To generate FeV-co, it is hypothesized that NifB-co is transferred to a scaffold specific for the V-nitrogenase (VnfEN), after which the V-nitrogenase reductase (VnfH) is involved in incorporating homocitrate and V.[44] To date, no scaffold specific to the Fe-nitrogenase has been identified. Instead, evidence supports that FeFe-co is synthesized directly on AnfDGK. Fe-nitrogenase expressed *in vivo* and recombinantly is functional without VnfEN or NifEN.[44,45] Spectroscopic analysis of purified Fe-

nitrogenase identifies an additional signal that is not FeFe-co or the P-cluster but is likely a FeFe-co precursor, supporting that cluster maturation occurs within AnfDGK.[44]

3. Nitrogen Fixation in Methanogens

Methanogens are predicted to be the originators of what would become the Mo-nitrogenase.[2] After transferring the Mo-nitrogenase to bacteria, gene duplication in bacteria likely resulted in the V-nitrogenase. The V-nitrogenase was then transferred to more recently evolved methanogens, where a second duplication yielded the Fe-nitrogenase.[4] Methanogens are underrepresented in nitrogenase research, yet their nitrogenases offer advantages for recombinant expression as detailed below.

3.1 Recombinant Nitrogenase

To produce functional recombinant nitrogenase is exceedingly complex, let alone integrating the energy demands of nitrogen fixation with the physiology of hosts such as crop plants. Expression of minimal *Paenibacillus* sp. WLY78 nitrogenase genes in non-diazotroph *Escherichia coli* leads to nitrogenase with only 10% activity compared to nitrogenase expressed in *Paenibacillus*; increasing activity to ~50% required addition of numerous genes for Fe-S cluster biosynthesis and generation of reduced electron carriers.[46]

One major roadblock is expression of Mo-nitrogenase NifDK in eukaryotes. Attempts thus far have resulted in protein that can correctly oligomerize but is nonfunctional and/or degraded.[47] To confer enzyme stability and function, it is essential to incorporate the necessary Fe-S clusters. Utilizing nitrogenase maturation proteins from methanogens has already proven fruitful. In contrast to recombinant NifB from *A. vinelandii*, which is unstable and aggregates,

methanogen NifB expressed in eukaryotes is soluble and functional in *in vitro* FeMo-co biogenesis.[48–50] Additionally, recombinant *K. pneumoniae* NifH is unstable and not functional without expression of maturase NifM, while methanogen NifH is stable when expressed alone.[51,52]

While the Fe-nitrogenase is least efficient at N_2 reduction, it offers benefits for recombinant expression. FeFe-co does not require insertion of Mo or V, relieving the burden of supplying and delivering those metals. Unlike NifDK, AnfHDGK expressed in yeast is functional after *in vitro* incorporation of FeMo-co, implying successful P-cluster formation.[53]As mentioned before, the Fe-nitrogenase also does not require scaffold proteins. The Fe-nitrogenase is functional in an *E. coli* strain expressing AnfHDGK, NifSU, NifB, NifV, and electron donors.[45] Because the Fe-nitrogenase originated in methanogens, methanogen Fe-nitrogenase may represent an even simpler system for recombinant expression, such using host ISC and SUF instead of needing to add NifSU. Consequently, a thorough investigation of the formation and activity of methanogen nitrogenase is needed to optimize recombinant expression. To do so, we must first understand the mechanisms of producing of nitrogenases in methanogens, which has not been explored in detail beyond the Mo-nitrogenase.

3.2 Energetics of Nitrogen Fixation

The energetics of nitrogen fixation in methanogens, such as how many ATP are needed to support N_2 reduction, are largely unknown. Methanogens live at the thermodynamic edge of life, receiving at most 2 ATP per mol growth substrate.[54] Understanding how methanogens cope with diverting ATP and electrons to diazotrophic growth may reveal methods to increase the efficiency of recombinant nitrogenase. For example, *M. acetivorans* VnfH may be more energy

efficient than other homologs. The [4Fe-4S] cluster of MaVnfH can reach an all-ferrous state *in vitro* at physiologically relevant reduction potentials.[55] An all-ferrous cluster would be able to donate 2 electrons at a time instead of one, halving the ATP requirements of nitrogen fixation when using MaVnfH. Understanding the mechanism of energy-consuming steps of nitrogen fixation in methanogens such as electron transfer and H_2 evolution may provide methods of mitigating the energetic burden of nitrogen fixation in recombinant hosts.

4. Regulation of Nitrogen Fixation

Due to high energy demands, nitrogen fixation is tightly regulated at transcriptional, post-transcriptional, and post-translational levels. Much research has been done on how nitrogenase is regulated in methanogens containing the Mo-nitrogenase and in bacterial diazotrophs. This dissertation focuses on model methanogen *M. acetivorans* which encodes all three nitrogenases, the regulation of which is unknown. In addition to key differences in basal transcription machinery between archaea and bacteria, other regulatory measures have been gained and lost over evolutionary time, as described below.[56]

While there are numerous factors that have been identified among clades of diazotrophs which impact nitrogenase expression and activity—salinity, temperature, oxygen, light/dark cycles—this introduction will focus on fixed nitrogen and metal availability, which are key effectors controlling nitrogenase within diazotrophs expressing more than one nitrogenase.[57–59]

4.1 Fixed Nitrogen Availability

Cellular nitrogen availability is sensed through levels of 2-oxoglutarate (2-OG). During nitrogen sufficiency, 2-OG and ammonium are converted to glutamate. During nitrogen

limitation, there is less ammonium for this reaction and 2-OG levels increase. 2-OG is sensed directly or indirectly through signaling proteins to repress or activate nitrogen fixation.[60] Overall, if fixed nitrogen is available, nitrogenase is not made. If fixed nitrogen becomes available during nitrogen fixation, nitrogenase is inactivated. The only known instances of nitrogenase production in the presence of fixed nitrogen are in strains engineered to bypass all modes of repression.[61,62] Lack of fixed nitrogen can affect transcriptional, post-transcriptional, and post-translational regulation, which differs between bacteria and methanogens.

4.1.1 Bacteria

If fixed nitrogen becomes available after nitrogenase is produced, nitrogenase activity can be turned off to eliminate unnecessary energy expenditure. This occurs through reversible ADP-ribosylation of NifH (Fe protein), which blocks its interactions with NifDK (Fig. 4).[63–66] However, most regulation of nitrogen fixation in bacteria—especially aerobes—occurs before translation.[56] Many diazotrophic bacteria regulate nitrogenases through transcription regulators that are in turn controlled by fixed nitrogen and metal availability at the transcriptional level. The ones most studied are *A. vinelandii* NifA, VnfA, and AnfA, which activate expression of their corresponding nitrogenase and may repress others, with a preference for the relatively energy-efficient Mo-nitrogenase, followed by the V-nitrogenase then the Fe-nitrogenase (Fig. 5).[57] Typically, each nitrogenase is made when metal is available to produce its specific catalytic cluster.[57] In the presence of Mo, *vnfA* and *anfA* are repressed; the Mo-nitrogenase is expressed and the Mo-independent alternative nitrogenases are not.[67,68] In the absence of Mo, *vnfA* is expressed and represses Mo-nitrogenase expression.[69] Vanadium acts at the post-translational level; V-nitrogenase transcripts are produced in the absence of Mo, but the protein is only made

in the presence of V.[70] In the absence of both Mo and V, *anfA* is expressed and the Fe-nitrogenase is made.[69] However, in *Rhodobacter capsulatus*, which encodes the Mo- and Fe-nitrogenases, both nitrogenases are produced and are functional during Mo limitation; in this case the Fe-nitrogenase is hypothesized to be complementary to the Mo-nitrogenase.[71,72] The need for fixed nitrogen supersedes metal-dependent regulation; in an *A. vinelandii* mutant unable to make *nif*, the Fe-nitrogenase is expressed even in the presence of Mo.[68] Similarly, in *R. palustris*, a lack of *nif* results in expression of V- and Fe-nitrogenases that are not repressed by Mo or V.[73] Additional regulatory elements include small RNAs in *Pseudomonas stutzeri* which are induced under nitrogen limitation, stabilizing *nif* transcripts and allowing full nitrogenase activity.[74,75]

4.1.2 Methanogens

While bacteria use ADP-ribosylation to inhibit nitrogenase activity, methanogens use regulatory proteins (NifI) that reversibly associate with NifDK to impede catalysis in the presence of fixed nitrogen (Fig. 4).[76] Two transcription regulators of nitrogen fixation have been identified in methanogens: NrpR, a repressor, and NrpA, an activator (Fig. 6). NrpR binds the promoter of the *nif* operon when fixed nitrogen is available, but when fixed nitrogen is limiting, NrpR binds 2-OG and the conformational change derepresses *nif*.[77,78] NrpR also represses *nrpA*, the gene product of which activates *nif* expression.[79] Small RNA molecules are involved in post-transcriptional regulation in methanogens. A sRNA induced during nitrogen limitation in *Methanosarcina mazei* stabilizes the transcripts of *nif* and *nrpA*.[80] These regulatory studies have focused entirely on the Mo-nitrogenase. It is expected that there are additional regulatory factors

in methanogens than can produce all three nitrogenases, and this regulation is likely metal-dependent, as in bacteria.

4.2 Metal Availability

There is little information on metal-dependent regulation in methanogens expressing more than one nitrogenase, but it is likely that alternative nitrogenase regulation is metal-dependent. *Methanosarcina barkeri* strain 227 encodes Mo- and V-nitrogenases and its diazotrophic growth was measured during growth with Mo or V.[82] In the absence of Mo and presence of V, diazotrophic growth is less robust than when Mo is added, suggesting use of the more energetically demanding V-nitrogenase, likely expressed only in the absence of Mo.[83] Methanogens do not encode homologs of the NifA/VnfA/AnfA activators, but putative Mo-binding regulatory proteins have been identified.[81]

4.2.1 Molybdenum-Binding Transcription Regulators

The ModE protein family provides Mo-dependent transcription regulation in numerous microbes. As characterized in *E. coli*, ModE comprises an N-terminal helix-turn-helix DNA binding domain and two C-terminal Mop domains which bind molybdate.[81] ModE has been shown to regulate genes encoding molybdate transport proteins and Mo-containing enzymes.[81] The affinity of ModE for DNA increases when ModE binds molybdate, and ModE can act as a repressor or activator.[58] In *R. capsulatus*, ModE homologs MopA and MopB directly repress *anfA*.[84] While the ModE regulon has not been fully characterized in *A. vinelandii*, ModE is involved in repression of *anfA*, and there are predicted ModE binding sites upstream of *anfA* and *vnfA*.[58,67] In *Anabaena variabilis*, encoding the Mo- and V-nitrogenases, two Mo-binding

repressor proteins VnfR1 and VnfR2 directly repress V-nitrogenase expression in a Mo-dependent manner.[85]

Methanogens also encode ModE homologs which have not been characterized. In contrast to bacterial ModE, methanogen ModE only has one C-terminal Mop domain. *M. acetivorans* encodes a ModE homolog and predicted ModE binding sites in the intergenic region between V- and Fe-nitrogenase genes, suggesting ModE may be involved in Mo-dependent alternative nitrogenase regulation as in other diazotrophs.[81]

4.3 Nitrogenase-Dependent Regulation

Another possibility for regulation of methanogen alternative nitrogenases is through nitrogenases themselves. Through mechanisms currently unknown, nitrogenase structural proteins can regulate nitrogenase gene expression in bacteria. In *A. vinelandii*, V-dependent repression of the Fe-nitrogenase requires the presence of the V-nitrogenase.[68] Promoter assays show the *K. pneumoniae* Mo-nitrogenase operates in a feedback loop, with maximal expression from the *nif* promoter occurring in the presence of NifHDK.[86]

5. Nitrogenase-Like Proteins

Numerous bacteria and archaea—even those that cannot fix nitrogen—encode genes that are homologous to nitrogenase structural genes (Fig. 7). Like nitrogenase, these comprise a NifDK-like catalytic component and NifH-like electron donor but reduce different substrates. Nitrogenase-like proteins conserved among all methanogens function in the biosynthesis of coenzyme F430, the cofactor of methyl-CoM reductase which catalyzes the final methane-releasing step of methanogenesis. CfbC (NifH homolog) and CfbD (NifD homolog) contribute to

the reduction of the coenzyme F430 precursor.[87] Similar to NifH and NifD, CfbC and CfbD interact with each other, though CfbD is homomeric, unlike heterotetramer NifDK. Like NifH, CfbC dimerizes when bound to a [4Fe-4S] cluster and has ATP-dependent changes in EPR spectra.[88] CfbD also contains a [4Fe-4S] cluster per dimer rather than a P-cluster. CfbD reduces the F430 precursor substrate in its active site that is similar to where FeMo-co resides in NifDK.[89]

Nitrogenase-like proteins are also involved in the biosynthesis of chlorophyll and bacteriochlorophyll. Akin to NifH and NifDK, generating chlorophyll uses a homodimeric electron donor protein (BchL) and a heterotetrameric catalytic complex (BchNB). Instead of a P-cluster, BchNB coordinates a [4Fe-4S] cluster. BchNB catalyzes the reduction of a C=C double bond in its chlorophyll precursor substrate, which binds in place of FeMo-co. Bacteriochlorophyll synthesis uses a similar mechanism using BchX and BchYZ to reduce the bacteriochlorophyll precursor.[89]

A nitrogenase-like enzyme complex with a novel role in sulfur metabolism was identified in *Rhodospirillum rubrum*. The Mar system reduces C-S bonds in volatile organic sulfur compounds during methionine biosynthesis, producing methane and ethylene byproducts. *marBHDK* genes are analogous to NifB, NifH, NifD, and NifK. MarB and MarH share conserved [4Fe-4S] binding motifs with NifB and NifH, as well as radical SAM and ATPase domains, respectively. MarDK contains residues that coordinate the P-cluster in NifDK, but MarD does not have a conserved histidine that coordinates FeMo-co. Details of catalysis are unknown, but the presence of MarB implies MarDK uses a unique catalytic cluster, unlike the other systems described above where substrates occupy the space of a catalytic cluster.[90] Nitrogenase-like systems identified thus far are integral to elemental cycles by contributing to

photosynthesis, production of methane, and degradation of volatile sulfur species. There are still nitrogenase-like proteins which have yet to be characterized which may perform important biochemistry.

6. Experimental Sections Included in this Dissertation

The overarching goal of this dissertation is to characterize the expression, usage, and function of Mo-, V-, and Fe-nitrogenases, and role of uncharacterized nitrogenase-like proteins in the model methanogen *M. acetivorans*. One of the few methanogens encoding all three nitrogenases, *M. acetivorans* also has a robust genetic system allowing *in vivo* characterization. *M. acetivorans* nitrogenase proteins (NifH and NifB) have already proven adept at recombinant expression, and *M. acetivorans* VnfH may achieve an all-ferrous state and be more energy efficient, so there is practical relevance for a deeper understanding of its alternative nitrogenase proteins.[48,55] Lastly, *M. acetivorans* encodes two uncharacterized nitrogenase-like gene clusters. This dissertation explores the following questions:

1. How does availability of metals and fixed nitrogen regulate nitrogenase expression? What are the functions of each nitrogenase?
2. Does ModE contribute to Mo-dependent transcription regulation and controlling alternative nitrogenase expression?
3. What are the roles of nitrogenase-like proteins?

References

1. Stüeken, E. E., Buick, R., Guy, B. M. & Koehler, M. C. Isotopic evidence for biological nitrogen fixation by molybdenum-nitrogenase from 3.2 Gyr. *Nature* **520**, 666–669 (2015).

2. Boyd, E. S. *et al.* A late methanogen origin for molybdenum-dependent nitrogenase. *Geobiology* **9**, 221–232 (2011).

3. Poudel, S. *et al.* Electron Transfer to Nitrogenase in Different Genomic and Metabolic Backgrounds. *J. Bacteriol.* **200**, (2018).

4. Boyd, E. S., Hamilton, T. L. & Peters, J. W. An Alternative Path for the Evolution of Biological Nitrogen Fixation. *Front. Microbiol.* **2**, (2011).

5. Galloway, J. N., Leach, A. M., Bleeker, A. & Erisman, J. W. A chronology of human understanding of the nitrogen cycle. *Philos. Trans. R. Soc. B Biol. Sci.* **368**, 20130120 (2013).

6. Smith, B. E. Nitrogenase Reveals Its Inner Secrets. *Science* **297**, 1654–1655 (2002).

7. Bulen, W. A. & LeComte, J. R. The nitrogenase system from *Azotobacter*: two-enzyme requirement for N_2 reduction, ATP-dependent H_2 evolution, and ATP hydrolysis. *Proc. Natl. Acad. Sci. U. S. A.* **56**, 979–986 (1966).

8. Hageman, R. V. & Burris, R. H. Nitrogenase and nitrogenase reductase associate and dissociate with each catalytic cycle. *Proc. Natl. Acad. Sci.* **75**, 2699–2702 (1978).

9. Mortenson, L. E. FERREDOXIN AND ATP, REQUIREMENTS FOR NITROGEN FIXATION IN CELL-FREE EXTRACTS OF CLOSTRIDIUM PASTEURIANUM. *Proc. Natl. Acad. Sci. U. S. A.* **52**, 272–279 (1964).

10. Shah, V. K., Stacey, G. & Brill, W. J. Electron transport to nitrogenase. Purification and characterization of pyruvate:flavodoxin oxidoreductase, the *nifJ* gene product. *J. Biol. Chem.* **258**, 12064–12068 (1983).

11. Ljones, T. & Burris, R. H. ATP hydrolysis and electron transfer in the nitrogenase reaction with different combinations of the iron protein and the molybdenum-iron protein. *Biochim. Biophys. Acta BBA - Bioenerg.* **275**, 93–101 (1972).

12. Hageman, R. V., Orme-Johnson, W. H. & Burris, R. H. Role of magnesium adenosine 5'-triphosphate in the hydrogen evolution reaction catalyzed by nitrogenase from *Azotobacter vinelandii*. *Biochemistry* **19**, 2333–2342 (1980).

13. Lukoyanov, D. *et al.* Identification of a Key Catalytic Intermediate Demonstrates That Nitrogenase Is Activated by the Reversible Exchange of N_2 for H_2. *J. Am. Chem. Soc.* **137**, 3610–3615 (2015).

14. Simpson, F. B. & Burris, R. H. A nitrogen pressure of 50 atmospheres does not prevent evolution of hydrogen by nitrogenase. *Science* **224**, 1095–1097 (1984).

15. Dingler, C., Kuhla, J., Wassink, H. & Oelze, J. Levels and activities of nitrogenase proteins in *Azotobacter vinelandii* grown at different dissolved oxygen concentrations. *J. Bacteriol.* **170**, 2148–2152 (1988).

16. Hales, B. J., Case, E. E., Morningstar, J. E., Dzeda, M. F. & Mauterer, L. A. Isolation of a new vanadium-containing nitrogenase from *Azotobacter vinelandii*. *Biochemistry* **25**, 7251–7255 (1986).

17. Schneider, K., Müller, A., Schramm, U. & Klipp, W. Demonstration of a molybdenum- and vanadium-independent nitrogenase in a *nifHDK*-deletion mutant of *Rhodobacter capsulatus*. *Eur. J. Biochem.* **195**, 653–661 (1991).

18. Chisnell, J. R., Premakumar, R. & Bishop, P. E. Purification of a second alternative nitrogenase from a *nifHDK* deletion strain of *Azotobacter vinelandii*. *J. Bacteriol.* **170**, 27–33 (1988).

19. Sippel, D. & Einsle, O. The structure of vanadium nitrogenase reveals an unusual bridging ligand. *Nat. Chem. Biol.* **13**, 956–960 (2017).

20. Krahn, E. *et al.* The Fe-only nitrogenase from *Rhodobacter capsulatus*: identification of the cofactor, an unusual, high-nuclearity iron-sulfur cluster, by Fe K-edge EXAFS and 57Fe Mössbauer spectroscopy. *JBIC J. Biol. Inorg. Chem.* **7**, 37–45 (2002).

21. Addo, M. A. & Dos Santos, P. C. Distribution of Nitrogen-Fixation Genes in Prokaryotes Containing Alternative Nitrogenases. *ChemBioChem* **21**, 1749–1759 (2020).

22. Gollan, U., Schneider, K., Müller, A., Schüddekopf, K. & Klipp, W. Detection of the *in vivo* incorporation of a metal cluster into a protein. *Eur. J. Biochem.* **215**, 25–35 (1993).

23. Pau, R. N., Eldridge, M. E., Lowe, D. J., Mitchenall, L. A. & Eady, R. R. Molybdenum-independent nitrogenases of *Azotobacter vinelandii*: a functional species of alternative nitrogenase-3 isolated from a molybdenum-tolerant strain contains an iron-molybdenum cofactor. *Biochem. J.* **293**, 101–107 (1993).

24. Rebelein, J. G., Lee, C. C., Newcomb, M., Hu, Y. & Ribbe, M. W. Characterization of an M-Cluster-Substituted Nitrogenase VFe Protein. *mBio* **9**, (2018).

25. Moore, V. G., Tittsworth, R. C. & Hales, B. J. Construction and Characterization of Hybrid Component 1 from V-Nitrogenase Containing FeMo Cofactor. *J. Am. Chem. Soc.* **116**, 12101–12102 (1994).

26. Eady, R. R., Robson, R. L., Richardson, T. H., Miller, R. W. & Hawkins, M. The vanadium nitrogenase of *Azotobacter chroococcum*. Purification and properties of the VFe protein. *Biochem. J.* **244**, 197–207 (1987).

27. Dilworth, M. J., Eldridge, M. E. & Eady, R. R. The molybdenum and vanadium nitrogenases of *Azotobacter chroococcum*: effect of elevated temperature on N_2 reduction. *Biochem. J.* **289(Pt 2)**, 395–400 (1993).

28. Schneider, K., Gollan, U., Dröttboom, M., Selsemeier-Voigt, S. & Müller, A. Comparative Biochemical Characterization of the Iron-Only Nitrogenase and the Molybdenum Nitrogenase from *Rhodobacter capsulatus*. *Eur. J. Biochem.* **244**, 789–800 (1997).

29. Hu, Y., Lee, C. C. & Ribbe, M. W. Extending the Carbon Chain: Hydrocarbon Formation Catalyzed by Vanadium/Molybdenum Nitrogenases. *Science* **333**, 753–755 (2011).

30. Lee, C. C., Hu, Y. & Ribbe, M. W. Vanadium Nitrogenase Reduces CO. *Science* **329**, 642–642 (2010).

31. Zheng, Y. *et al.* A pathway for biological methane production using bacterial iron-only nitrogenase. *Nat. Microbiol.* **3**, 281–286 (2018).

32. Burén, S., Jiménez-Vicente, E., Echavarri-Erasun, C. & Rubio, L. M. Biosynthesis of Nitrogenase Cofactors. *Chem. Rev.* (2020) doi:10.1021/acs.chemrev.9b00489.

33. Santos, P. C. D., Johnson, D. C., Ragle, B. E., Unciuleac, M.-C. & Dean, D. R. Controlled Expression of *nif* and *isc* Iron-Sulfur Protein Maturation Components Reveals Target Specificity and Limited Functional Replacement between the Two Systems. *J. Bacteriol.* **189**, 2854–2862 (2007).

34. Johnson, D. C., Dean, D. R., Smith, A. D. & Johnson, M. K. Structure, Function, and Formation of Biological Iron-Sulfur Clusters. *Annu. Rev. Biochem.* **74**, 247–81 (2005).

35. Garcia, P. S., Gribaldo, S., Py, B. & Barras, F. The SUF system: an ABC ATPase-dependent protein complex with a role in Fe–S cluster biogenesis. *Res. Microbiol.* **170**, 426–434 (2019).

36. Garcia, P. S. *et al.* An early origin of iron–sulfur cluster biosynthesis machineries before Earth oxygenation. *Nat. Ecol. Evol.* **6**, 1564–1572 (2022).

37. Kennedy, C. & Dean, D. The *nifU*, *nifS* and *nifV* gene products are required for activity of all three nitrogenases of *Azotobacter vinelandii*. *Mol. Gen. Genet. MGG* **231**, 494–498 (1992).

38. Roberts, G. P., MacNeil, T., MacNeil, D. & Brill, W. J. Regulation and characterization of protein products coded by the *nif* (nitrogen fixation) genes of *Klebsiella pneumoniae*. *J. Bacteriol.* **136**, 267–279 (1978).

39. Balk, J. & Pilon, M. Ancient and essential: the assembly of iron–sulfur clusters in plants. *Trends Plant Sci.* **16**, 218–226 (2011).

40. Burén, S. & Rubio, L. M. State of the art in eukaryotic nitrogenase engineering. *FEMS Microbiol. Lett.* **365**, (2018).

41. Lee, C. C. *et al.* Stepwise formation of P-cluster in nitrogenase MoFe protein. *Proc. Natl. Acad. Sci.* **106**, 18474–18478 (2009).

42. Waugh, S. I. *et al.* The genes encoding the delta subunits of dinitrogenases 2 and 3 are required for Mo-independent diazotrophic growth by *Azotobacter vinelandii*. *J. Bacteriol.* **177**, 1505–1510 (1995).

43. Chatterjee, R., Ludden, P. W. & Shah, V. K. Characterization of VNFG, the δ Subunit of the *vnf*-Encoded Apodinitrogenase from *Azotobacter vinelandii*. *J. Biol. Chem.* **272**, 3758–3765 (1997).

44. Pérez-González, A. *et al.* Specificity of NifEN and VnfEN for the Assembly of Nitrogenase Active Site Cofactors in *Azotobacter vinelandii*. *mBio* **12**, e01568-21.

45. Yang, J., Xie, X., Wang, X., Dixon, R. & Wang, Y.-P. Reconstruction and minimal gene requirements for the alternative iron-only nitrogenase in *Escherichia coli*. *Proc. Natl. Acad. Sci. U. S. A.* **111**, E3718–E3725 (2014).

46. Li, X.-X., Liu, Q., Liu, X.-M., Shi, H.-W. & Chen, S.-F. Using synthetic biology to increase nitrogenase activity. *Microb. Cell Factories* **15**, 43 (2016).

47. Burén, S. *et al.* Formation of Nitrogenase NifDK Tetramers in the Mitochondria of *Saccharomyces cerevisiae*. *ACS Synth. Biol.* **6**, 1043–1055 (2017).

48. Fay, A. W., Wiig, J. A., Lee, C. C. & Hu, Y. Identification and characterization of functional homologs of nitrogenase cofactor biosynthesis protein NifB from methanogens. *Proc. Natl. Acad. Sci.* **112**, 14829–14833 (2015).

49. Burén, S. *et al.* Biosynthesis of the nitrogenase active-site cofactor precursor NifB-co in *Saccharomyces cerevisiae*. *Proc. Natl. Acad. Sci.* **116**, 25078–25086 (2019).

50. Burén, S., Jiang, X., López-Torrejón, G., Echavarri-Erasun, C. & Rubio, L. M. Purification and *In Vitro* Activity of Mitochondria Targeted Nitrogenase Cofactor Maturase NifB. *Front. Plant Sci.* **8**, (2017).

51. Howard, K. S. *et al.* Klebsiella pneumoniae *nifM* gene product is required for stabilization and activation of nitrogenase iron protein in *Escherichia coli*. *J. Biol. Chem.* **261**, 772–778 (1986).

52. Hiller, C. J., Stiebritz, M. T., Lee, C. C., Liedtke, J. & Hu, Y. Tuning Electron Flux through Nitrogenase with Methanogen Iron Protein Homologues. *Chem. - Eur. J.* **23**, 16152–16156 (2017).

53. López-Torrejón, G., Burén, S., Veldhuizen, M. & Rubio, L. M. Biosynthesis of cofactor-activatable iron-only nitrogenase in *Saccharomyces cerevisiae*. *Microb. Biotechnol.* **14**, 1073–1083 (2021).

54. Buan, N. R. Methanogens: pushing the boundaries of biology. *Emerg. Top. Life Sci.* **2**, 629–646 (2018).

55. Solomon, J. B. *et al.* Probing the All-Ferrous States of Methanogen Nitrogenase Iron Proteins. *JACS Au* **1**, 119–123 (2021).

56. Boyd, E. S., Costas, A. M. G., Hamilton, T. L., Mus, F. & Peters, J. W. Evolution of Molybdenum Nitrogenase during the Transition from Anaerobic to Aerobic Metabolism. *J. Bacteriol.* **197**, 1690–1699 (2015).

57. Mus, F., Alleman, A. B., Pence, N., Seefeldt, L. C. & Peters, J. W. Exploring the alternatives of biological nitrogen fixation. *Metallomics* **10**, 523–538 (2018).

58. Demtröder, L., Narberhaus, F. & Masepohl, B. Coordinated regulation of nitrogen fixation and molybdate transport by molybdenum. *Mol. Microbiol.* **111**, 17–30 (2019).

59. Mus, F., Colman, D. R., Peters, J. W. & Boyd, E. S. Geobiological feedbacks, oxygen, and the evolution of nitrogenase. *Free Radic. Biol. Med.* **140**, 250–259 (2019).

60. Huergo, L. F. & Dixon, R. The Emergence of 2-Oxoglutarate as a Master Regulator Metabolite. *Microbiol. Mol. Biol. Rev.* **79**, 419–435 (2015).

61. Rey, F. E., Heiniger, E. K. & Harwood, C. S. Redirection of Metabolism for Biological Hydrogen Production. *Appl. Environ. Microbiol.* **73**, 1665–1671 (2007).

62. Drepper, T. *et al.* Role of GlnB and GlnK in ammonium control of both nitrogenase systems in the phototrophic bacterium *Rhodobacter capsulatus*. *Microbiology,* **149**, 2203–2212 (2003).

63. Lowery, R. G., Saari, L. L. & Ludden, P. W. Reversible regulation of the nitrogenase iron protein from *Rhodospirillum rubrum* by ADP-ribosylation in vitro. *J. Bacteriol.* **166**, 513–518 (1986).

64. Pope, M. R., Murrell, S. A. & Ludden, P. W. Covalent modification of the iron protein of nitrogenase from *Rhodospirillum rubrum* by adenosine diphosphoribosylation of a specific arginine residue. *Proc. Natl. Acad. Sci.* **82**, 3173–3177 (1985).

65. Masepohl, B., Krey, R. & Klipp, W. The *draTG* gene region of *Rhodobacter capsulatus* is required for post-translational regulation of both the molybdenum and the alternative nitrogenase. *Microbiology,* **139**, 2667–2675 (1993).

66. Heiniger, E. K. & Harwood, C. S. Posttranslational modification of a vanadium nitrogenase. *MicrobiologyOpen* **4**, 597–603 (2015).

67. Premakumar, R., Pau, R. N., Mitchenall, L. A., Easo, M. & Bishop, P. E. Regulation of the transcriptional activators AnfA and VnfA by metals and ammonium in *Azotobacter vinelandii*. *FEMS Microbiol. Lett.* **164**, 63–68 (1998).

68. Luque, F. & Pau, R. N. Transcriptional regulation by metals of structural genes for *Azotobacter vinelandii* nitrogenases. *Mol. Gen. Genet. MGG* **227**, 481–487 (1991).

69. Joerger, R. D., Jacobson, M. R. & Bishop, P. E. Two *nifA*-like genes required for expression of alternative nitrogenases by *Azotobacter vinelandii*. *J. Bacteriol.* **171**, 3258–3267 (1989).

70. Jacobitz, S. & Bishop, P. E. Regulation of nitrogenase-2 in *Azotobacter vinelandii* by ammonium, molybdenum, and vanadium. *J. Bacteriol.* **174**, 3884–3888 (1992).

71. Hoffmann, M.-C. *et al.* Proteome Profiling of the *Rhodobacter capsulatus* Molybdenum Response Reveals a Role of IscN in Nitrogen Fixation by Fe-Nitrogenase. *J. Bacteriol.* **198**, 633–643 (2016).

72. Demtröder, L., Pfänder, Y., Schäkermann, S., Bandow, J. E. & Masepohl, B. NifA is the master regulator of both nitrogenase systems in *Rhodobacter capsulatus*. *MicrobiologyOpen* **8**, e921 (2019).

73. Oda, Y. *et al.* Functional Genomic Analysis of Three Nitrogenase Isozymes in the Photosynthetic Bacterium *Rhodopseudomonas palustris*. *J. Bacteriol.* **187**, 7784–7794 (2005).

74. Zhan, Y. *et al.* The novel regulatory ncRNA, NfiS, optimizes nitrogen fixation via base pairing with the nitrogenase gene *nifK* mRNA in *Pseudomonas stutzer*i A1501. *Proc. Natl. Acad. Sci.* **113**, E4348–E4356 (2016).

75. Zhan, Y. *et al.* NfiR, a New Regulatory Noncoding RNA (ncRNA), Is Required in Concert with the NfiS ncRNA for Optimal Expression of Nitrogenase Genes in *Pseudomonas stutzeri* A1501. *Appl. Environ. Microbiol.* **85**, (2019).

76. Kessler, P. S., Daniel, C. & Leigh, J. A. Ammonia Switch-Off of Nitrogen Fixation in the Methanogenic Archaeon *Methanococcus maripaludis*: Mechanistic Features and Requirement for the Novel GlnB Homologues, $NifI_1$ and $NifI_2$. *J. Bacteriol.* **183**, 882–889 (2001).

77. Lie, T. J. & Leigh, J. A. A novel repressor of *nif* and *glnA* expression in the methanogenic archaeon *Methanococcus maripaludis*. *Mol. Microbiol.* **47**, 235–246 (2003).

78. Lie, T. J., Wood, G. E. & Leigh, J. A. Regulation of *nif* Expression in *Methanococcus maripaludis*: roles of the euryarchaeal repressor NrpR, 2-oxoglutarate, and two operators. *J. Biol. Chem.* **280**, 5236–5241 (2005).

79. Weidenbach, K., Ehlers, C. & Schmitz, R. A. The transcriptional activator NrpA is crucial for inducing nitrogen fixation in *Methanosarcina mazei* Gö1 under nitrogen-limited conditions. *FEBS J.* **281**, 3507–3522 (2014).

80. Prasse, D., Förstner, K. U., Jäger, D., Backofen, R. & Schmitz, R. A. $sRNA_{154}$ a newly identified regulator of nitrogen fixation in *Methanosarcina mazei* strain Gö1. *RNA Biol.* **14**, 1544–1558 (2017).

81. Studholme, D. J. & Pau, R. N. A DNA element recognised by the molybdenum-responsive transcription factor ModE is conserved in Proteobacteria, green sulphur bacteria and Archaea. *BMC Microbiol.* **3**, 24 (2003).

82. Chien, Y.-T., Auerbuch, V., Brabban, A. D. & Zinder, S. H. Analysis of Genes Encoding an Alternative Nitrogenase in the Archaeon *Methanosarcina barkeri* 227. *J. Bacteriol.* **182**, 3247–3253 (2000).

83. Lobo, A. L. & Zinder, S. H. Diazotrophy and Nitrogenase Activity in the Archaebacterium *Methanosarcina barkeri* 227. *Appl. Environ. Microbiol.* **54**, 1656–1661 (1988).

84. Kutsche, M., Leimkühler, S., Angermüller, S. & Klipp, W. Promoters controlling expression of the alternative nitrogenase and the molybdenum uptake system in *Rhodobacter capsulatus* are activated by NtrC, independent of sigma54, and repressed by molybdenum. *J. Bacteriol.* **178**, 2010–2017 (1996).

85. Pratte, B. S., Sheridan, R., James, J. A. & Thiel, T. Regulation of V-nitrogenase genes in *Anabaena variabilis* by RNA processing and by dual repressors. *Mol. Microbiol.* **88**, 413–424 (2013).

86. Dixon, R. *et al.* Analysis of regulation of *Klebsiella pneumoniae* nitrogen fixation (*nif*) gene cluster with gene fusions. *Nature* **286**, 128–132 (1980).

87. Zheng, K., Ngo, P. D., Owens, V. L., Yang, X. & Mansoorabadi, S. O. The biosynthetic pathway of coenzyme F430 in methanogenic and methanotrophic archaea. *Science* **354**, 339–342 (2016).

88. Moore, S. J. *et al.* Elucidation of the biosynthesis of the methane catalyst coenzyme F430. *Nature* **543**, 78–82 (2017).

89. Ghebreamlak, S. M. & Mansoorabadi, S. O. Divergent Members of the Nitrogenase Superfamily: Tetrapyrrole Biosynthesis and Beyond. *ChemBioChem* **21**, 1723–1728 (2020).

90. North, J. A. *et al.* A nitrogenase-like enzyme system catalyzes methionine, ethylene, and methane biogenesis. *Science* **369**, 1094–1098 (2020).

Figures

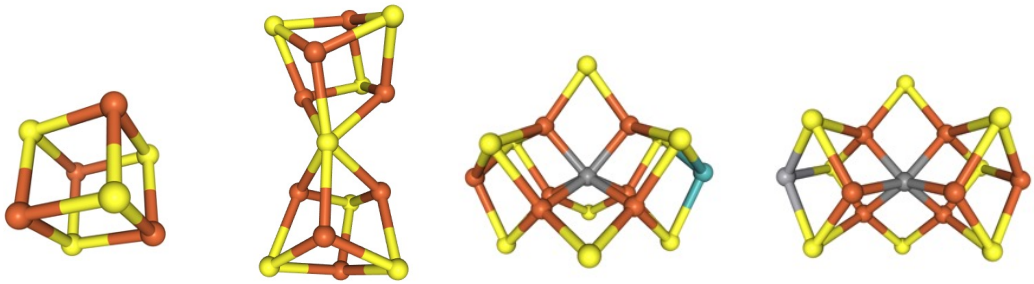

Figure 1. The simple and complex iron-sulfur clusters involved in nitrogen fixation. FeMo-co and FeV-co are bound to homocitrate (not pictured) through Mo and V, respectively. Images are of PDB structures SF4, CLF, ICS, and 8P8. The crystal structure of FeFe-co has not been determined.

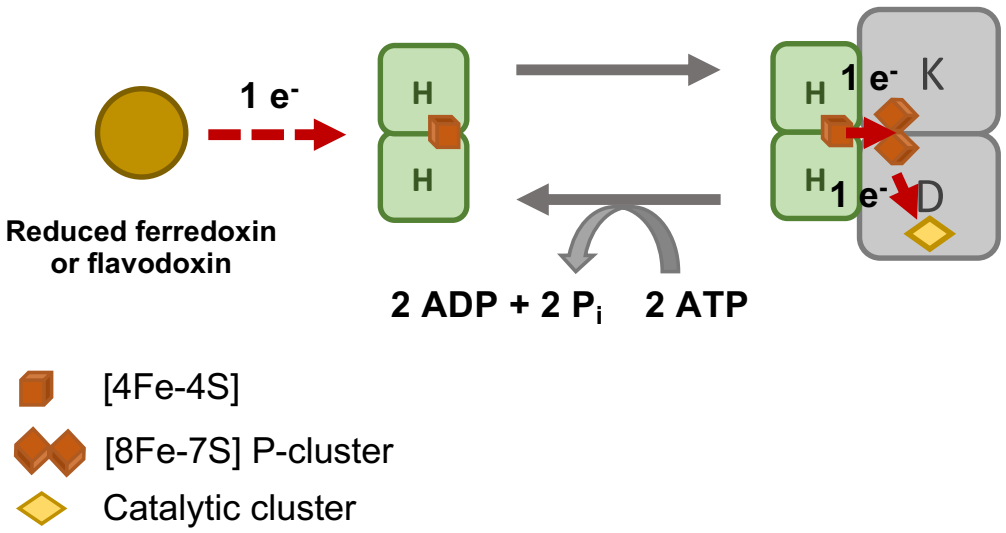

Figure 2. The general mechanism of electron flow for one half of the Mo nitrogenase. Electrons are delivered from reduced ferredoxin or flavodoxin to NifH. NifH donates one electron at a time to the P-cluster of NifDK, hydrolyzing 2 ATP to dissociate. One electron is transferred from the P-cluster to the M-cluster.

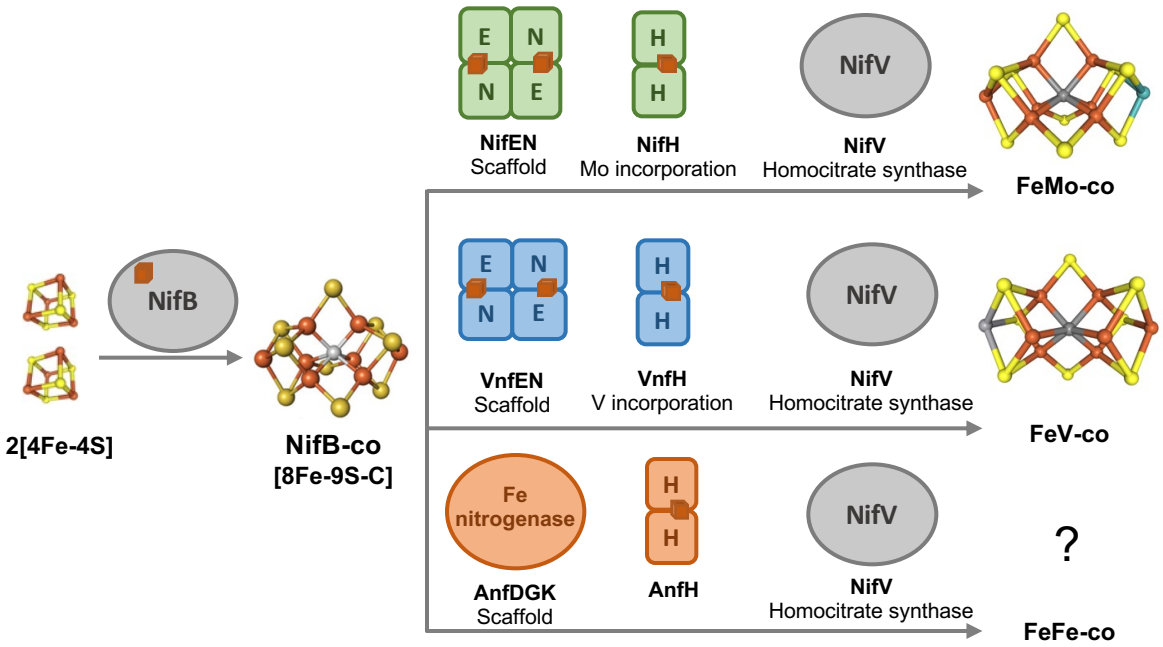

Figure 3. The minimal machinery required for nitrogenase catalytic cluster formation. Two [4Fe-4S] clusters are used by NifB to generate NifB-co. NifB-co is transferred to scaffolds NifEN or VnfEN, where Mo/V and homocitrate are incorporated using NifH/VnfH and NifV. FeMo-co and FeV-co are transferred to their respective nitrogenases. FeFe-co formation is unknown but the final cluster is assembled within the Fe-nitrogenase.

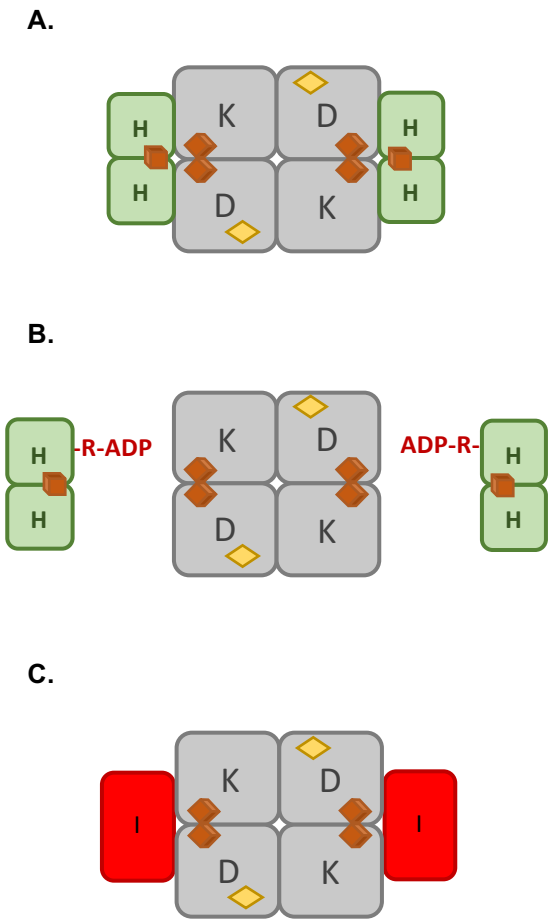

Figure 4. Post-translational regulation of nitrogenase in bacteria and methanogens. In the absence of fixed nitrogen, NifH donates electrons to NifDK as normal (A). In the presence of fixed nitrogen, NifH is ADP-ribosylated in bacteria (B), preventing association with NifDK. In methanogens (C), a NifI complex associates with NifDK and hinders NifH association.

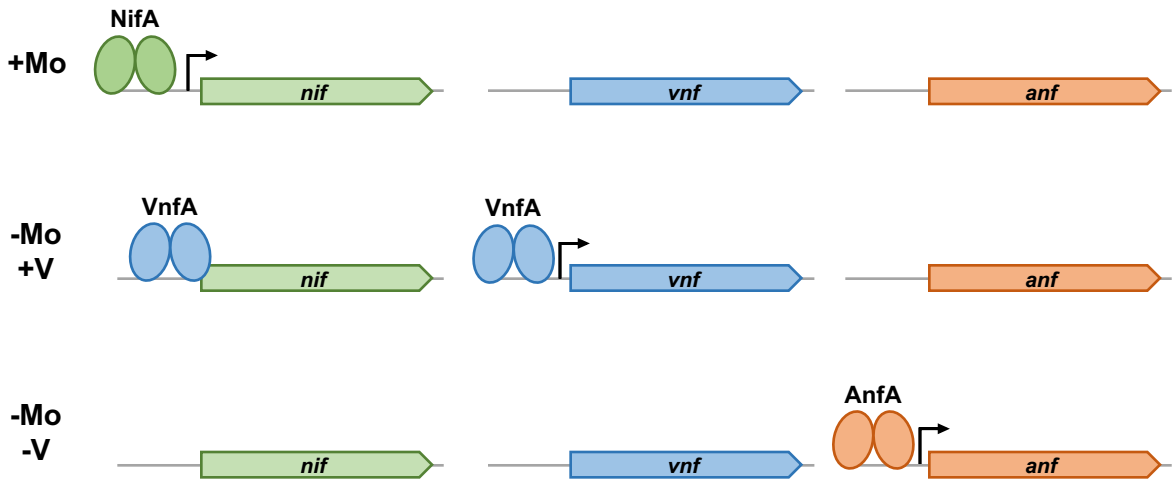

Figure 5. Transcriptional regulation of the three nitrogenases based on metal availability in *Azotobacter vinelandii.* In the presence of Mo, NifA activates *nif* while *vnfA* and *anfA* are repressed. In the absence of Mo and presence of V, VnfA activates *vnf* and represses *nif*. In the absence of Mo and V, AnfA is produced and activates *anf*.

Figure 6. Transcriptional regulation of the Mo-nitrogenase in methanogens. In the presence of fixed nitrogen, NrpR represses *nif* and *nrpA*. In the absence of fixed nitrogen, *nif* and *nrpA* are derepressed and NrpA activates *nif*.

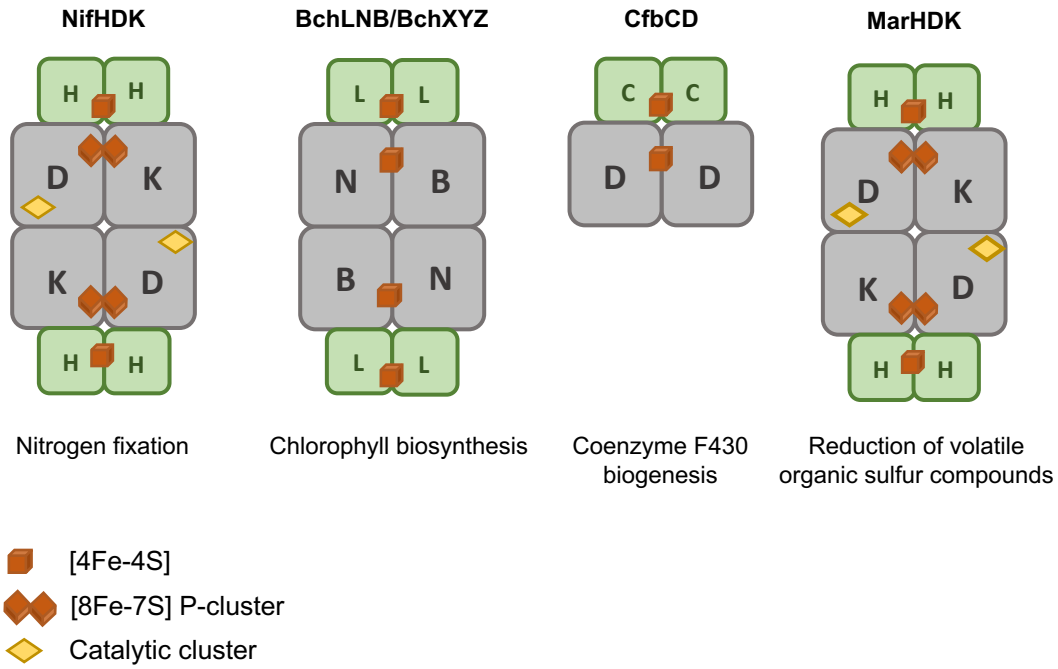

Figure 7. Nitrogenase family proteins and characterized or putative oligomerization and cofactors.

Chapter I

Methanosarcina acetivorans simultaneously produces molybdenum, vanadium, and iron-only nitrogenases in response to fixed nitrogen and molybdenum depletion

Melissa Chanderban, Ahmed E. Dhamad, Christopher A. Hill, and Daniel J. Lessner

Cell and Molecular Biology Program, University of Arkansas,

Fayetteville AR, 72701, USA

Introduction

Microbes are the primary drivers of the global biological nitrogen (N) cycle.[1,2] For example, only select bacteria and archaea are capable of biological nitrogen fixation, whereby dinitrogen gas (N_2) is reduced to ammonia (NH_3), the ion of which (NH_4^+) is the preferred "fixed" form of N used directly by most organisms. The biological reduction of the triple bond of N_2 is difficult and is catalyzed by nitrogenase, a unique metalloenzyme.[3,4] To date, all known and predicted N_2-fixing prokaryotes (diazotrophs) possess molybdenum (Mo) nitrogenase that contains a Mo atom within the unique iron (Fe) Mo-cofactor or M-cluster of the active site.[5,6] Mo-nitrogenase consists of two components: the Fe protein, which contains a single iron-sulfur (Fe-S) cluster, and the MoFe protein that contains the active site FeMo-cofactor and the [8Fe-7S] P-cluster. The Fe protein, encoded by *nifH*, is the dinitrogenase reductase that donates electrons to the MoFe protein, the dinitrogenase composed of a heterotetramer of subunits encoded by *nifD* and *nifK*. Together NifH and NifDK catalyzes the energy intensive reduction of N_2 as shown: $N_2 + 16ATP + 8e^- + 8H^+ \rightarrow 2NH_3 + H_2 + 16ADP + 16P_i$.[7] As such, Mo-nitrogenase production and activity is highly regulated in diazotrophs and is only synthesized when a fixed N source is unavailable. When needed, Mo-nitrogenase is produced in high quantities and can comprise as much as 10% of the total protein of the cell.[8]

In addition to having Mo-nitrogenase, some diazotrophs possess alternative nitrogenases that lack Mo.[9,10] The vanadium (V) nitrogenase and the Fe-only (Fe) nitrogenase contain an active site FeV-cofactor and FeFe-cofactor, respectively, instead of FeMo-cofactor.[11,12] The understanding of the genetic, biochemical, and catalytic properties of the alternative nitrogenases has primarily come from a few model bacteria (e.g., *Azotobacter vinelandii*). V-nitrogenase and Fe-nitrogenase have a similar subunit composition as Mo-nitrogenase, comprised of

VnfH/VnfDK and AnfH/AnfDK subunits, respectively. However, a distinguishing feature of V- and Fe-nitrogenases is the presence of an additional subunit (G) that associates with the dinitrogenase component (i.e., VnfDGK and AnfDGK).[9,11] The precise role of the G subunit is unknown, but it is required for diazotrophy in the absence of Mo.[13] V- and Fe-nitrogenases are less efficient at reducing N_2 than Mo-nitrogenase. More electron flux is directed to obligate H_2 production during reduction of N_2 by the alternative nitrogenases leading to substantially more ATP consumption. The V- and Fe-nitrogenases are estimated to consume 24 ATPs and 40 ATPs, respectively, during the reduction of a single N_2 to $2NH_3$.[14,15] As such, alternative nitrogenases in bacteria are only produced when insufficient levels of Mo are present to support usage of Mo-nitrogenase. In studied bacteria that possess all three nitrogenases, the expression and activity of each nitrogenase is highly regulated in response to metal and fixed N availability.[9,16]

Most characterized bacterial diazotrophs, such as *A. vinelandii*, use each nitrogenase isozyme during availability of its preferred metal, e.g., expressing only the V-nitrogenase during Mo limitation in the presence of vanadium (V).[16] Exceptions lie within the purple phototrophic bacteria. *Rhodobacter capsulatus* (*nif*, *anf*) produces the Mo-nitrogenase in the presence of Mo, but both Mo- and Fe-nitrogenases in the absence of Mo.[47] *Rhodopseudomonas palustris* (*nif*, *vnf*, *anf*) expresses each nitrogenase when its corresponding metal is available.[52] However, in a mutant with *nif* inactivation, both V- and Fe-nitrogenases are made, regardless of the presence of Mo or V.[52] Similarly, Fe-nitrogenase is produced in the presence of Mo in *Rhodospirillum rubrum* (*nif*, *anf*) when Mo-nitrogenase is inactive.

In addition to N_2, nitrogenases from bacteria can reduce other double and triple-bonded substrates (e.g., CO, CO_2, acetylene). Moreover, in the absence of another substrate, nitrogenase reduces protons to H_2, a feature that has been exploited to use nitrogenase to produce H_2 as a

biofuel.[17,18] The substrate, product, and activity profiles are also different between the three nitrogenases. The reduction of acetylene (C_2H_2) to ethylene (C_2H_4) is commonly used to measure nitrogenase activity.[19] Mo-nitrogenase reduces acetylene at a higher rate than both V- and Fe-nitrogenases, which also further reduce ethylene, producing ethane (C_2H_6) as a minor product.[20] Mo-nitrogenase does not produce ethane. Moreover, bacterial V-nitrogenase is more adept at reducing CO to alkanes than the Mo-nitrogenase, and the Fe-nitrogenase is better at reducing CO_2 to CH_4 than the V-nitrogenase.[11,21-23]

In contrast to bacterial diazotrophs, the regulation, assembly, and activity of nitrogenase, especially the alternative nitrogenases, is largely unknown in archaeal diazotrophs. Among archaea, only anaerobic methanogens and the closely related anerobic methanotrophs are known or predicted to fix N_2.[5,24,25] N_2 fixation has been studied in a few species of methanogens. The primary models are the obligate CO_2-reducing methanogen *Methanococcus maripaludis*, and the more versatile species *Methanosarcina mazei* and *Methanosarcina barkeri*.[26,27] *Methanosarcina* species can grow using methylated compounds (e.g., methanol) and acetate, in addition to reducing CO_2 with H_2.[28] *M. maripaludis* and *M. mazei* only contain Mo-nitrogenase, whereas strains of *M. barkeri* contain all three nitrogenases.[29,30] Mo-dependent and V-dependent N_2 fixation has been demonstrated in *M. barkeri*.[31-33] To our knowledge, diazotrophy under Fe-only conditions using the Fe-nitrogenase has not been documented for any methanogen. Previous research has primarily focused on elucidating the mechanisms that regulate the production and activity of Mo-nitrogenase in methanogens, revealing that the regulatory proteins used to control transcription and activity of Mo-nitrogenase are distinct from those used by most bacteria.[34,35] Recently, small RNAs (sRNA) have also been demonstrated to play roles in N_2 fixation and assimilation in methanogens.[36,37]

Methanosarcina acetivorans serves as an ideal model methanogen to understand the regulation and usage of the alternative nitrogenases in methanogens, since its genome encodes all three nitrogenases and it has a robust genetic system.[38-41] Recently, it was shown that *M. acetivorans* can fix N_2 using Mo-nitrogenase. Like *M. maripaludis*, *M. mazei*, and *M. barkeri*, Mo-nitrogenase is only produced in *M. acetivorans* when cells are grown in the absence of a fixed N source (e.g., NH_4Cl). Silencing of the *nif* operon in *M. acetivorans* using the recently developed CRISPRi-dCas9 system confirmed that Mo-nitrogenase is required for diazotrophy when cells are supplied with Mo.[41] However, to our knowledge, the ability of *M. acetivorans* to fix N_2 when Mo is not available has not been documented nor have the activities of *M. acetivorans* V-nitrogenase or Fe-nitrogenase been reported. Presumably, *M. acetivorans* produces V-nitrogenase and/or Fe-nitrogenase when both fixed N and Mo are limiting. An understanding of the properties of nitrogenases from methanogens could lead to new avenues for nitrogenase-based biofuel production and for the genetic engineering of crop plants capable of N_2-fixation. In this study we show that *M. acetivorans* can grow by fixing N_2 during Mo limitation with production of both V- and Fe-nitrogenases. We also determined the requirement of each nitrogenase during diazotrophy with and without Mo. These results provide a foundation to understand the regulation and properties of the three nitrogenases in methanogens.

Materials and Methods

M. acetivorans strains and growth

M. acetivorans strain WWM73 was used for genetic manipulation and for wild-type experiments.[40] Anoxic high-salt (HS) medium was prepared as previously described with some modifications.[42] To prepare Mo-deplete HS medium, all glassware was washed twice with 1 M

HCl, once with 1 M H_2SO_4, and then rinsed with ultrapure water to remove any residual molybdate prior to use. NH_4Cl and molybdate were omitted and the HS medium was reduced with 1.5 mM DTT. Methanol, NH_4Cl, sodium sulfide (Na_2S), sodium molybdate (Na_2MoO_4), and sodium vanadate (Na_3VO_4) were added from anoxic sterile stocks using sterile syringes prior to inoculation. *M. acetivorans* strain WWM73 was grown in Balch tubes containing 10 ml of HS medium with 125 mM methanol and 0.025 % Na_2S (w/v). Molybdate (1 μM), vanadate (1 μM), and NH_4Cl (18 mM) were added to cultures as indicated. Strains were grown for more than 100 generations in Mo-depleted HS medium containing methanol and NH_4Cl prior to the growth experiments. Growth was measured by monitoring optical density at 600 nm (OD_{600}) using a spectrophotometer. Cell density was determined from OD_{600} using a standard curve generated by direct cell counts with a hemocytometer.

Quantitative PCR analysis of gene expression

M. acetivorans cells were harvested during mid-log phase (0.3-0.4 OD_{600}) by anaerobic centrifugation of 4-8 mL of culture. Cell pellets were resuspended in 1 mL Trizol and frozen at -80 °C. RNA was extracted using the Zymo Direct-zol Miniprep kit (#R2052) and further purified using the Invitrogen DNA-free DNA Removal Kit (#AM1906). cDNA was generated using the Bio-Rad iScript Select cDNA Synthesis Kit (#1708896). qPCR primers were designed using Geneious Prime (*nifD* forward: CGCCCGCTGTGAAGGATATA; *nifD* reverse: TTATGTCAAAGGGAGTGGGGTC; *vnfD* forward: GTCGGAAAGAGGTTGCAGCTA; *vnfD* reverse: GCTTCGTGTGCCAGGTATCA; *anfD* forward: GTCTCCCTGATGGCCGAATT; *anfD* reverse: AGATCTGTCTCTGGCCTGGT; 16S rRNA forward: GGTACGGGTTGTGAGAGCAA; 16S rRNA reverse: CTCGGTGTCCCCTTATCACG). qPCR

of three biological replicates and two technical replicates was performed with the SsoAdvanced Universal SYBR Green Supermix (Bio-Rad, #1725271). Relative quantification was determined using the $2^{-\Delta\Delta Cq}$ method with 16S rRNA internal control.

Western blot analysis

Separate custom polyclonal antibodies specific for *M. acetivorans* NifD, VnfD, or AnfD were generated using the PolyExpress Silver package (two epitopes) from Genscript. Specificity of the antibodies was confirmed using recombinant NifD, VnfD, and AnfD expressed in *E. coli* (data not shown). *M. acetivorans* cells were harvested during mid-log phase (0.3-0.4 OD_{600}) by aerobic centrifugation (8500 x *g* for 10 minutes at 4°C) of 6 mL of culture. The cell pellet was resuspended in 50 mM Tris, 150 mM NaCl pH 7.2 with 1 mM PMSF and 1 mM benzamidine, normalized based on OD_{600}, and frozen at -80°C. Whole cell lysate was generated by five freeze/thaw cycles and a one hour DNase (5 µg) treatment at 37°C. Protein concentration was determined using the Bradford assay. After blocking for one hour in TBST (20 mM Tris, 150 mM NaCl, 0.1% Tween pH 7.6) with 5% milk, membranes were incubated for 18 hours with the primary antibodies specific for NifD, VnfD, or AnfD, then washed three times with TBST. Membranes were then incubated with an HRP-conjugated secondary antibody (Promega) for one hour, followed by three washes with TBST. Finally, membranes were visualized using an enhanced chemiluminescent reagent (Thermo Scientific) and an Alpha Innotech imaging system.

Construction of CRISPRi gene repression strains

CRISPRi repression of the *vnf* and *anf* operons in *M. acetivorans* was designed and strains constructed as previously described for CRISPRi repression of the *nif* operon in strain DJL74.[41]

Briefly, 20 bp guide RNAs (gRNA) targeting dCas9 to *vnf* and *anf* gene clusters were designed using Geneious Prime (Fig. 1). Synthetic DNA oligos (IDT) were designed for assembly with CRISPRi-dCas9 plasmid pDL734 as described.[41] gBlocks and pDL734 were assembled using the Gibson assembly Ultra Kit (Synthetic Genomics). The assembly mix was used to transform *Escherichia coli* strain WM4489, and transformants were screened for assembled plasmids using standard methods and final plasmids sequenced. Each plasmid was used to transform *M. acetivorans* strain WWM73 as described.[43] Integration of each plasmid integration into the chromosome of strain WWM73 was screened using PCR. Repression of the *vnf* and/or *anf* operons in the resultant CRISPRi repression strains was confirmed by western blot as described above. *M. acetivorans* strains used in this study are listed in Table 1.

Methane determination by gas chromatography

After the cessation of growth, the total volume of gas produced by each culture was measured using a glass syringe, which also normalized the pressure to 1 atm. The amount of CH_4 produced was determined by injection of 50 µl of headspace gas into a Shimadzu Nexis GC-2030 gas chromatograph fitted with a Rt-Q-BOND fused silica PLOT column with a 0.32 mm internal diameter, a 30 m length, and a 10.00 µm film thickness (Restek, VWR #89166-308) and BID detector. The sample split ratio was 42.6, and the carrier gas was helium at 4.44 mL/min. The injection port temperature was 100 °C, column temperature 27 °C, and BID temperature 220 °C. Peak integration was performed using Shimadzu LabSolutions software and moles of CH_4 determined using methane standards.

Results

Organization of nitrogenase genes in *M. acetivorans* and prevalence of alternative nitrogenases in methanogens. The genome of *M. acetivorans* contains three separate nitrogenase gene clusters (Fig. 2), designated *nif*, *vnf*, and *anf*, encoding putative Mo-nitrogenase, V-nitrogenase, and Fe-nitrogenase, respectively. The gene arrangement of the *nif* cluster is similar to the characterized *nif* operons from *M. maripaludis*, *M. barkeri*, and *M. mazei*.[30,44,45] The sequence of *M. acetivorans* NifDK is homologous to *Clostridium pasteurianum* NifDK, including an insertion in NifD and smaller NifK. In addition to encoding the nitrogenase structural components (NifH and NifDK), the operon also encodes the regulatory proteins $NifI_1$ and $NifI_2$ and the FeMo-cofactor scaffold proteins NifEN.[12,46] The *M. acetivorans vnf* cluster contains the same gene arrangement as *nif*, including its own regulatory and scaffold genes, but also includes *vnfG* and a homolog of *nifX*, designated *vnfX*. NifX is involved in FeMo-cofactor assembly in bacteria.[12] The gene arrangement of the *M. acetivorans anf* cluster is like the *vnf* cluster, except *anfH* encoding the putative Fe-protein is downstream of *anfK* and is not in the operon. The *vnf* and *anf* clusters are designated as such due to the presence of a G subunit, and all *anf* genes to date lack a designated scaffold. The *anf* and *vnf* gene clusters are divergent in the chromosome of *M. acetivorans* (Fig. 2), indicating there could be coordinated regulation. Interestingly, the amino acid sequences of VnfH and AnfH are identical, indicating the same Fe-protein functions with both V- and Fe-nitrogenases. Also unique to the *anf* cluster is the presence of homologs of Anf3 and AnfO found in *anf* operons of bacteria. The function of Anf3 is unknown. However, Anf3 is essential for diazotrophy with the Fe-nitrogenase in *Rhodobacter capsulatus*.[47] An Anf3 homolog characterized in *A. vinelandii* is a heme- and FAD-binding oxidase that may protect the Fe-nitrogenase from oxygen.[48] AnfO was recently shown to control

fidelity of Fe-nitrogenase maturation by preventing incorporation of the incorrect active site cofactor.[49]

The *nif*, *vnf*, and *anf* gene clusters are widely distributed within genera of bacteria. However, nitrogenase genes are found only in a subset of archaea, restricted to methanogens and closely related anerobic methanotrophs. The *nif* operon is distributed across six of the seven orders of methanogens, whereas the *vnf* and *anf* genes are restricted to the Methanosarcinales, with few exceptions, namely *Methanobacterium lacus*, which contains a cluster of putative *anf* genes.[5,24,25] Like bacteria, all methanogens that contain putative *vnf* and *anf* clusters also contain the *nif* operon. Of the 41 complete Methanosarcinales genome sequences currently available in the NCBI database, ~66 % contain the *nif* genes. Of those containing *nif*, ~44 % contain the *vnf* and/or *anf* genes (Table 2). The arrangement of the *vnf* and *anf* gene clusters are similar across the Methanosarcinales (Fig. 3). Of note is a hypothetical protein encoded by a gene between *vnfDGK* and *vnfEN* in several *Methanosarcina* species.

Molybdenum and vanadium availability affect diazotrophic growth of *M. acetivorans*. To ascertain the effect of molybdenum and vanadium availability on nitrogenase utilization by *M. acetivorans*, WWM73 was passed in HS standard medium lacking Mo for >100 generations to deplete molybdate, the biological available form of Mo, to <1 ppb as confirmed with ICP-MS. Vanadium is not added to standard HS medium (<1 ppb). Mo-deplete cells were used to inoculate Mo-deplete HS medium devoid of NH_4Cl (fixed N source). Methanol was used as the carbon and energy source in all experiments. Molybdate, vanadate, and NH_4Cl were added from sterile anaerobic stocks to separate cultures to compare the effect of Mo, V, and fixed N on growth and nitrogenase expression. Neither the depletion of Mo nor the addition of V affects the

growth, generation time, or cell yield when NH_4Cl is supplied as the fixed N source (Fig. 4 and Table 3). However, the depletion of Mo and the addition of V significantly affects growth, generation time and cell yield in cultures without NH_4Cl (diazotrophic growth). When *M. acetivorans* is provided Mo in the absence of NH_4Cl, the generation time increases approximately 3-fold, and the cell yield decreases approximately 37% compared to non-diazotrophic cultures (Table 3). Diazotrophic cultures lacking Mo but provided V have an even longer generation time and further reduction in cell yield (~50% that of non-diazotrophic cultures). Diazotrophic growth is further impacted by the limitation of both Mo and V, with an ~10-fold increase in generation time and an ~70% reduction in cell yield compared to non-diazotrophic cultures (Fig. 4 and Table 3). Diazotrophic cultures lacking Mo also have an extended lag phase compared to diazotrophic cultures containing Mo (Fig. 4 and Table 3). These data reveal that *M. acetivorans* is capable of diazotrophy during Mo limitation, and that V availability impacts N_2 fixation. These results are consistent with *M. acetivorans* utilizing Mo-, V-, and Fe-nitrogenases to fix N_2 according to Mo and V availability.

Methylotrophic methanogenesis is not altered by diazotrophy or the availability of molybdenum or vanadium. Growth of *M. acetivorans* with methanol utilizes the methylotrophic pathway of methanogenesis, where one methyl group of methanol is oxidized to CO_2, and the resulting three electron pairs are used to reduce three additional methyl groups to CH_4.[50] To determine if diazotrophy and metal availability affect the flux of carbon during methylotrophic methanogenesis, contributing to the slower growth rate and lower cell yields with limited Mo, total CH_4 was determined after the cessation of growth of non-diazotrophic and diazotrophic cultures. Similar amounts of CH_4 were observed across all growth conditions (Table

4), revealing N_2 fixation and differences in Mo and V availability does not significantly alter the flux of carbon during methylotrophic methanogenesis. Therefore, the observed hierarchical decrease in cell yields during diazotrophic growth under Mo + Fe, V + Fe, or Fe-only conditions (Table 3) is not due to decreased energy availability from altered methanogenesis but is likely due to the increased ATP consumption needed to support N_2 reduction by Mo-, V-, and Fe-nitrogenases, as seen in bacteria.[9]

Molybdenum availability affects the expression of V-nitrogenase and Fe-nitrogenase but not Mo-nitrogenase in *M. acetivorans*. Previous results demonstrated that Mo-nitrogenase is not produced in *M. acetivorans* cells grown in the presence of NH_4Cl. Removal of NH_4Cl results in a modest increase in *nif* transcription and production of Mo-nitrogenase, allowing growth with N_2. Repression of the *nif* operon using CRISPRi-dCas9, in which catalytically dead Cas9 is targeted to *nif* and blocks transcription, abolishes the ability to grow with N_2 in medium containing Mo.[41] To determine the effect of fixed N and Mo depletion on Mo-nitrogenase, V-nitrogenase and Fe-nitrogenase expression, qPCR was performed using primers specific for *nifD*, *vnfD*, and *anfD* to analyze transcript abundance in cells grown in medium with or without NH_4Cl and containing Mo + Fe, V + Fe, or Fe only (Fig. 5). An increase in transcript abundance for *nifD* and *vnfD* was observed in cells grown in Mo + Fe medium without NH_4Cl, relative to the transcript abundance in cells grown with NH_4Cl (Fig. 5A). However, only the fold change for *vnfD* was significant. Comparison of *nifD*, *vnfD*, *anfD* transcript abundance from cells grown with V + Fe showed a significant fold change for *vnfD* and *anfD* (Fig. 5B). The transcript abundance of *vnfD* is ~180-fold higher in cells grown in V + Fe medium without NH_4Cl compared to cells grown with NH_4Cl. Transcript abundance for *anfD* is ~60-fold higher in cells

grown in V + Fe medium without NH_4Cl compared to cells grown with NH_4Cl. In contrast, only a slight increase (~3-fold) was observed for *nifD* transcript abundance. Like the transcript abundance of *vnfD* and *anfD* in cells grown with V + Fe, cells grown in Fe-only medium lacking NH_4Cl had a significant increase in *vnfD* and *anfD* transcript abundance compared to cells grown with NH_4Cl (Fig. 5C**).** No change in the expression of *nifD* was detected in cells grown in Fe-only medium lacking NH_4Cl relative to that with NH_4Cl (Fig. 5C).

To further determine the effect of Mo removal on transcription of each nitrogenase gene cluster, the fold change in *nifD*, *vnfD* and *anfD* transcript abundance was also calculated by comparing the relative abundance in cells grown in V + Fe or Fe-only medium to the transcript abundance in cells grown in Mo + Fe medium (Fig. 6). The expression of *nifD* did not significantly change in cells grown in medium with or without Mo, regardless of the presence or absence of NH_4Cl. However, removal of Mo significantly affected the transcription of both *vnfD* and *anfD* in cells grown with or without NH_4Cl. The transcript abundance of *vnfD* is highest in cells grown in Fe-only medium, with the fold-change higher than when V is present. A similar pattern was observed for the expression of *anfD*. However, the fold change in expression of *anfD* in cells grown with Fe only compared to Mo + Fe was much higher (~300-600-fold). These results indicate there is significant regulatory control of transcription of the *vnf* and *anf* gene clusters, whereas there is only modest transcriptional control of the *nif* operon. The results also show that the depletion of Mo is the key signal that increases transcription of the *vnf* and *anf* gene clusters. Removal of a fixed N source (NH_4Cl) when Mo is available has only a slight effect on the transcription of the *vnf* and *anf* gene clusters.

The production of Mo-, V-, and Fe-nitrogenases in *M. acetivorans* grown under the same conditions for qPCR analysis was determined by Western blot using antibodies specific to NifD,

VnfD, and AnfD (Fig. 7). Consistent with previous results, NifD was only detected in lysate from *M. acetivorans* cells grown in Mo + Fe medium lacking NH_4Cl.[41] Neither VnfD nor AnfD were detected in lysate from cells grown in Mo + Fe medium regardless of the presence or absence of NH_4Cl. However, both VnfD and AnfD were detected in lysate from cells grown in Mo-depleted medium lacking NH_4Cl. Interestingly, NifD was also detected in lysate from cells grown in Mo-deplete medium. The availability of V does not appear to affect production of VnfD or AnfD. These results indicate that both the depletion of fixed N and Mo are required for production of V-nitrogenase and Fe-nitrogenase in *M. acetivorans*.

V- or Fe-nitrogenase expression is required for Mo-independent diazotrophy. Since all three nitrogenases were detected during Mo-independent diazotrophy (Fig. 7), it is unclear which nitrogenase(s) is required to support growth. CRISPRi repression of the *nif* operon in strain DJL74 was previously shown to abolish production of Mo-nitrogenase and Mo-dependent diazotrophy. Therefore, to test the importance of V- or Fe-nitrogenases, three CRISPRi repression strains expressing gRNAs to target repression of the *vnf* or *anf* operons (**Table 1**). Strains DJL107, DJL119, and DJL120 were grown in HS medium lacking NH_4Cl with the different metal availabilities (Mo+Fe, V+Fe, and Fe only) to assess the ability of each strain to grow by Mo-dependent or independent diazotrophy (Fig. 8). Strain DJL107 (gRNA-*vnfH*) grew comparable to control strain DJL72 (gRNA-free) under all conditions: however, the addition of V did not result in a stimulation of growth as seen with strain DJL72. Strain DJL120 (gRNA-*anf*) also grew similar to the control with the exception of the Fe only condition, where growth was abolished, consistent with the Fe-nitrogenase essential for diazotrophy in Fe only medium. Finally, strain DJL119 that contains both gRNAs is unable to grow by Mo-independent

diazotrophy, indicating that V- and/or Fe-nitrogenase is required for N_2 fixation in the absence of Mo.

To confirm that production of V- and Fe-nitrogenases is abolished in strains DJL107, DJL119, and DJL120, lysates from cells grown under the conditions in Fig. 8 were probed for the presence of NifD, VnfD, and AnfD by Western blot (Fig. 9). NifD was detected in lysates from all strains grown in Mo + Fe medium, indicating repression of *vnf* and *anf* does not affect Mo-nitrogenase expression. Importantly, VnfD and AnfD are below the detection limit in lysates from strains DJL107, DJL119, and DJL120 grown under conditions where each protein is detected in lysate from control strain DJL72 (gRNA-free) (Fig. 9). These results demonstrate that production of V-nitrogenase is abolished in strain DJL107, production of Fe-nitrogenase is abolished in strain DJL120, and production of both nitrogenases is abolished in strain DJL119. Finally, since Mo-independent diazotrophy by strain DJL107 in the presence of V is not abolished (Fig. 8), this suggest that the expressed Fe-nitrogenase is active both in the presence and absence of V.

Mo-nitrogenase is required for V- and Fe-nitrogenase expression. To understand why *M. acetivorans* produces Mo-nitrogenase when fixing N_2 in medium lacking Mo, strain DJL74 was used to test the effect of the repression of the *nif* operon on Mo-independent diazotrophy and alternative nitrogenase expression. As shown previously, DJL74 (gRNA-P_{nif}) does not grow in the absence of fixed nitrogen and in Mo +Fe medium (Fig. 10A). Surprisingly, Mo-independent diazotrophy by strain DJL74 is also abolished, regardless of the presence or absence of V (Fig. 10A). Importantly, strain DJL119 that is only capable of expressing Mo-nitrogenase cannot grow by Mo-independent diazotrophy (Fig. 8), indicating the Mo-nitrogenase that is produced cannot

support nitrogen fixation (i.e., the alternative nitrogenases are required for Mo-independent diazotrophy). To test if expression of inactive Mo-nitrogenase is required for expression of the alternative nitrogenases in *M. acetivorans*, cells of strains DJL72 and DJL74 were harvested at the indicated times (Fig. 10A) and lysates probed for the presence of VnfD and AnfD by western blot (Fig. 10B). In both V + Fe and Fe only conditions, AnfD and VnfD are detected in lysates from cells of strain DJL72. However, both AnfD and VnfD are below the detection limit in all lysates from cells of strain DJL74. These results reveal that expression of the *nif* operon is required for expression of both V- and Fe-nitrogenases in *M. acetivorans* when cells are grown in the absence of fixed nitrogen and Mo.

Discussion

The regulation, assembly, and activity of the three forms of nitrogenase is well understood in diazotrophic bacteria, especially in the principal model *A. vinelandii* that contains all three nitrogenases. In contrast to methanogens which are strict anaerobes, *A. vinelandii* is an obligate aerobe; thus, in addition to nitrogenase structural proteins, *A. vinelandii* requires accessory proteins to prevent oxidative damage to nitrogenase and to integrate nitrogen fixation into central metabolism. At least 82 genes are predicted to be involved in the formation and regulation of Mo-, V-, and Fe-nitrogenases in *A. vinelandii*.[16] Moreover, there is complex regulatory control over hierarchal nitrogenase expression, with only one nitrogenase produced at a time. When fixed N is absent and Mo is available, Mo-nitrogenase is preferentially produced over V- and Fe-nitrogenase, followed by V-nitrogenase if Mo is absent and V is present. If neither Mo nor V is available, then Fe-nitrogenase is produced [24]. Among methanogens, the alternative nitrogenases are restricted primarily to the Methanosarcinales, the most metabolically

diverse methanogens with the largest genomes. Nonetheless, the genomes of sequenced Methanosarcinales contain simpler nitrogenase gene clusters and lack many of the accessory and regulatory proteins found in *A. vinelandii* and other diazotrophic bacteria.[25] The formation and regulation of the alternative nitrogenases is likely simpler in methanogens compared to aerobic diazotrophic bacteria. The results presented here demonstrate that *M. acetivorans* produces all three nitrogenases and is capable of diazotrophy during limitation of available Mo and V (Fe-only condition). To our knowledge, this is first direct evidence of a methanogen producing an Fe-nitrogenase and capable of diazotrophy in conditions limited in both Mo and V.

Like other diazotrophs, *M. acetivorans* only produces nitrogenase in the absence of fixed N. The diazotrophic growth pattern of *M. acetivorans* correlates with reported ATP requirements by Mo-, V-, and Fe-nitrogenase from bacteria.[14] *M. acetivorans* has the fastest growth rate and highest cell yield during diazotrophic growth when utilizing only Mo-nitrogenase. Only a modest increase in transcription of the *nif* operon was observed in response to fixed N depletion. The high basal level of transcription of the *nif* operon likely allows *M. acetivorans* to be poised for rapid Mo-nitrogenase production. The relatively short lag time before the onset of diazotrophic growth in Mo + Fe medium (Table 2 and Fig. 2) supports the rapid production of Mo-nitrogenase.

The results indicating minimal transcriptional control of the *nif* operon further support that post-transcriptional regulation is a key factor controlling Mo-nitrogenase production. Previous studies investigated the role of NrpR in regulating the expression of Mo-nitrogenase in *M. acetivorans*. NrpR is the repressor of the *nif* operon in methanogens and indirectly senses fixed N availability by directly sensing intracellular 2-oxogluatrate levels.[51] A mutant strain of *M. acetivorans* where *nrpR* transcription was silenced using the CRISPRi-dCas9 system revealed

that the depletion of NrpR results in an increase in the transcription of the *nif* operon, but the mutant still fails to produce detectable nitrogenase when grown with fixed N.[41] In *M. mazei*, a small RNA ($sRNA_{154}$) is exclusively expressed when fixed N is limiting and functions to stabilize the polycistronic mRNA produced from the *nif* operon.[36] The genome of *M. acetivorans* encodes a $sRNA_{154}$ homolog, indicating similar post-transcriptional regulation of the *nif* operon. Interestingly, removal of Mo did not significantly alter transcription of the *nif* operon or the production of nitrogenase (Fig. 4A and 5). Therefore, the critical and likely only signal for Mo-nitrogenase production in *M. acetivorans* is fixed N limitation. This is distinct from diazotrophic bacteria that contain V- and Fe-nitrogenases. For example, *A. vinelandii* and the purple non-sulfur phototroph *Rhodopseudomonas palustris* both stop producing Mo-nitrogenase when Mo is depleted.[24,52]

While Mo-depletion had little effect on Mo-nitrogenase expression, it is critical for the expression of V- and Fe-nitrogenase in *M. acetivorans*. Both fixed N and Mo depletion are required for production of V-nitrogenase and Fe-nitrogenase (Fig. 5). Importantly, Mo depletion resulted in a significant increase in the relative transcript abundance of *vnfD* and *anfD* (Fig. 3 and 4). Thus, unlike production of Mo-nitrogenase, transcriptional regulation is a key mechanism to control production of V- and Fe-nitrogenases in *M. acetivorans*. The overall transcript abundance profiles for *vnfD* and *anfD* are similar across all growth conditions. Mo depletion appears to be a key effector as cells grown with NH_4Cl exhibited a significant increase in transcript abundance of *vnfD* and *anfD* (Fig. 4). Nonetheless, neither VnfD nor AnfD were detected in cells grown with NH_4Cl in Mo-depleted medium (Fig. 5), indicating post-transcriptional regulation of *vnf* and *anf* genes is also likely involved. Unexpectedly, during Mo limitation, the presence of V does not increase the transcript abundance of *vnfD* and *anfD* as

much as the increase during Fe-only conditions (Fig. 4). The role V plays in nitrogenase regulation is unknown in most diazotrophs. Nevertheless, when comparing the effect of fixed N depletion, a large relative fold change in transcript abundance for *vnfD* and *anfD* was observed in cells grown in V + Fe medium (Fig. 3B). Expression of the *vnf* and *anf* operons in *A. vinelandii* in the absence of Mo results in the production of either V-nitrogenase or Fe-nitrogenase depending on V availability, but not both.[16] In contrast, V availability had no effect on V-nitrogenase or Fe-nitrogenase production in *M. acetivorans*, as each was produced in cells grown in Mo-depleted medium (Fig. 5). Notably, VnfH and AnfH are identical in amino acid sequence, indicating a single dinitrogenase reductase (VnfH/AnfH) can support the *in vivo* activities of separate dinitrogenases (VnfDGK and AnfDGK).

Production of both V-nitrogenase and Fe-nitrogenase in *M. acetivorans* clearly requires fixed N depletion since neither VnfD nor AnfD were detected by immunoblot in lysate from cells grown with NH_4Cl regardless of Mo availability. Regulation of V-nitrogenase and Fe-nitrogenase expression in response to fixed N availability does not likely involve direct control of *vnf* and *anf* transcription since fixed N depletion in the presence of Mo did not alter *anfD* transcript abundance and only had a modest effect on *vnfD* transcript abundance (Fig. 3A). These results are consistent with the promotor regions of both the *vnf* and *anf* gene clusters lacking the identified NrpR operator sequence.[53] The promoter regions also lack identified binding sites for NrpA, an activator of the *nif* operon in *M. mazei*, though *M. acetivorans* encodes two homologs (MA0545 and MA0546).[54] Thus, post-transcriptional regulation is likely the primary mechanism of control of V-nitrogenase and Fe-nitrogenase production in response to fixed N availability. It is possible $sRNA_{154}$, or another sRNA, is responsive to fixed N depletion and functions to

stabilize *vnf* and *anf* mRNAs, which allows for V-nitrogenase and Fe-nitrogenase production only when fixed N is depleted.

Mo availability is the key factor controlling transcription of both the *vnf* and *anf* gene clusters in *M. acetivorans*. In non-diazotrophic (e.g., *E. coli*) and diazotrophic bacteria, the molybdate-responsive transcriptional regulator ModE controls the expression of the high-affinity molybdate transporter ModABC as well as Mo-dependent enzymes.[55] In *A. vinelandii*, ModE indirectly represses expression of both V-nitrogenase and Fe-nitrogenase by directly repressing the transcription of the genes encoding the regulators VnfA and AnfA. VnfA activates transcription of the *vnf* operon and AnfA activates transcription of the *anf* operon in *A. vinelandii*.[55] The genome of *M. acetivorans* encodes several homologs of ModABC (MA0325-27, MA1235-37, and MA2280-82), including an additional homolog of ModBC (MA3902-03) downstream of the *nif* operon. *M. acetivorans* contains a ModE homolog (MA0283) but lacks homologs to VnfA and AnfA. Potential ModE-binding sites are located upstream of *vnfH* and $anfI_1$, the first genes in the *vnf* and *anf* gene clusters.[56] Therefore, it is highly plausible that ModE is responsible for repressing transcription of *vnf* and *anf* when sufficient Mo is available to support Mo-nitrogenase activity. Depletion of Mo (corepressor) likely results in removal of DNA-bound ModE and de-repression of transcription of the *vnf* and *anf* gene clusters, leading to the simultaneous production of V-nitrogenase and Fe-nitrogenase in *M. acetivorans*. The results are consistent with this regulatory mechanism. Interestingly, the starter inoculum used in all expression studies was maintained in Mo-deplete medium, which should result in an increase in *vnf* and *anf* transcription even during growth with NH_4Cl (Fig. 4). As such, the starter inoculum should be primed to use the alternative nitrogenases once fixed N is depleted, yet there was a much longer lag period before the onset of growth in Mo-deplete medium compared to the onset

of growth in Mo-deplete medium with added Mo (Table 2 and Fig. 2). This result indicates that there are likely other unknown regulatory factors involved in controlling the production of V-nitrogenase and Fe-nitrogenase in response to fixed N and Mo depletion.

The simultaneous production of all three nitrogenases in *M. acetivorans* during diazotrophy in Mo-deplete medium raises interesting questions. Why would *M. acetivorans* continue to produce Mo-nitrogenase under conditions when the enzyme is likely not functional? One plausible explanation is that because the energy conservation (i.e., ATP generation) during methanogenesis by *M. acetivorans* is significantly lower even during optimal conditions compared to studied diazotrophic bacteria, that *M. acetivorans* continues to produce Mo-nitrogenase when fixed N is limiting regardless of Mo availability to be poised to use the most efficient nitrogenase.[57] However, we cannot rule out that the small amount of residual Mo present in the Mo-deplete medium is enough to maintain expression of Mo-nitrogenase.

The simultaneous production of all three nitrogenases under Mo-deplete conditions begs the question, which nitrogenase(s) are functional? Although only NifD, VnfD, and AnfD were detected in cells growing in Mo-deplete medium, it is likely that NifDK, VnfDGK, and AnfDGK complexes are present since NifD is unstable in the absence of NifK.[58] Therefore, metal-dependent regulation of metallocluster insertion into NifDK, VnfDGK, and AnfDGK may control which nitrogenase is active. NifDK likely lacks FeMo-cofactor when produced in cells growing in Mo-deplete medium, while VnfDGK likely lacks FeV-cofactor when produced in the absence of V. AnfDGK could contain the FeFe-cofactor cluster regardless of the presence of V and always be active in cells grown in Mo-deplete medium. Moreover, the formation of hybrid nitrogenases is possible, as both VnfDGK and AnfDGK can incorporate the FeMo-cofactor

resulting in a functional hybrid nitrogenase.[59,60] It is unlikely that NifDK can incorporate the FeV-cofactor or FeFe-cofactor, although this cannot be ruled out.

To begin answering these questions, we used CRISPRi-dCas9 to repress each nitrogenase. First, to investigate why the Mo-nitrogenase is expressed during all diazotrophic conditions, we grew DJL74 in Mo-deplete medium. Because *M. acetivorans* produces Vnf and Anf during these conditions, we predicted there would be no phenotype. However, DJL74 still struggles to grow, suggesting either the Mo-nitrogenase is the dominant nitrogenase used during Mo limitation, or genes in the *nif* operon are required for some aspect of using the alternative nitrogenases. To test the former, DJL119 was generated to repress both *vnf* and *anf* and produces the Mo-nitrogenase as its only detectable nitrogenase. Because this strain also struggles to grow with limited Mo, the Mo-nitrogenase is likely not contributing to nitrogen fixation. We probed for Vnf and Anf expression in DJL74 grown in the absence of Mo, revealing Vnf and Anf are not detected. This suggests a role for Mo-nitrogenase proteins in controlling alternative nitrogenase expression and/or maturation. While the *nif* gene cluster (*nifHI$_1$I$_2$DKEN*) does not encode any gene clearly required for alternative nitrogenase expression or activity, one suspect is a biosynthetic role of NifH. NifH, in addition to providing electrons to NifDK during N_2 reduction, serves multiple roles in nitrogenase maturation in bacteria, including synthesis of the complex metalloclusters within NifDK (e.g., P-cluster).[3,12,61] Therefore, NifH could be required for metallocluster synthesis in VnfDGK and AnfDGK. Another possibility is that cluster-deficient NifDK is a signal for *vnf* and *anf* expression. This result is opposite that of the purple bacteria, in which mutationally inactive Mo-nitrogenase is tied to activation of *vnf* and/or *anf* when they would be repressed by Mo. In *M. acetivorans*, *vnf* and *anf* are repressed when they would ordinarily be produced. A role for NifEN in V-and Fe-nitrogenase maturation is less likely, as

the V-nitrogenase operon encodes its own putative scaffold (*vnfEN*) and Fe-nitrogenase maturation likely does not require a scaffold.[62] Further experimentation is required to determine how *nif* operon proteins are involved in alternative nitrogenase regulation in *M. acetivorans*.

We also sought to understand why the V-nitrogenase is expressed even in the absence of V, and why the Fe-nitrogenase is produced in the presence of V. DJL107 grows like the control in both V+Fe and Fe-only conditions, indicating wild-type growth yields can be supported by the Fe-nitrogenase. DJL120 has no growth phenotype in the presence of V, likely due to V-nitrogenase activity, but this strain also has a growth deficiency in Fe-only conditions, suggesting that Fe-nitrogenase is the dominant nitrogenase during limitation of both Mo and V. V-nitrogenase production in Fe-only conditions may be a vestige of Mo-dependent regulation of transcriptionally divergent *vnf* and *anf* gene clusters.

Overall, the results from this study highlight the utility of *M. acetivorans* as a model to understand the regulation, maturation, and activity of the three forms of nitrogenase in methanogens. Further experimentation is necessary to understand the role of Mo-nitrogenase in alternative nitrogenase maturation as well as how *M. acetivorans* manages the simultaneous production of three nitrogenases.

References

1. Fowler, D. et al. (2013) The global nitrogen cycle in the twenty-first century, *Philos Trans R Soc Lond B Biol Sci.* **368**, 20130164.

2. Stein, L. Y. & Klotz, M. G. (2016) The nitrogen cycle, *Current biology : CB.* **26**, R94-8.

3. Rubio, L. M. & Ludden, P. W. (2008) Biosynthesis of the iron-molybdenum cofactor of nitrogenase, *Annu Rev Microbiol.* **62**, 93-111.

4. Dixon, R. & Kahn, D. (2004) Genetic regulation of biological nitrogen fixation, *Nat Rev Microbiol.* **2**, 621-31.

5. Dos Santos, P. C., Fang, Z., Mason, S. W., Setubal, J. C. & Dixon, R. (2012) Distribution of nitrogen fixation and nitrogenase-like sequences amongst microbial genomes, *BMC Genomics.* **13**, 162.

6. Burris, R. H. (1991) Nitrogenases, *J Biol Chem.* **266**, 9339-42.

7. Peters, J. W., Fisher, K. & Dean, D. R. (1995) Nitrogenase structure and function: a biochemical-genetic perspective, *Annu Rev Microbiol.* **49**, 335-66.

8. Dingler, C. et al. (1988) Levels and activities of nitrogenase proteins in *Azotobacter vinelandii* grown at different dissolved oxygen concentrations, *J Bacteriol.* **170**, 2148-52.

9. Eady, R. R. (1996) Structure-Function Relationships of Alternative Nitrogenases, *Chem Rev.* **96**, 3013-3030.

10. Harwood, C. S. (2020) Iron-Only and Vanadium Nitrogenases: Fail-Safe Enzymes or Something More?, *Annu Rev Microbiol.* **74**, 247-266.

11. Hu, Y. & Ribbe, M. W. (2015) Nitrogenase and homologs, *J Biol Inorg Chem.* **20**, 435-45.

12. Hu, Y. & Ribbe, M. W. (2016) Biosynthesis of the Metalloclusters of Nitrogenases, *Annu Rev Biochem.* **85**, 455-83.

13. Waugh, S. I. et al. (1995) The genes encoding the delta subunits of dinitrogenases 2 and 3 are required for Mo-independent diazotrophic growth by *Azotobacter vinelandii*, *J Bacteriol.* **177**, 1505-10.

14. Harris, D. F. et al. (2019) Mo-, V-, and Fe-Nitrogenases Use a Universal Eight-Electron Reductive-Elimination Mechanism To Achieve N_2 Reduction, *Biochemistry.* **58**, 3293-3301.

15. Eady, R. R. et al. (1987) The vanadium nitrogenase of *Azotobacter chroococcum.* Purification and properties of the VFe protein, *Biochem J.* **244**, 197-207.

16. Hamilton, T. L. et al. (2011) Transcriptional profiling of nitrogen fixation in *Azotobacter vinelandii*, *J Bacteriol.* **193**, 4477-86.

17. McKinlay, J. B. & Harwood, C. S. (2010) Photobiological production of hydrogen gas as a biofuel, *Curr Opin Biotechnol.* **21**, 244-51.

18. McKinlay, J. B. & Harwood, C. S. (2011) Calvin cycle flux, pathway constraints, and substrate oxidation state together determine the H_2 biofuel yield in photoheterotrophic bacteria, *mBio.* **2**.

19. Postgate, J. R. (1982) Biological Nitrogen-Fixation - Fundamentals, *Philos T Roy Soc B.* **296**, 375-385.

20. Dilworth, M. J., Eady, R. R. & Eldridge, M. E. (1988) The vanadium nitrogenase of *Azotobacter chroococcum*. Reduction of acetylene and ethylene to ethane, *Biochem J.* **249**, 745-51.

21. Hu, Y., Lee, C. C. & Ribbe, M. W. (2011) Extending the carbon chain: hydrocarbon formation catalyzed by vanadium/molybdenum nitrogenases, *Science.* **333**, 753-5.

22. Seefeldt, L. C. et al. (2013) Nitrogenase reduction of carbon-containing compounds, *Biochimica et biophysica acta.* **1827**, 1102-11.

23. Zheng, Y. et al. (2018) A pathway for biological methane production using bacterial iron-only nitrogenase, *Nature microbiology.* **3**, 281-286.

24. Mus, F. et al. (2018) Exploring the alternatives of biological nitrogen fixation, *Metallomics : integrated biometal science.* **10**, 523-538.

25. Mus, F. et al. (2019) Geobiological feedbacks, oxygen, and the evolution of nitrogenase, *Free radical biology & medicine.* **140**, 250-259.

26. Kessler, P. S. & Leigh, J. A. (1999) Genetics of nitrogen regulation in *Methanococcus maripaludis*, *Genetics.* **152**, 1343-51.

27. Kessler, P. S., McLarnan, J. & Leigh, J. A. (1997) Nitrogenase phylogeny and the molybdenum dependence of nitrogen fixation in *Methanococcus maripaludis, J Bacteriol.* **179**, 541-3.

28. Thauer, R. K. et al. (2008) Methanogenic archaea: ecologically relevant differences in energy conservation, *Nat Rev Microbiol.* **6**, 579-91.

29. Hendrickson, E. L. et al. (2004) Complete genome sequence of the genetically tractable hydrogenotrophic methanogen *Methanococcus maripaludis*, *J Bacteriol.* **186**, 6956-69.

30. Ehlers, C., Veit, K., Gottschalk, G. & Schmitz, R. A. (2002) Functional organization of a single nif cluster in the mesophilic archaeon *Methanosarcina mazei* strain Gö1, *Archaea.* **1**, 143-50.

31. Chien, Y. T. et al. (2000) Analysis of genes encoding an alternative nitrogenase in the archaeon *Methanosarcina barkeri* 227, *J Bacteriol.* **182**, 3247-53.

32. Lobo, A. L. & Zinder, S. H. (1988) Diazotrophy and Nitrogenase Activity in the Archaebacterium *Methanosarcina barkeri* 227, *Appl Environ Microbiol.* **54**, 1656-61.

33. Lobo, A. L. & Zinder, S. H. (1990) Nitrogenase in the archaebacterium *Methanosarcina barkeri* 227, *J Bacteriol.* **172**, 6789-96.

34. Leigh, J. A. (2000) Nitrogen fixation in methanogens: the archaeal perspective, *Current issues in molecular biology.* **2**, 125-31.

35. Leigh, J. A. & Dodsworth, J. A. (2007) Nitrogen regulation in bacteria and archaea, *Annu Rev Microbiol.* **61**, 349-77.

36. Prasse, D. et al. (2017) $sRNA_{154}$ a newly identified regulator of nitrogen fixation in *Methanosarcina mazei* strain Gö1, *RNA biology.* **14**, 1544-1558.

37. Buddeweg, A. et al. (2018) $sRNA_{41}$ affects ribosome binding sites within polycistronic mRNAs in *Methanosarcina mazei* Gö1, *Mol Microbiol.* **107**, 595-609.

38. Galagan, J. E. et al. (2002) The genome of *Methanosarcina acetivorans* reveals extensive metabolic and physiological diversity, *Genome Res.* **12**, 532-42.

39. Nayak, D. D. & Metcalf, W. W. (2017) Cas9-mediated genome editing in the methanogenic archaeon *Methanosarcina acetivorans*, *Proc Natl Acad Sci U S A.* **114**, 2976-2981.

40. Guss, A. M. et al. (2008) New methods for tightly regulated gene expression and highly efficient chromosomal integration of cloned genes for *Methanosarcina* species, *Archaea.* **2**, 193-203.

41. Dhamad, A. E. & Lessner, D. J. (2020) A CRISPRi-dCas9 System for Archaea and Its Use To Examine Gene Function during Nitrogen Fixation by *Methanosarcina acetivorans*, *Appl Environ Microbiol.* **86**.

42. Sowers, K. R., Boone, J. E. & Gunsalus, R. P. (1993) Disaggregation of *Methanosarcina* spp. and growth as single cells at elevated osmolarity, *Appl Environ Microbiol.* **59**, 3832-9.

43. Metcalf, W. W. et al. (1997) A genetic system for Archaea of the genus *Methanosarcina*: liposome-mediated transformation and construction of shuttle vectors, *Proc Natl Acad Sci USA.* **94**, 2626-31.

44. Kessler, P. S., Blank, C. & Leigh, J. A. (1998) The *nif* gene operon of the methanogenic archaeon *Methanococcus maripaludis*, *J Bacteriol.* **180**, 1504-11.

45. Chien, Y. T. & Zinder, S. H. (1996) Cloning, functional organization, transcript studies, and phylogenetic analysis of the complete nitrogenase structural genes (*nifHDK2*) and associated genes in the archaeon *Methanosarcina barkeri* 227, *J Bacteriol.* **178**, 143-8.

46. Kessler, P. S., Daniel, C. & Leigh, J. A. (2001) Ammonia switch-off of nitrogen fixation in the methanogenic archaeon *Methanococcus maripaludis*: mechanistic features and requirement for the novel GlnB homologues, NifI(1) and NifI(2), *J Bacteriol.* **183**, 882-9.

47. Sicking, C. et al. (2005) Identification of two new genes involved in diazotrophic growth via the alternative Fe-only nitrogenase in the phototrophic purple bacterium *Rhodobacter capsulatus*, *J Bacteriol.* **187**, 92-8.

48. Varghese, F. et al. (2019) A low-potential terminal oxidase associated with the iron-only nitrogenase from the nitrogen-fixing bacterium *Azotobacter vinelandii*, *J Biol Chem.* **294**, 9367-9376.

49. Perez-Gonzalez, A. et al. (2022) AnfO controls fidelity of nitrogenase FeFe protein maturation by preventing misincorporation of FeV-cofactor, *Mol Microbiol.* **117**, 1080-1088.

50. Ferry, J. G. (1999) Enzymology of one-carbon metabolism in methanogenic pathways, *FEMS microbiology reviews.* **23**, 13-38.

51. Lie, T. J. & Leigh, J. A. (2002) Regulatory response of *Methanococcus maripaludis* to alanine, an intermediate nitrogen source, *J Bacteriol.* **184**, 5301-6.

52. Oda, Y. et al. (2005) Functional genomic analysis of three nitrogenase isozymes in the photosynthetic bacterium *Rhodopseudomonas palustris*, *J Bacteriol.* **187**, 7784-94.

53. Lie, T. J. et al. (2007) Diverse homologues of the archaeal repressor NrpR function similarly in nitrogen regulation, *FEMS Microbiol Lett.* **271**, 281-8.

54. Weidenbach, K., Ehlers, C. & Schmitz, R. A. (2014) The transcriptional activator NrpA is crucial for inducing nitrogen fixation in *Methanosarcina mazei* Gö1 under nitrogen-limited conditions, *FEBS J.* **281**, 3507-22.

55. Demtroder, L., Narberhaus, F. & Masepohl, B. (2019) Coordinated regulation of nitrogen fixation and molybdate transport by molybdenum, *Mol Microbiol.* **111**, 17-30.

56. Studholme, D. J. & Pau, R. N. (2003) A DNA element recognised by the molybdenum-responsive transcription factor ModE is conserved in Proteobacteria, green sulphur bacteria and Archaea, *BMC Microbiol.* **3**, 24.

57. Ferry, J. G. (2010) How to make a living by exhaling methane, *Annu Rev Microbiol.* **64**, 453-73.

58. Li, J. G. et al. (1990) Analysis of *Azotobacter vinelandii* strains containing defined deletions in the *nifD* and *nifK* genes, *J Bacteriol.* **172**, 5884-91.

59. Gollan, U. et al. (1993) Detection of the in vivo incorporation of a metal cluster into a protein. The FeMo cofactor is inserted into the FeFe protein of the alternative nitrogenase of *Rhodobacter capsulatus*, *Eur J Biochem.* **215**, 25-35.

60. Rebelein, J. G. et al. (2018) Characterization of an M-Cluster-Substituted Nitrogenase VFe Protein, *mBio.* **9**.

61. Rangaraj, P., Shah, V. K. & Ludden, P. W. (1997) ApoNifH functions in iron-molybdenum cofactor synthesis and apodinitrogenase maturation, *Proc Natl Acad Sci U S A.* **94**, 11250-5.

62. Perez-Gonzalez, A. et al. (2021) Specificity of NifEN and VnfEN for the Assembly of Nitrogenase Active Site Cofactors in *Azotobacter vinelandii*, *mBio.* **12**, e0156821.

Figures and Tables

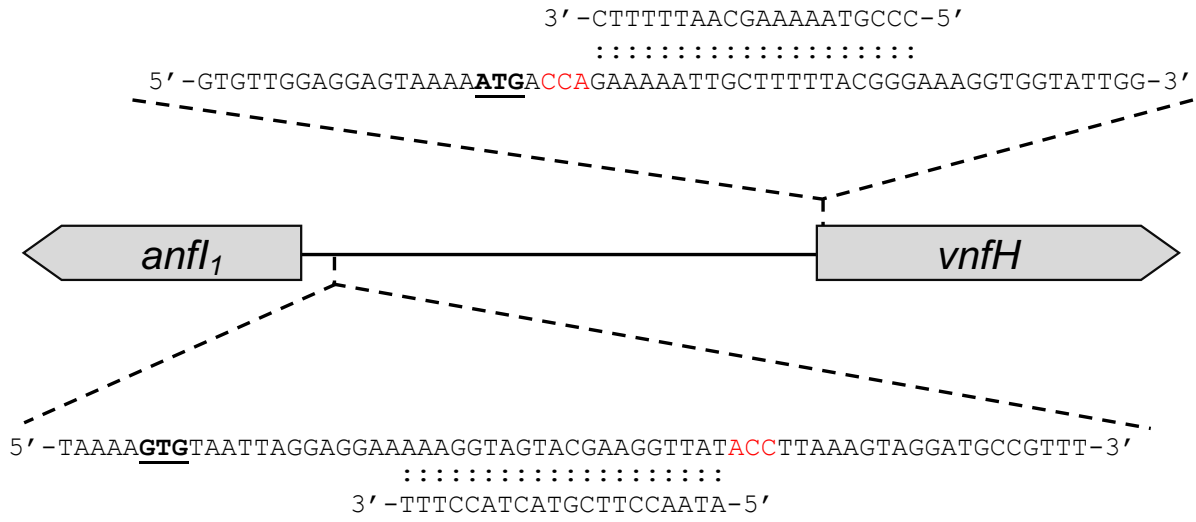

Figure 1. The location of gRNA binding to target dCas9 to *vnf* and *anf* gene clusters. The PAM sequence is in red and the start codon is bolded and underlined.

Table 1. *M. acetivorans* strains used in this study.

Strain	Description	gRNA	Reference
WWM73	Wild type strain used for genetic analysis	-	
DJL72	WWM73 with integrated CRISPRi plasmid	None	
DJL74	WWM73 with integrated CRISPRi plasmid	gRNA-*nifH*	
DJL107	WWM73 with integrated CRISPRi plasmid	gRNA-*vnfH*	This study
DJL120	WWM73 with integrated CRISPRi plasmid	gRNA-$anfI_1$	This study
DJL119	WWM73 with integrated CRISPRi plasmid	gRNA-*vnfH* + gRNA-$anfI_1$	This study

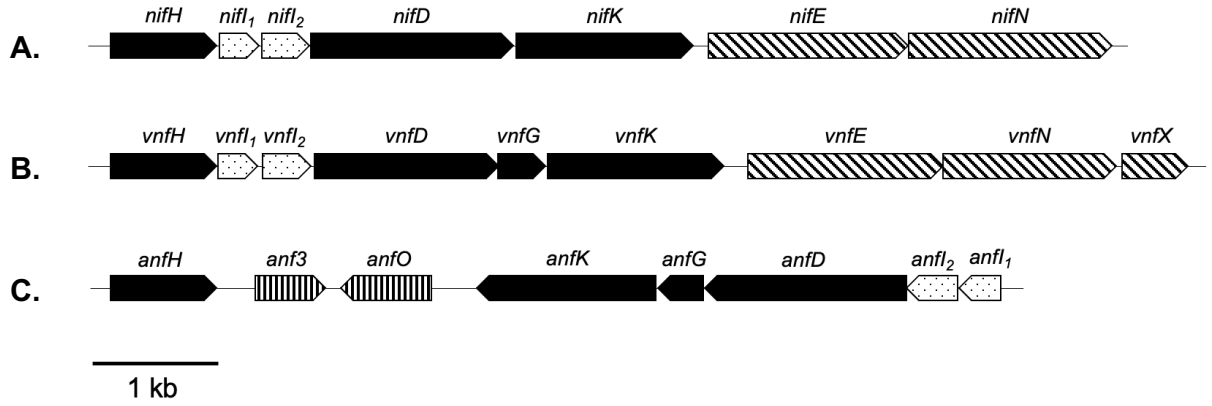

Figure 2. Arrangement of nitrogenase gene clusters in the genome of *M. acetivorans*. A) *nif*; Mo-nitrogenase, B) *vnf*; V-nitrogenase, C) *anf*; Fe-nitrogenase. Black arrows: nitrogenase subunits, diagonal striped arrows: cofactor assembly proteins, dotted arrows: regulatory proteins and vertical striped arrows: unknown function.

Table 2. Nitrogenase distribution among genome-sequenced Methanosarcinales.

Species	Mo-nitrogenase (*nif*)	V-nitrogenase (*vnf*)	Fe-nitrogenase (*anf*)
Methanococcoides burtonii DSM 6242			
Methanococcoides methylutens MM1			
Methanohalobium evestigatum Z-7303			
Methanohalophilus halophilus			
Methanohalophilus mahii DSM 5219			
Methanolobus psychrophilus R15	•		
Methanolobus zinderi	•		
Methanomethylovorans hollandica DSM 15978			
Methanosaeta harundinacea 6Ac			
Methanosalsum zhilinae DSM 4017			
Methanosarcina acetivorans C2A	•	•	•
Methanosarcina barkeri 227	•	•	
Methanosarcina barkeri 3	•	•	•
Methanosarcina barkeri CM1	•	•	
Methanosarcina barkeri MS	•	•	
Methanosarcina barkeri str. Fusaro	•	•	—[a]
Methanosarcina barkeri str. Wiesmoor	•	•	—[a]
Methanosarcina flavescens			
Methanosarcina horonobensis HB-1	•		
Methanosarcina lacustris Z-7289			
Methanosarcina mazei zm-15	•		
Methanosarcina mazei C16	•		
Methanosarcina mazei Gö1	•		
Methanosarcina mazei LYC	•		
Methanosarcina mazei S-6	•		
Methanosarcina mazei SarPi	•		
Methanosarcina mazei Tuc01	•		
Methanosarcina mazei WWM610	•		
Methanosarcina siciliae C2J	•	•	•
Methanosarcina siciliae HI350	•	•	
Methanosarcina siciliae T4/M	•	•	•
Methanosarcina sp. Kolksee	•	•	
Methanosarcina sp. MTP4			
Methanosarcina sp. WH1	•		
Methanosarcina sp. WWM596	•		
Methanosarcina thermophila MT-1	—[b]		
Methanosarcina thermophila CHTI-55			
Methanosarcina thermophila TM-1			
Methanosarcina vacuolata Z-761	•	•	
Methanothrix soehngenii GP6	•		
Methanothrix thermoacetophila PT			

[a]AnfH is truncated and likely non-functional.

[b]*nif*-like genes present but not in an operon.

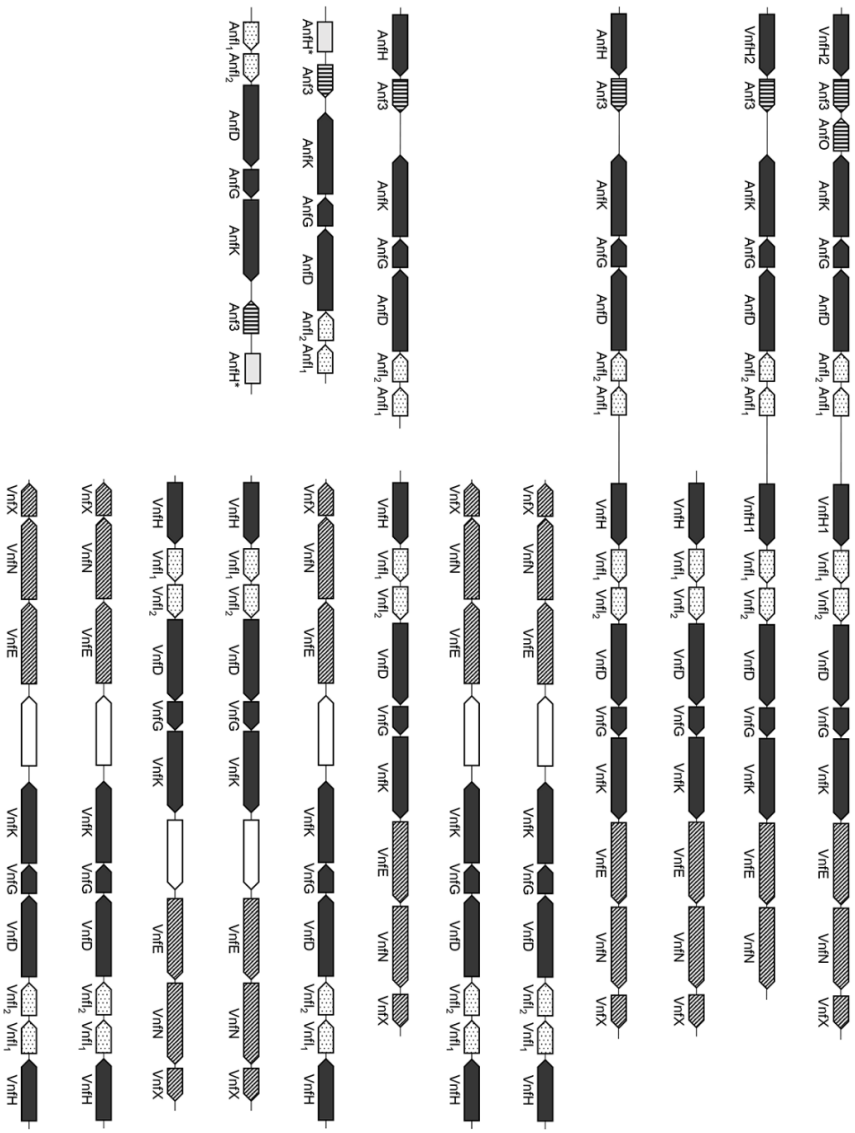

Figure 3. Arrangement of the *vnf* and *anf* gene clusters in Methanosarcinales species that contain both alternative nitrogenases.

Table 3. Effect of metal and NH_4Cl availability on growth of *M. acetivorans* strain WWM73 with methanol.

Relevant Metals	Nitrogen Source	Lag time[a] (hours)	Generation Time[b] (hours)	Cell Yield[b] (cells/mL)
Mo + Fe	NH_4Cl	30	8.2 ± 0.5	3.02×10^8
	N_2	48	28.5 ± 4	1.92×10^8
V + Fe	NH_4Cl	30	8.5 ± 0.1	3.08×10^8
	N_2	90	44.5 ± 4.1	1.53×10^8
Fe only	NH_4Cl	30	8.7 ± 0.1	3.34×10^8
	N_2	96	82 ± 4.1	9.88×10^7

[a]Approximate time until the first observed increase in OD_{600}.
[b]Generation time and cell yield represent the mean ± 1 SD from at least three biological replicates.

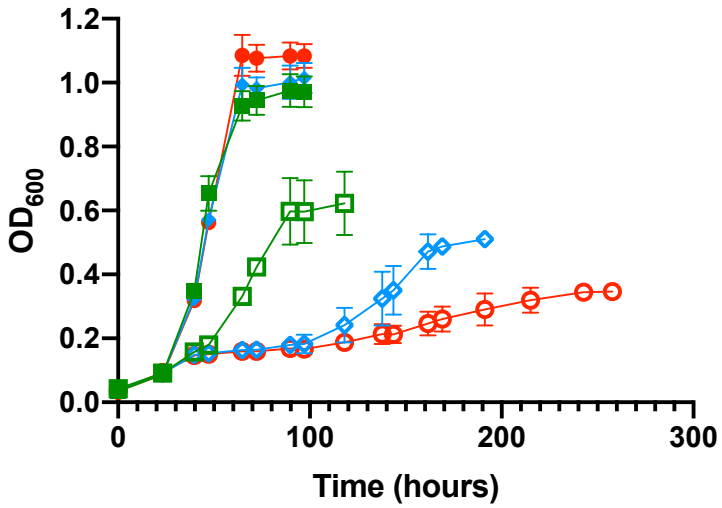

Figure 4. Comparison of the growth of *M. acetivorans* in the presence (closed) or absence (open) of NH_4Cl in HS medium with Mo + Fe (green squares), V + Fe (blue diamonds), or Fe alone (red circles). Error bars represent mean ± 1 SD from at least three biological replicates.

Table 4. Effect of metal and NH_4Cl availability on total CH_4 production by *M. acetivorans* strain WWM73 with methanol.

Relevant Metals	Nitrogen Source	CH_4 Produced (μmol)
Mo + Fe	NH_4Cl	1004 ± 109
	N_2	1092 ± 58
V + Fe	NH_4Cl	926 ± 193
	N_2	823 ± 24
Fe only	NH_4Cl	1031 ± 48
	N_2	1079 ± 41

Data represent the mean ± 1 SD from at least three biological replicates.

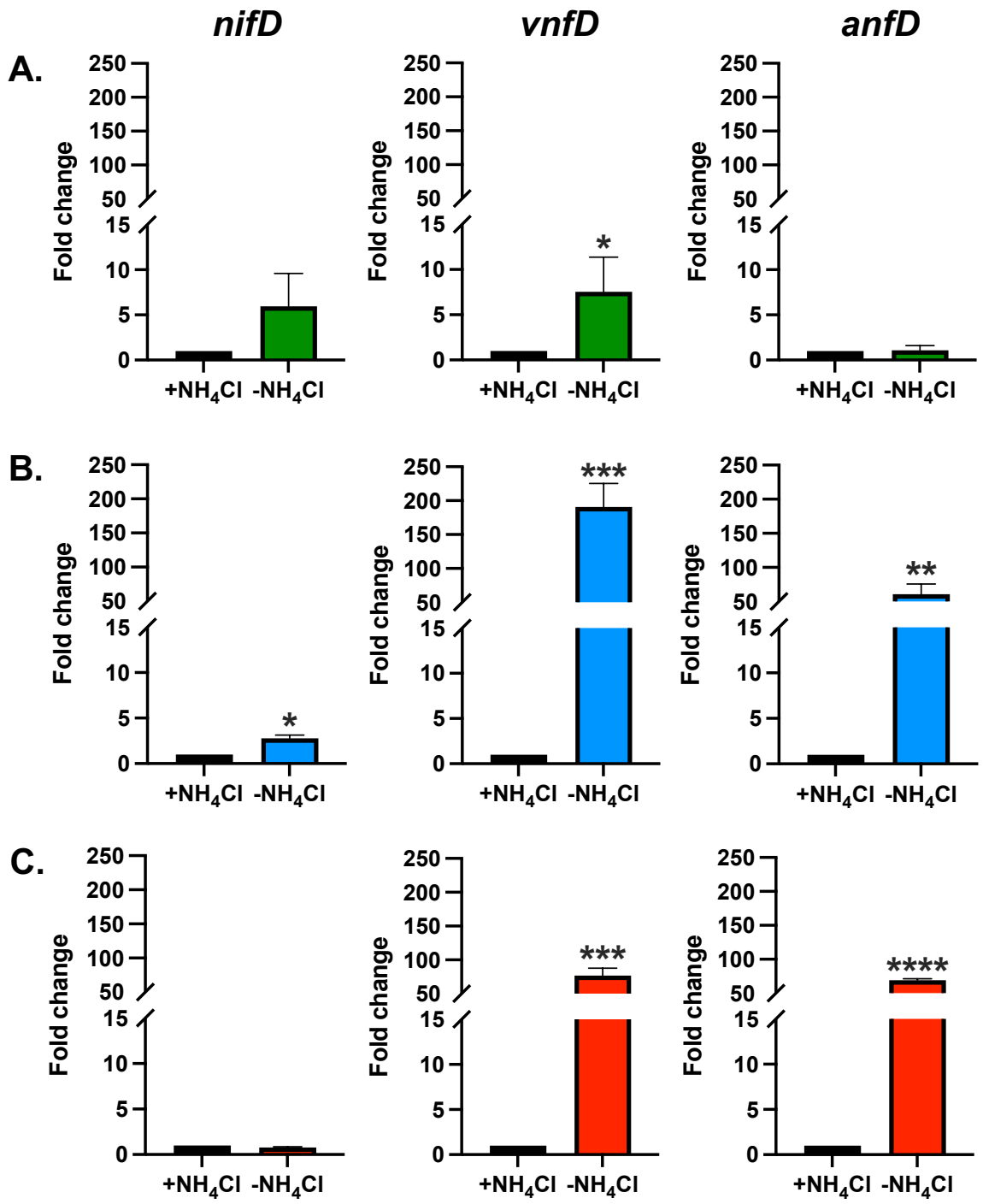

Figure 5. Effect of fixed N availability on the transcription of the *nif*, *vnf* and *anf* gene clusters in *M. acetivorans* as determined by qPCR. The relative abundance of *nifD*, *vnfD*, and *anfD* transcripts in *M. acetivorans* cells grown with NH_4Cl (normalized to one) were compared to cells grown without NH_4Cl. *M. acetivorans* was grown with methanol in HS medium containing A) Mo + Fe B) V + Fe or C) Fe only. Error bars represent mean ± 1 SD for two technical replicates and three biological replicates. *, $P < 0.05$; **, $P < 0.01$; ***, $P < 0.001$; ****, $P < 0.0001$.

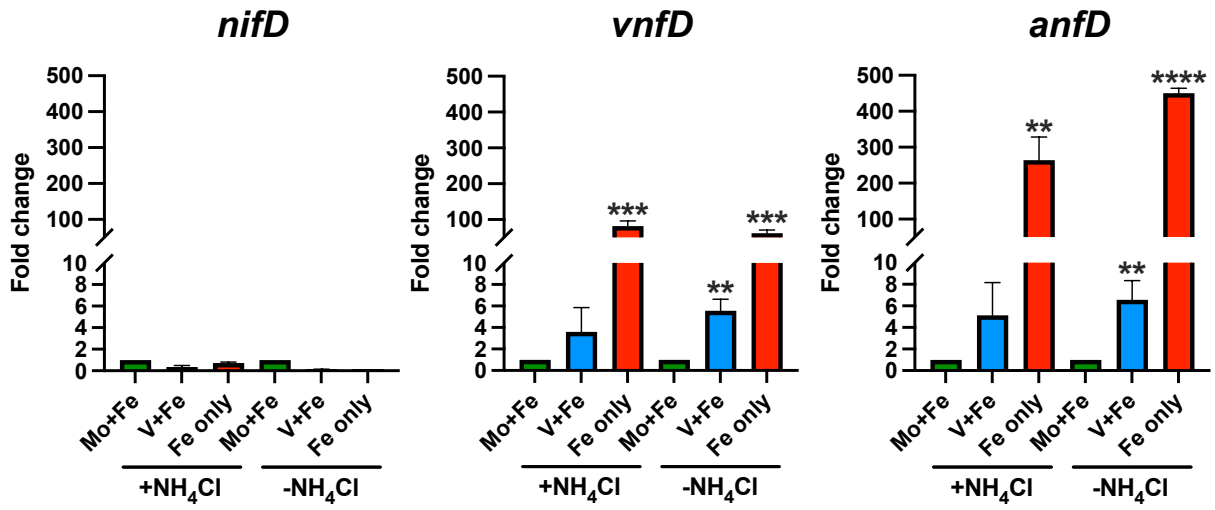

Figure 6. Effect of molybdenum availability on the transcription of the *nif*, *vnf* and *anf* gene clusters in *M. acetivorans* as determined by qPCR. The relative abundance of A) *nifD*, B) *vnfD*, and C) *anfD* transcripts in cells grown with molybdenum (normalized to one) were compared to cells grown without molybdenum. Error bars represent mean ± 1 SD for two technical replicates and three biological replicates. *, $P < 0.05$; **, $P < 0.01$; ***, $P < 0.001$; ****, $P < 0.0001$.

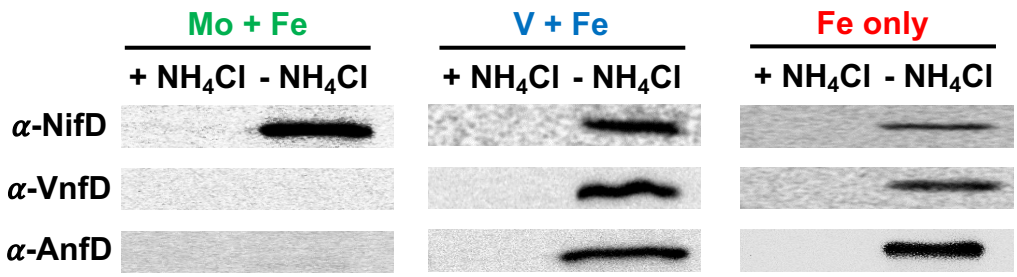

Figure 7. Western blot analysis using NifD-, VnfD-, and AnfD-specific antibodies on lysate from *M. acetivorans* cells grown with or without NH_4Cl and the indicated metals. SDS-PAGE of the same lysates for loading control is shown in Fig. S1.

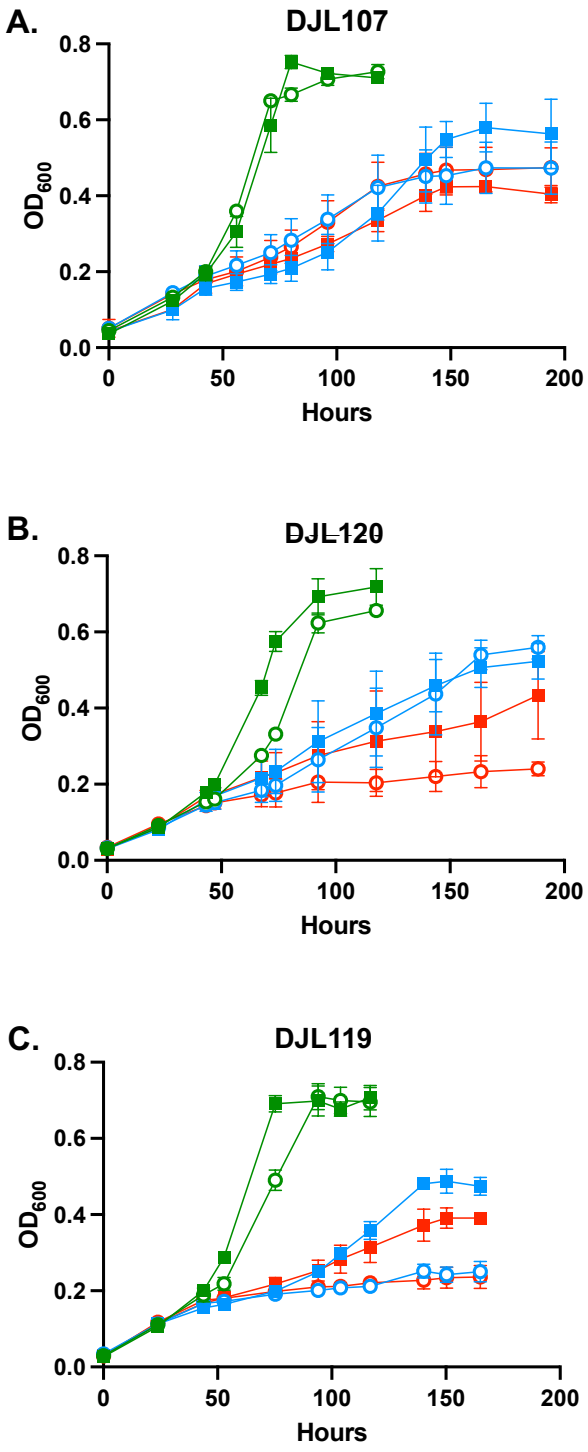

Figure 8. Comparison of the growth of *M. acetivorans* CRISPRi repression strains DJL107 (A), DJL120 (B) and DJL119 (C) to control strain DJL72 (gRNA-free) in medium lacking NH_4Cl. Growth of DJL72 (squares) and each CRISPRi repression strain (circles) is shown in HS medium with Mo + Fe (green), V + Fe (blue), or Fe alone (red). Error bars represent mean ± 1 SD from at least three biological replicates.

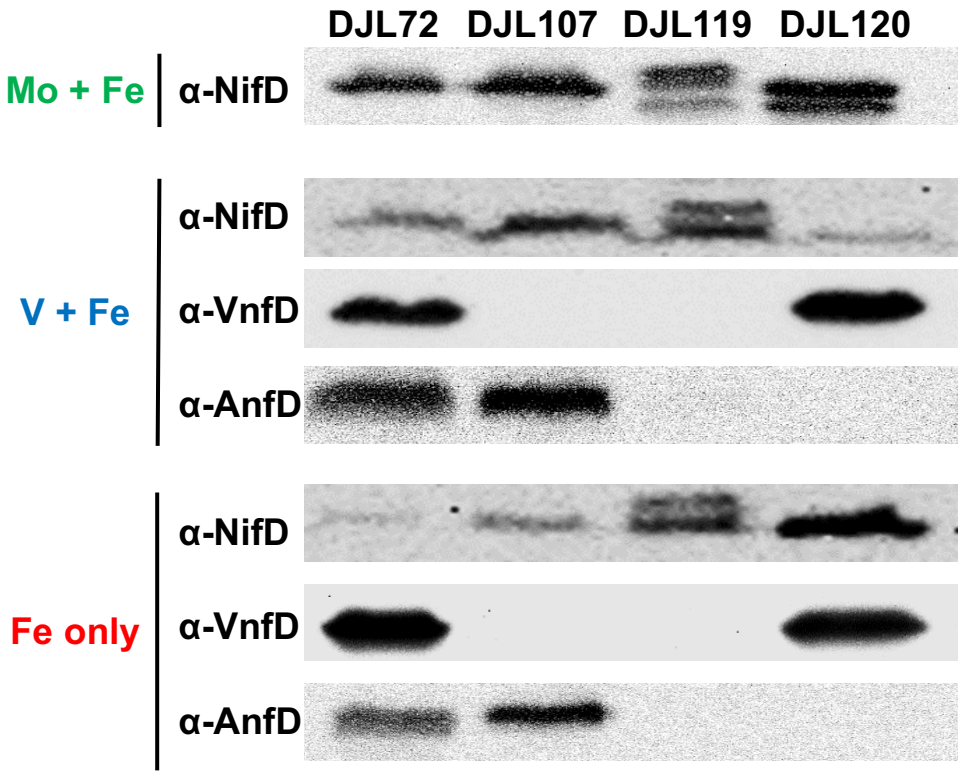

Figure 9. Western blot analysis using NifD-, VnfD-, and AnfD-specific antibodies on lysate from cells of the indicated *M. acetivorans* strains grown without NH_4Cl and the indicated metals. SDS-PAGE of the same lysates for loading control is shown in Fig. S2.

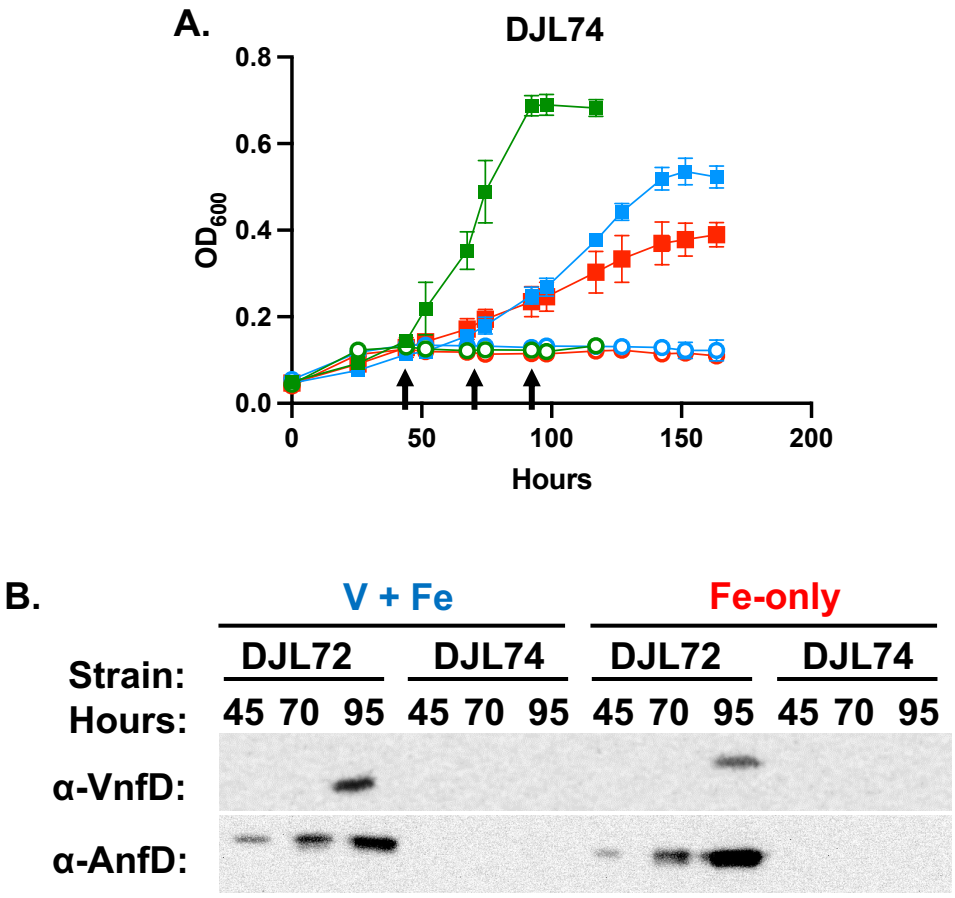

Figure 10. A) Comparison of the growth of *M. acetivorans* CRISPRi repression strain DJL74 to control strain DJL72 (gRNA-free) in medium lacking NH_4Cl. Growth of DJL74 (squares) and DJL72 (circles) is shown in HS medium with Mo + Fe (green), V + Fe (blue), or Fe alone (red). B) Western blot detection of VnfD and AnfD in lysates from cells of strains DJL72 and DJL74 grown with V + Fe and and Fe-only harvested at the times indicated by arrows in panel A. SDS-PAGE of the same lysates for loading control is shown in Fig. S3.

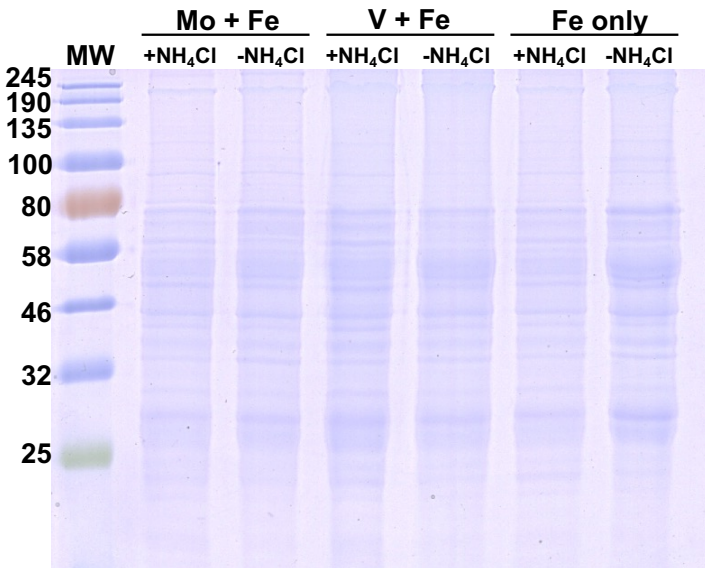

Supplemental Figure 1. SDS-PAGE of cell lysates used for western blot in Fig. 7. MW, molecular weight standard.

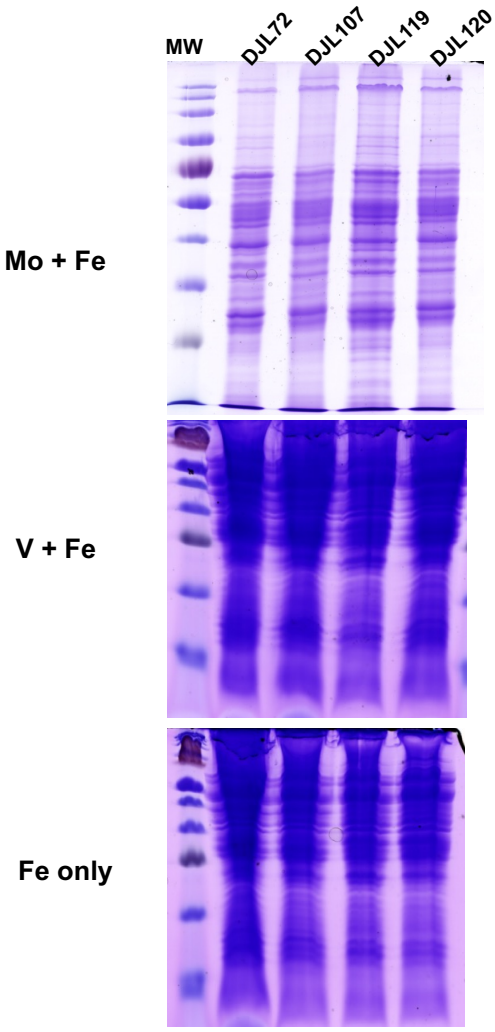

Supplemental Figure 2. SDS-PAGE of cell lysates used for western blot in Fig. 9. MW, molecular weight standard.

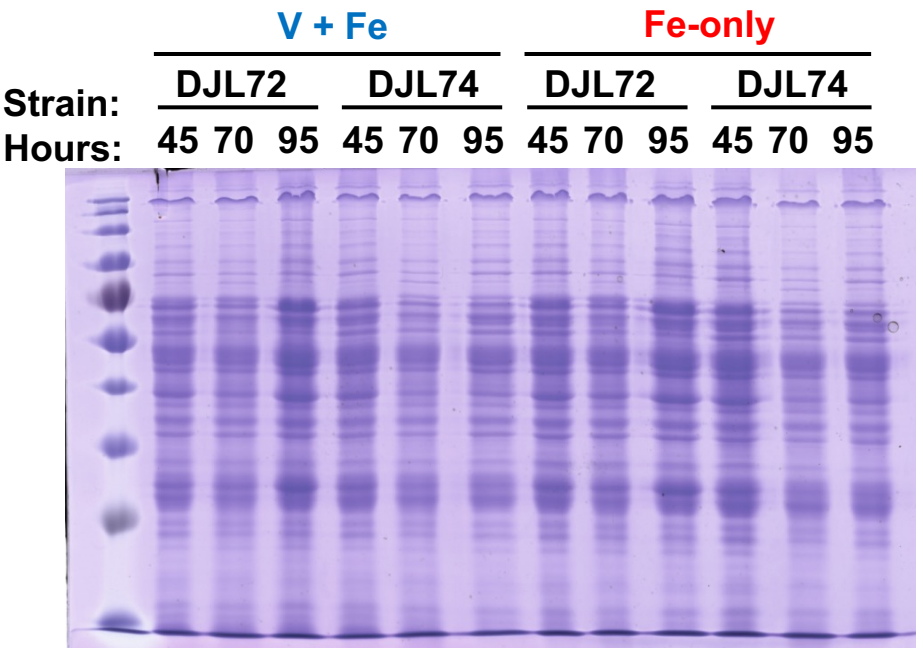

Supplemental Figure 3. SDS-PAGE of cell lysates used for western blot in Fig. 10B. MW, molecular weight standard.

Chapter II

Alternative nitrogenase expression in *Methanosarcina acetivorans* is directly controlled by the repressor ModE

Melissa Chanderban

Cell and Molecular Biology Program, University of Arkansas,

Fayetteville AR, 72701, USA

Introduction

Biological nitrogen fixation is accomplished by three nitrogenase isozymes. The three nitrogenases are named for their catalytic cofactors, each differentiated by containing molybdenum (Mo), vanadium (V), or iron (Fe) within the catalytic cofactor. The Mo-, V-, and Fe-nitrogenases—encoded by *nif*, *vnf*, and *anf* gene clusters, respectively—have different catalytic properties; while all three reduce inert nitrogen gas (N_2) into biologically available ammonia (NH_3), each nitrogenase requires different amounts of energy for this reaction. The Mo-nitrogenase uses at least 16 ATP per dinitrogen fixed, and the alternative V- and Fe-nitrogenases require a minimum of 24 and 40 ATP respectively. Because the alternative nitrogenases represent an even greater energetic burden, diazotrophs preferentially express the Mo-nitrogenase and produce the others when the Mo-nitrogenase cannot function, such as when Mo is limited.[1]

One regulatory mechanism is transcriptional repression of the alternative nitrogenases at Mo concentrations that support Mo-nitrogenase activity, such as through Mo-binding transcription regulators, including ModE. ModE as characterized in non-diazotrophic *Escherichia coli* has an N-terminal winged-helix-turn-helix DNA-binding domain (HTH_9) and two C-terminal molybdate-binding Mop (or TOBE) domains. ModE can function as an activator or repressor, with its affinity for binding DNA typically increased in the presence of molybdate.[2] In proteobacteria, ModE indirectly controls alternative nitrogenase expression by regulating nitrogenase activators VnfA and AnfA.[3,4] *Azotobacter vinelandii*, which produces all three nitrogenases, encodes two copies of ModE. Both copies repress *vnfA* and *anfA* expression in the presence of Mo, preventing VnfA and AnfA from activating *vnf* and *anf* gene clusters. *Rhodobacter capsulatus*, which has Mo and Fe-nitrogenases, encodes two ModE homologs

MopA and MopB, either of which can repress *anfA* and control Fe-nitrogenase expression.[3] The cyanobacterium *Anabaena variabilis* uses Mo-dependent repressors VnfR1 and VnfR2 to directly repress expression of V-nitrogenase structural genes.[5] While ModE and MopAB have conserved domains, VnfR proteins have different DNA-binding and molybdate-binding domains (HTH_3 and periplasmic binding protein domain PBP-2, respectively).[2]

Transcriptional regulators of alternative nitrogenase expression in methanogens have not been identified. We have previously shown that production of the alternative nitrogenases in *Methanosarcina acetivorans* is dependent upon low concentrations of Mo and fixed nitrogen. In the presence of Mo, only the Mo-nitrogenase is made. In the absence of Mo, all three nitrogenases are produced whether V is present or not. Transcription of the *vnf* and *anf* operons is upregulated in the absence of Mo, indicating Mo-responsive transcriptional repression. *M. acetivorans* does not encode homologs of VnfA or AnfA but does encode ModE. Potential ModE binding sites have been identified computationally in the intergenic region between the *vnf* and *anf* gene clusters.[2] Thus, ModE likely functions as the Mo-dependent repressor of the *vnf* and *anf* operons encoding the alternative nitrogenases. This hypothesis was tested using genetic and biochemical methods. The recently developed *M. acetivorans* CRISPR interference (CRISPRi) system was used to generate a strain with expression of *modE* knocked down. Results from analyses of this mutant strain combined with *in vitro* studies with recombinant ModE reveal that ModE functions to directly repress transcription of the *vnf* and *anf* operons in *M. acetivorans*.

Materials and Methods

Growth

Methanosarcina acetivorans cultures were maintained in standard high-salt medium supplemented with 125 mM methanol, 0.025% Na_2S (w/v), and 2 μg/mL puromycin as needed. Growth experiments were conducted in molybdenum-deplete, DTT-reduced high-salt medium lacking cysteine as described in chapter 1. Other additives for the growth experiments included 18.7 mM NH_4Cl, 1 μM Na_2MoO_4, and 1 μM Na_3VO_4 as indicated. Mo-deplete inocula contained 18.7 mM NH_4Cl and 3 mM L-cysteine.

Construction of knockdown strain

A gRNA targeting dCas9 to the coding sequence of *modE* (MA0283; MA_RS01505) was designed using the CRISPR site finder tool in Geneious Prime (Fig. 1). A synthetic gBlock (IDT) containing this gRNA was used in Gibson assembly (Synthetic Genomics) with dCas9 vector pDL734 linearized with *Asc*I.[6] The assembly mix was used to transform *Escherichia coli* strain WM4489 with 34 μg/mL chloramphenicol, and the gBlock insertion was verified with PCR screening and sequencing.[7] *M. acetivorans* strain WWM73 was transformed with this plasmid using liposome-mediated methods and selection with 2 μg/mL puromycin, yielding strain DJL89 (gRNA-*modE*).[8] Plasmid integration was verified with PCR. *modE* repression was confirmed using qPCR. *M. acetivorans* strain DJL72, expressing dCas9 with no gRNA, was used as a control for all experiments with strain DJL89. See Table 1 for a list of primers used and Table 2 for a list of strains used in this study.

Quantitative PCR analysis of gene expression

M. acetivorans cultures were harvested at mid-log phase (OD_{600} ~0.4) and used for RNA extraction and qPCR as described previously in chapter 1. Relative expression was calculated using the 2^{-ddCt} method.

Western blot analysis of protein expression

M. acetivorans cultures were harvested aerobically at mid-log phase. Whole cell lysate was used for western blotting as described previously in chapter 1 with custom antibodies (GenScript) specific for the catalytic subunit of each nitrogenase.

Purification of recombinant ModE from E. coli

The gene encoding ModE was amplified from *M. acetivorans* C2A genomic DNA using Q5 polymerase and primers to add restriction sites NcoI and BamHI as well as a C-terminal strep tag. Because the NcoI site (CCATGG) contains a start codon, this replaced the GTG start codon of ModE. Additional bases were added to keep *modE* in frame, resulting in an extra alanine after the start codon. The PCR product was cloned into pET28a following digestion for 16 hours at 37°C and ligation using T4 DNA ligase for 16 hours at 16°C. The plasmid was used to transform *E. coli* DH5alpha for maintenance using 100 μg/mL kanamycin for selection. Colony PCR and sequencing confirmed *modE* insertion.

The plasmid was used to transform *E. coli* Rosetta DE3 for protein expression. The strain was grown in LB medium with 50 μg/mL kanamycin and 17 μg/mL chloramphenicol. Overexpression was induced with 400 mM IPTG at an OD_{600} of 0.5-0.7. After 4 hours, cells were harvested and the pellet was frozen. The cell pellet was thawed and resuspended in buffer

A (1 M NaCl, 50 mM NaH_2PO_4 pH 8) with protease inhibitors PMSF and benzamidine. Cells were lysed by sonication, followed by treatment with lysozyme and DNase at 37°C for 30 minutes. Lysate was incubated with 50 mM EDTA shaking on ice for 30 minutes. Cell debris was removed by centrifugation at 39200 x g for 35 minutes at 4°C. Cleared lysate was passed twice over Streptactin Superflow Plus column (Qiagen). The column was washed once with buffer A and once with buffer NP (300 mM NaCl, 50 mM NaH_2PO_4 pH 8). ModE was eluted with NPD (NP buffer with 2.5 mM desthiobiotin). Lack of bound Mo was confirmed using ICP-MS (Thermo Scientific iCAP Q, University of Arkansas Stable Isotope Laboratory).

Electrophoretic mobility shift assays

Complementary synthetic oligos (IDT) were annealed to generate 49-50 bp DNA probes. Lyophilized DNA was resuspended in 10 mM Tris, 50 mM KCl pH 8. Equal volumes were mixed and incubated at 95°C for 2 minutes followed by a ramp cool to 25°C over 45 minutes. EMSA reaction buffer comprised 20 mM Tris pH 8, 15 mM $MgCl_2$, 120 mM KCl, 10% glycerol, 12.5 µg/mL heparin, 100 nM DNA, and 8 µM protein unless otherwise indicated. Additives included 1 mM Na_2MoO_4 and 1 mM DTT as indicated. Eluted ModE was deemed >95% pure (Fig. 7), so this was used for assays directly after eluting or after one freeze-thaw. Reactions were incubated at 37°C for 30 min and loaded onto a 6% acrylamide gel pre-run at room temperature (100 V, 1 hour) in 0.5x TBE buffer. The gel was run at 75 V for 1 hour, stained with SYBR Gold, and imaged with Bio-Rad Gel Doc XR+.

Results

CRISPRi repression of *modE* in *M. acetivorans* affects alternative nitrogenase expression and Mo-dependent diazotrophy. To ascertain the role of ModE in regulating the alternative nitrogenases in *M. acetivorans*, CRISPRi repression strain DJL89 was generated which contains the recently developed CRISPRi plasmid expressing a gRNA targeting *modE* for dCas9-dependent repression. The location of gRNA binding is shown in Fig. 1. Under diazotrophic growth conditions, the transcript abundance of *modE* was reduced by ~70% in strain DJL89 compared to control strain DJL72 (gRNA-free), confirming dCas9-dependent repression of *modE* (Fig. 2). Next, the effect of *modE* repression on growth and alternative nitrogenase expression was analyzed. Notably, strain DJL89 grows identical to control strain DJL72 under all conditions tested, except in Mo + Fe medium lacking NH_4Cl (Mo-dependent diazotrophy) (Fig. 3). Specifically, strain DJL89 exhibits a delay in the onset of Mo-dependent diazotrophic growth compared to strain DJL72. To determine if the Mo-dependent diazotrophy phenotype is due to aberrant expression of V- and/or Fe-nitrogenases, the transcript abundance of *vnfD* and *anfD* was compared in DJL89 and DJL72. The abundance of *vnfD* and *anfD* is 40-fold and 10-fold higher, respectively, in strain DJL89 compared to strain DJL72 during Mo-dependent diazotrophy (Fig. 4). These results indicate that ModE functions in Mo-dependent repression of the *vnf* and *anf* operons in *M. acetivorans*.

To determine if the production of Mo-nitrogenase, V-nitrogenase, or Fe-nitrogenase is altered in strain DJL89 cells grown in Mo + Fe medium, the presence of NifD, VnfD, and AnfD in cell lysates was analyzed by western blot. Consistent with previous results in chapter 1, only NifD is detected in lysate from strain DJL72 cells grown in Mo + Fe medium lacking NH_4Cl (Fig. 5).[9] However, AnfD was detected in addition to NifD in lysate from strain DJL89 cells

grown in Mo + Fe medium lacking NH_4Cl (Fig. 5). Surprisingly, VnfD was not detected in lysate from strain DJL89 cells grown in Mo + Fe medium lacking NH_4Cl, despite the significant increase in the transcript abundance of *vnfD* (Fig. 4). The addition of V to the growth medium did not result in detection of VnfD, indicating the presence of V is not required for production of V-nitrogenase.

The predicted ModE binding motif is required for binding of recombinant ModE to the *anf* operon promoter region. The predicted consensus ModE binding palindromic motif (RTTATGT-N_8-RCATAAY) was previously identified upstream of several genes in the chromosome of *M. acetivorans*.[2] Genes that contain the conserved motif upstream, and are therefore predicted to be regulated by ModE, are shown in Table 3. Notably, many of the putative ModE binding motifs are located near genes that neighbor the *anf* and *vnf* operons, including four motifs within the intergenic region between the operons (Fig. 6). Specifically, one binding site is located upstream of the *anf* operon and three binding sites are located upstream of the *vnf* operon (Table 3). To determine if ModE binds to the motif and therefore directly represses expression of the *vnf* and *anf* operons, *M. acetivorans* ModE was expressed in *E. coli* with a C-terminal Strep tag and purified to homogeneity by affinity chromatography (Fig. 7). Purified recombinant ModE was then used in electrophoretic mobility shift assays (EMSA) to test for binding to the motif. The single site upstream of the *anf* operon was chosen for initial optimization of EMSAs using recombinant ModE. An oligonucleotide (49 bp) encompassing the promoter region of *anf* with the predicted ModE binding motif within the center was used in EMSA and results compared to the promoter region of *ma2869* that lacks the motif (negative control). Recombinant ModE caused a complete shift of both P_{anf} and P_{ma2689} in the absence of

heparin. However, the addition of heparin (12.5 µg/ml) to decrease non-specific DNA binding resulted in the appearance of two shifted bands with P_{anf} when ModE was added (Fig. 8). No shift was observed when ModE was added to P_{ma2689}, indicating the predicted ModE binding site is required for the specific binding of ModE to P_{anf}. To further assess the specificity of ModE for P_{anf}, EMSAs were performed with increasing concentrations of heparin. The addition of 25 µg/ml heparin resulted in the loss of the lower MW band, while the addition of 50 µg/ml heparin abolished ModE binding to P_{anf} (Fig. 9). For all subsequent EMSAs either 12.5 or 25 µg/ml heparin was used. As a further control, the promoter region of four additional genes that lack the ModE binding motif were tested by EMSA for ModE binding. The addition of ModE failed to shift the DNA for any of the genes (Fig. 10).

To confirm the predicted motif is required for ModE binding, EMSAs with P_{anf} were compared to P_{anf} harboring mutations in the predicted motif (Fig. 11). Mutation or deletion of half of the palindrome (i.e., RTTATGT) decreased binding of ModE, whereas deletion of both sides of the palindrome abolished binding with results identical to the negative control P_{ma2689}. These results indicate that the RTTATGT-N_8-RCATAAY motif is required for direct binding of ModE to P_{anf}.

Molybdate does not alter the binding of ModE to P_{anf}. ICP-MS analysis revealed that recombinant ModE purified from *E. coli* does not contain molybdate (<1 ppb). The addition of excess molybdate (1 µM) to the EMSA mix does not alter the affinity of ModE for $P_{anf.}$ (Fig. 12). In addition, pre-incubation of ModE with molybdate and DTT prior to EMSA analysis also did not alter the affinity of ModE for $P_{anf.}$ (Fig. 13**).** These results indicate that ModE binding to DNA is independent of Mo under the conditions tested.

The expression of *modE* is not altered by the availability of fixed nitrogen or Mo.

Transcription of the *anf* and *vnf* operons increases significantly in *M. acetivorans* cells grown in the absence of molybdate and fixed nitrogen (Chapter 1). Moreover, CRISPRi-repression of *modE* in strain DJL89 clearly results in derepression of *anf* and *vnf* transcription in the presence of Mo and the detection of AnfD, consistent with ModE as a Mo-dependent repressor. However, recombinant ModE DNA binding is unresponsive to Mo *in vitro*, indicating ModE binding to *anf* and *vnf* operons is independent of Mo. Thus, it is unclear how regulation of *vnf* and *anf* transcription by ModE is controlled by Mo. One possibility is that *modE* expression is controlled by availability of Mo and/or fixed nitrogen, such that ModE levels increase in response to the presence of Mo that results in repression of *vnf* and *anf* operons. To test this hypothesis, the relative expression of *modE* was compared for the wild-type strain grown in the presence and absence of fixed nitrogen and the addition of Mo or V (Fig. 14). No significant difference (fold change >2) in the transcript abundance of *modE* was observed for any of the conditions, indicating alteration of *modE* expression is not the mode of regulation used.

Identification of additional genes in the *M. acetivorans* ModE regulon. DNA oligos containing the ModE binding motif upstream of *vnf*, *anfH*, *ma1204*, *ma1234,* and *vht* identified in Table 3 were analyzed by EMSA with recombinant ModE. ModE bound to all six oligonucleotides, resulting in a similar shift as seen with P_{anf} (Fig. 15). The shift with P_{vht} was the weakest, likely due to a single nucleotide substitution within the palindromic sequence (Table 4). These results are consistent with ModE controlling the expression of all the genes listed in Table 3.

Discussion

The presence of Mo represses the transcription of the genes encoding the alternative nitrogenases Vnf and Anf in *M. acetivorans* (Chapter 1). Bioinformatic analysis identified putative ModE binding sites in the intergenic region between *vnf* and *anf*, pointing to ModE as a possible mechanism of Mo-dependent transcriptional control.[2] To test this hypothesis, strain DJL89 was constructed where *modE* is repressed by dCas9. In strain DJL89, *anfD* is upregulated compared to the control strain and AnfD is produced in the presence of Mo during nitrogen fixation. Similarly, deleting *vnf* repressors VnfR1 and VnfR2 in *A. variabilis* leads to production of the V-nitrogenase when Mo is present.[5] However, even though *vnfD* transcript abundance is significantly increased in strain DJL89 during nitrogen fixation in the presence of Mo, VnfD is below the western blot detection limit, regardless of whether or not V is present. This difference between Fe-nitrogenase and V-nitrogenase production in strain DJL89 is likely due to Mo-dependent post-transcriptional regulation. *A. vinelandii vnf* is also post-transcriptionally regulated: protein is only made in the presence of V and absence of fixed nitrogen, even though transcript accumulates in Fe-only conditions and with fixed nitrogen.[10]

Repression of *modE* in strain DJL89 increases the lag time during diazotrophic growth in the presence of Mo. A similar phenotype is seen during diazotrophic growth of the wild-type strain in the absence of Mo (Chapter 1). *M. acetivorans* may require increased time to coordinate the production of multiple nitrogenases, or this may be an effect of other genes in the ModE regulon. It is unclear whether functional Fe-nitrogenase is made in strain DJL89 in the presence of Mo, and if so, which catalytic cluster is present (i.e., FeMo-co or FeFe-co). Some diazotrophs have been shown to incorporate a FeMo-co into the alternative nitrogenases if Mo becomes available in the absence of functional Mo-nitrogenase.[11,12]

Biochemical data further support that ModE is a direct repressor of the alternative nitrogenases. ModE specifically binds four regions of DNA in the intergenic region between *anf* and *vnf* with the sequence RTTATGT-N_8-RCATAAY, but not to DNA lacking this sequence. ModE binds other DNA with this sequence, including that upstream of genes putatively involved in nitrogen fixation: *anfH*, *ma1204*, and *ma1234*. AnfH is the Fe protein encoded separate from the other *anf* structural genes. As AnfH is identical to VnfH in *M. acetivorans*, it is unclear if both are expressed during nitrogen fixation. *ma1234* is the first gene in a cluster encoding iron transport proteins as well as *nifV*, the homocitrate synthase likely required for formation of all three nitrogenase catalytic cofactors.[13] ModE binding to these sites may be alleviated in the absence of Mo to allow derepression of the these genes, which would provide another Fe protein and potentially increase Fe uptake to accommodate the increased demand for Fe used by the alternative nitrogenases. *ma1204*, divergent from *anfH*, is a putative radical SAM protein. It is unknown if MA1204 has a role in nitrogen fixation, but the radical SAM enzyme NifB is required to form the catalytic cluster precursor in all three nitrogenases.[13].

The ModE binding motif is found upstream of other genes not directly tested by EMSA here, including another iron transporter (*ma1200*), molybdate transporters (*ma0325*, *ma2280*), and formylmethanofuran dehydrogenase (*ma0304*, two binding sites). As with *ma1234*, derepression of *ma1200* in *M. acetivorans* grown in the absence of Mo may increase Fe uptake needed to support maturation of the alternative nitrogenases. Formylmethanofuran dehydrogenase (Fmd) is a Mo-containing enzyme that catalyzes the reversible conversion of formylmethanofuran to CO_2 in methanogenesis.[14] In *E. coli*, ModE also regulates Mo-containing enzymes and high affinity molybdate transport genes.[2,3] A putative ModE binding site was identified upstream of *vht*, the membrane-bound hydrogenase which oxidizes H_2 to reduce

methanophenazine within select *Methanosarcinales* electron transport systems.[15] While Vht proteins have yet to be detected in *M. acetivorans*, unpublished data support a role for Vht in recycling electrons from hydrogen produced during nitrogen fixation. Since the alternative nitrogenases from bacteria are known to produce more H_2 during N_2 reduction,[16] it is possible Vht hydrogenase expression is increased during Mo limitation to increase H_2 uptake during N_2 reduction by the alternative nitrogenases in *M. acetivorans*. ModE binds P_{vht} with lower affinity than P_{anf}, potentially due to the G → A substitution in P_{vht} or other bases outside of the identified palindrome.

The lower of the two DNA-ModE shifts is absent with increased heparin and decreased protein concentration, suggesting this species is bound with lower affinity than the higher shift. The oligomerization of *M. acetivorans* ModE is unknown, but *E. coli* ModE binds DNA as a dimer.[17] ModE is unresponsive to molybdate under the conditions tested and binds DNA with relatively low affinity (in the micromolar range). This could be due to suboptimal *in vitro* binding assays or because of its single Mop domain. *E. coli* ModE has two Mop domains, and a variant lacking its C-terminal Mop domain is no longer dependent on Mo for DNA binding.[18]

Similarly, in *Desulfovibrio alaskensis*, *in vivo* data show tungstate-responsive regulator TaoR regulates genes in a tungstate-dependent manner, but DNA binding is unaffected by the presence of tungstate *in vitro*.[19] *A. variabilis* VnfR proteins regulate V-nitrogenase genes in a Mo-dependent manner as shown in reporter assays, but binding to the promoter is not dependent on Mo in EMSAs.[5] Expression of *vnfR* genes in *A. variabilis* is repressed by Mo, unlike *modE* in *M. acetivorans*.[5] It is unclear how the expression of ModE is regulated in *M. acetivorans*, as the presence and absence of Mo or fixed nitrogen have no effect on relative expression.

Overall, the results in this study support ModE as the direct repressor of V- and Fe-nitrogenase expression and the first regulator of alternative nitrogenases identified in archaea. The ModE regulon includes molybdoenzymes as well as genes involved in molybdate uptake and Mo-independent nitrogen fixation. Further work will need to be done to determine Mo sensing by ModE, the post-transcriptional regulation of Vnf and characteristics of Anf produced in the presence of Mo.

References

1. Mus, F., Alleman, A. B., Pence, N., Seefeldt, L. C. & Peters, J. W. Exploring the alternatives of biological nitrogen fixation. *Metallomics* **10**, 523–538 (2018).

2. Studholme, D. J. & Pau, R. N. A DNA element recognised by the molybdenum-responsive transcription factor ModE is conserved in Proteobacteria, green sulphur bacteria and Archaea. *BMC Microbiol.* **3**, 24 (2003).

3. Demtröder, L., Narberhaus, F. & Masepohl, B. Coordinated regulation of nitrogen fixation and molybdate transport by molybdenum. *Mol. Microbiol.* **111**, 17–30 (2019).

4. Kutsche, M., Leimkühler, S., Angermüller, S. & Klipp, W. Promoters controlling expression of the alternative nitrogenase and the molybdenum uptake system in *Rhodobacter capsulatus* are activated by NtrC, independent of sigma54, and repressed by molybdenum. *J. Bacteriol.* **178**, 2010–2017 (1996).

5. Pratte, B. S., Sheridan, R., James, J. A. & Thiel, T. Regulation of V-nitrogenase genes in *Anabaena variabilis* by RNA processing and by dual repressors. *Mol. Microbiol.* **88**, 413–424 (2013).

6. Gibson, D. G. *et al.* Enzymatic assembly of DNA molecules up to several hundred kilobases. *Nat. Methods* **6**, 343–345 (2009).

7. Woodyer, R. D. *et al.* Heterologous Production of Fosfomycin and Identification of the Minimal Biosynthetic Gene Cluster. *Chem. Biol.* **13**, 1171–1182 (2006).

8. Metcalf, W. W., Zhang, J. K., Apolinario, E., Sowers, K. R. & Wolfe, R. S. A genetic system for Archaea of the genus *Methanosarcina*: Liposome-mediated transformation and construction of shuttle vectors. *Proc. Natl. Acad. Sci.* **94**, 2626–2631 (1997).

9. Dhamad, A. E. & Lessner, D. J. A CRISPRi-dCas9 System for Archaea and Its Use To Examine Gene Function during Nitrogen Fixation by *Methanosarcina acetivorans*. *Appl. Environ. Microbiol.* **86**, (2020).

10. Jacobitz, S. & Bishop, P. E. Regulation of nitrogenase-2 in *Azotobacter vinelandii* by ammonium, molybdenum, and vanadium. *J. Bacteriol.* **174**, 3884–3888 (1992).

11. Gollan, U., Schneider, K., Müller, A., Schüddekopf, K. & Klipp, W. Detection of the *in vivo* incorporation of a metal cluster into a protein. *Eur. J. Biochem.* **215**, 25–35 (1993).

12. Rebelein, J. G., Lee, C. C., Newcomb, M., Hu, Y. & Ribbe, M. W. Characterization of an M-Cluster-Substituted Nitrogenase VFe Protein. *mBio* **9**, (2018).

13. Burén, S., Jiménez-Vicente, E., Echavarri-Erasun, C. & Rubio, L. M. Biosynthesis of Nitrogenase Cofactors. *Chem. Rev.* (2020) doi:10.1021/acs.chemrev.9b00489.

14. Karrasch, M., Börner, G., Enßle, M. & Thauer, R. K. Formylmethanofuran dehydrogenase from methanogenic bacteria, a molybdoenzyme. *FEBS Lett.* **253**, 226–230 (1989).

15. Guss, A. M., Kulkarni, G. & Metcalf, W. W. Differences in Hydrogenase Gene Expression between *Methanosarcina acetivorans* and *Methanosarcina barkeri*. *J. Bacteriol.* **191**, 2826–2833 (2009).

16. Harwood, C. S. Iron-Only and Vanadium Nitrogenases: Fail-Safe Enzymes or Something More? *Annu. Rev. Microbiol.* **74**, null (2020).

17. McNicholas, P. M., Mazzotta, M. M., Rech, S. A. & Gunsalus, R. P. Functional Dissection of the Molybdate-Responsive Transcription Regulator, ModE, from *Escherichia coli*. *J. Bacteriol.* **180**, 4638–4643 (1998).

18. McNicholas, P. M., Chiang, R. C. & Gunsalus, R. P. The *Escherichia coli modE* gene: effect of *modE* mutations on molybdate dependent *modA* expression. *FEMS Microbiol. Lett.* **145**, 117–123 (1996).

19. Rajeev, L. *et al.* A new family of transcriptional regulators of tungstoenzymes and molybdate/tungstate transport. *Environ. Microbiol.* **21**, 784–799 (2019).

Figures and Tables

Table 1. List of primers used.

Primer	Sequence	Description
modE_for	GGTGGTCCATGGCGATGAAAGCGAAAACAAAGCT CTGGTTTACTGAAGATGGAAGAACG	Forward primer to amplify *modE* for cloning into pET28a
modE_rev	GGTGGTGGATCCTCACTTTTCGAACTGAGGGTGG GACCAGTCTGAGGGACCGGACTT	Reverse primer to amplify *modE* for cloning into pET28a
modE_qPCR_for	GCCAGAAACTCGGAATCTCGT	Forward qPCR primer to amplify *modE* transcript
modE_qPCR_rev	AGGTCGGTCAGGAAGGTACC	Reverse qPCR primer to amplify *modE* transcript
16sRNA.qPCR.F	GGTACGGGTTGTGAGAGCAA	Forward qPCR primer to amplify 16S rRNA transcript
16sRNA.qPCR.R	CTCGGTGTCCCCTTATCACG	Reverse qPCR primer to amplify 16S rRNA transcript
vnfD.qPCR.F	GTCGGAAAGAGGTTGCAGCTA	Forward qPCR primer to amplify *vnfD* transcript
vnfD.qPCR.R	GCTTCGTGTGCCAGGTATCA	Reverse qPCR primer to amplify *vnfD* transcript
anfD.qPCR.F	GTCTCCCTGATGGCCGAATT	Forward qPCR primer to amplify *anfD* transcript
anfD.qPCR.R	AGATCTGTCTCTGGCCTGGT	Reverse qPCR primer to amplify *anfD* transcript

Table 2. List of methanogen strains.

Strain	Plasmid	Description
WWM73	n/a	Pseudo wild-type *M. acetivorans*
DJL72	pDL734	WWM73 expressing dCas9 with no gRNA (control)
DJL89	pDL535	WWM73 expressing dCas9 with a gRNA targeting *modE*

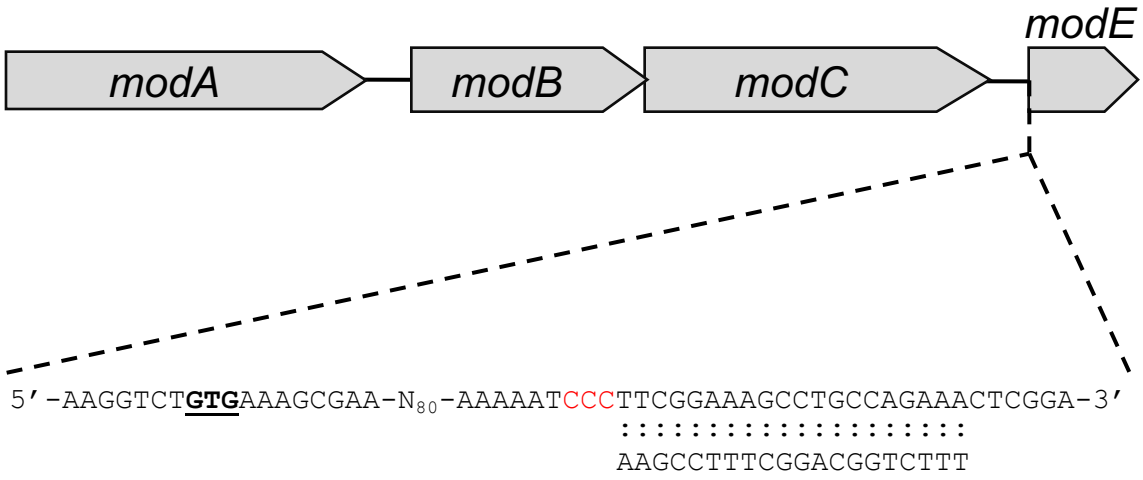

Fig. 1. The genomic context of *modE.* The gRNA targeting dCas9 to *modE* is located within the gene to avoid effects on upstream molybdate transporter *modABC*. The start codon is bolded and underlined and the PAM sequence is red.

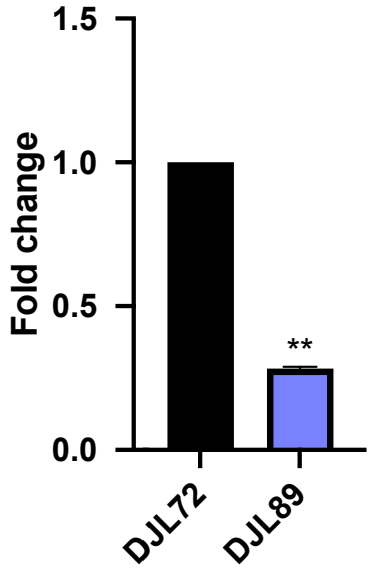

Figure 2. Relative expression of *modE* in strain DJL89 compared to the control strain DJL72 without fixed nitrogen. 16S rRNA was used as the internal control. ** $p < 0.01$.

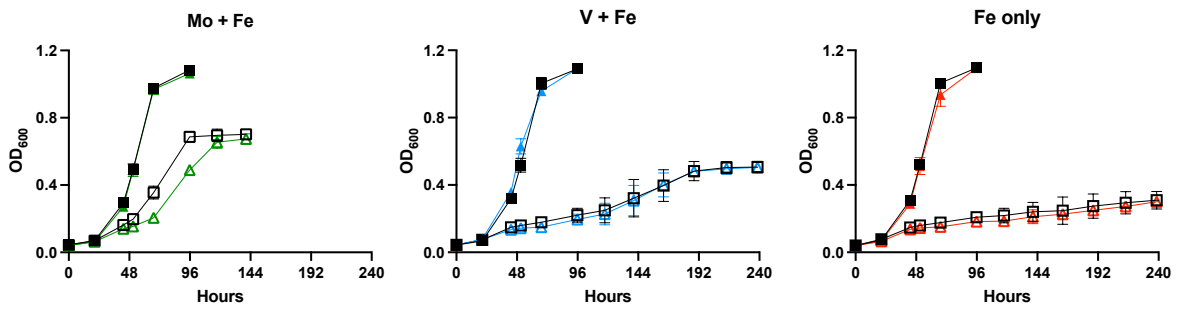

Figure 3. Comparison of the growth of strain DJL72 (black squares) and strain DJL89 (colored circles) with NH_4Cl (closed symbols) or without NH_4Cl (open symbols), and the indicated metals (Mo + Fe = green, V + Fe = blue, Fe only = red). Data represent at least three biological replicates ± 1 SD.

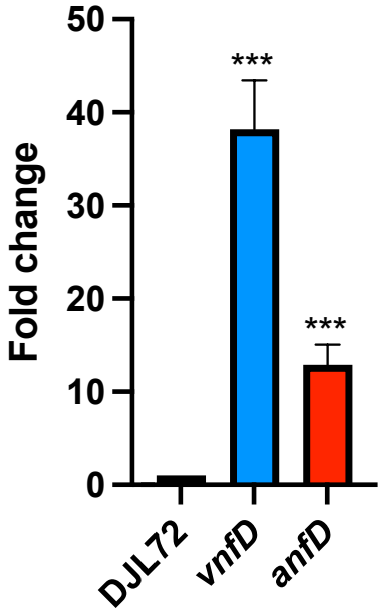

Figure 4. Relative expression of *vnfD* and *anfD* in strain DJL89 compared to the control strain DJL72 without fixed nitrogen. 16S rRNA was used as the internal control. *** $p < 0.001$.

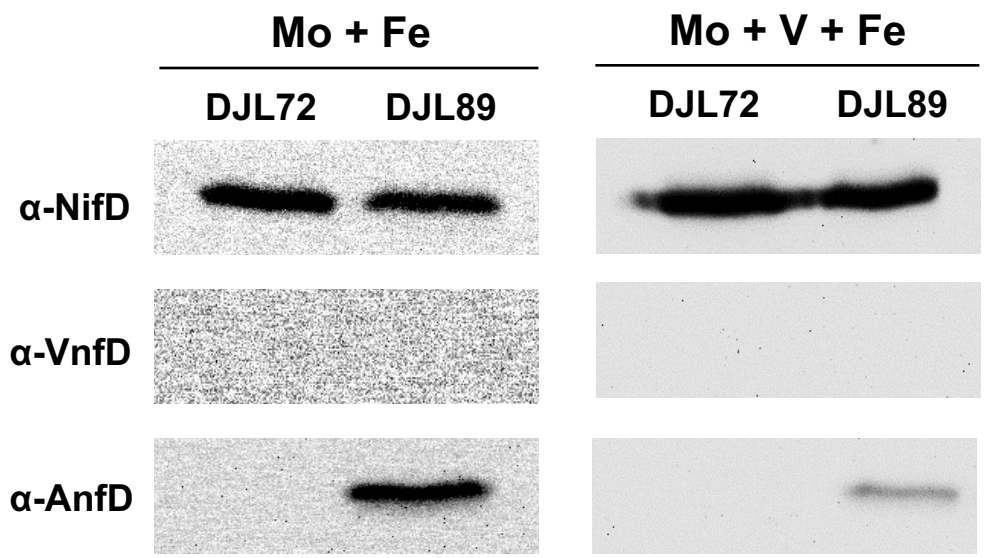

Figure 5. Western blots probing for the catalytic subunit of each nitrogenase (NifD, VnfD, AnfD). Cell lysates were generated from nitrogen-fixing cultures containing Mo + Fe or Mo + V+ Fe. SDS-PAGE gels showing normalization of loading Supplemental Fig. 1.

Table 3. List of putative ModE binding sites.

Gene	Details	Sequence(s)	Distance from Start Codon (bp)
ma1212	*anf* operon, divergent from *vnf*	G**TTATGT**AATTCTAA**ACATAA**C	314
ma1213	*vnf* operon, divergent from *anf*	G**TTATGT**TCAGTTAAG**CATAA**C	633
		G**TTATGT**TTACTTAA**ACATAA**C	555
		G**TTATGT**TTGAATAA**ACATAA**T	160
ma1205	*anfH*	G**TTATGT**TTGATTAA**ACATAA**C	161
ma1204	Radical SAM protein divergent from *anfH*	A**TTATGT**ATAACTGT**ACATAA**C	235
ma1234	Iron transport protein downstream of *vnf*	A**TTATGT**TTATTTGA**ACATAA**C	33
ma1141	*vht* hydrogenase	A**TTAT**A**T**AAATGTGT**A**T**ATAA**A	59
ma0304	Formylmethanofuran dehydrogenase	G**TTATGT**TGAAATCT**ACATAA**T	106
		G**TTATGT**TTATTTAA**ACATAA**C	24
ma2280	Molybdate transporter	G**TTATGT**TTAGGTAT**ACATAA**C	194
ma0325	Molybdate transporter	G**TTATGT**CTGAACTCG**CATAA**C	29
ma1200	Iron transport protein downstream of *anf*	G**TTATGT**TCGAATAA**ACATAA**T	33

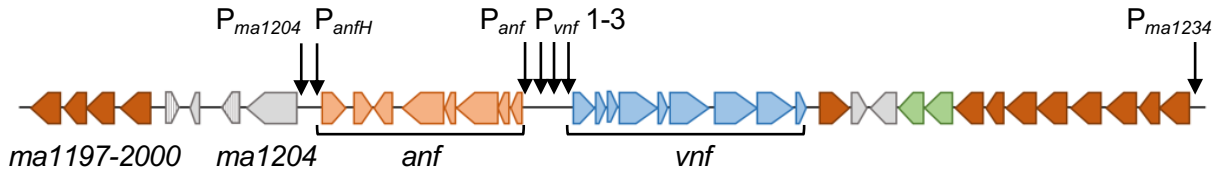

Figure 6. Location of sequences in the V- and Fe-nitrogenase gene neighborhood. Stripes = genes annotated as protein coding but containing stop codons. Green = *nifV* genes. Dark orange = iron transport genes. Gray = unknown function.

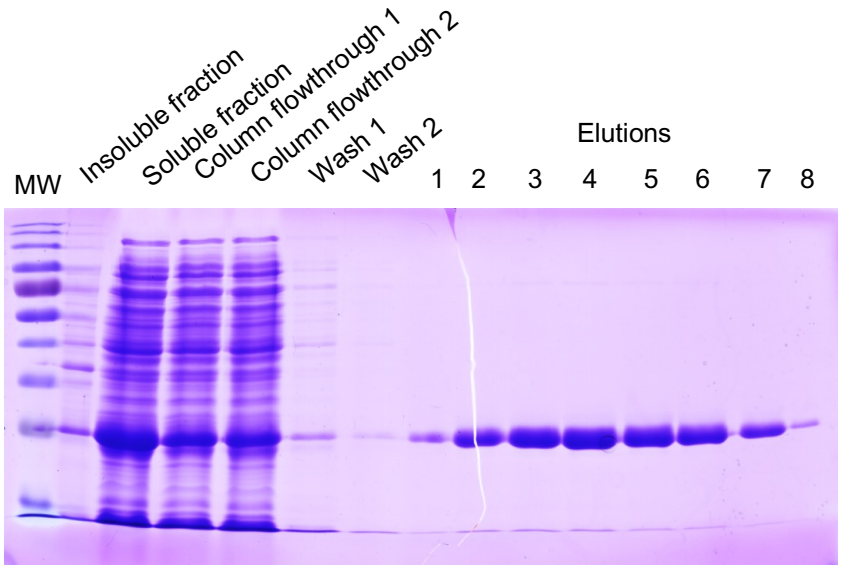

Figure 7. SDS-PAGE gel of samples from the purification of recombinant ModE from *E. coli*. MW = molecular weight marker.

P_{anf} GGAACAAAATATG**GTTATGT**AATTCTAA**ACATAAC**GAATAATAACCATG

P_{ma2689} AAAAACAGGAAGTAAGAATTCGAAGAAGCCGAAACCGAAAAAAAGCCGAT

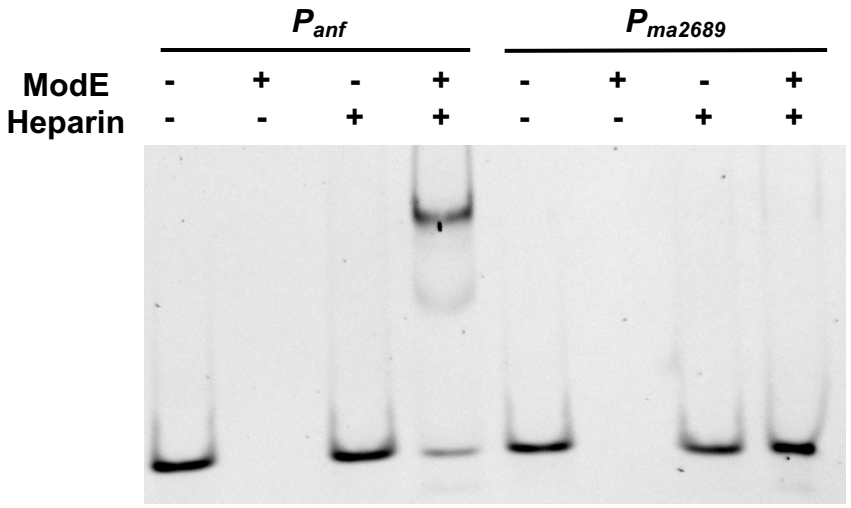

Figure 8. EMSA showing affinity of ModE for P_{anf} containing the predicted ModE binding site (bolded and underlined) compared P_{ma2869} that lacks the predicted ModE binding site. EMSA was performed as described in the Materials and Methods section using 8 μM ModE.

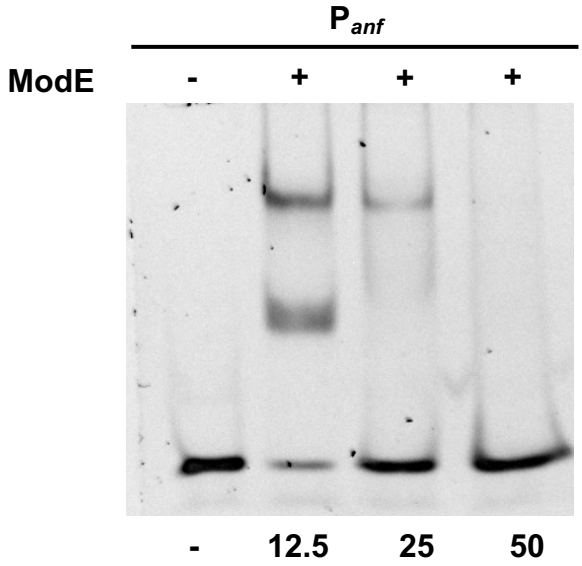

Figure 9. EMSA demonstrating the affinity of ModE for P_{anf} with increasing heparin concentrations.

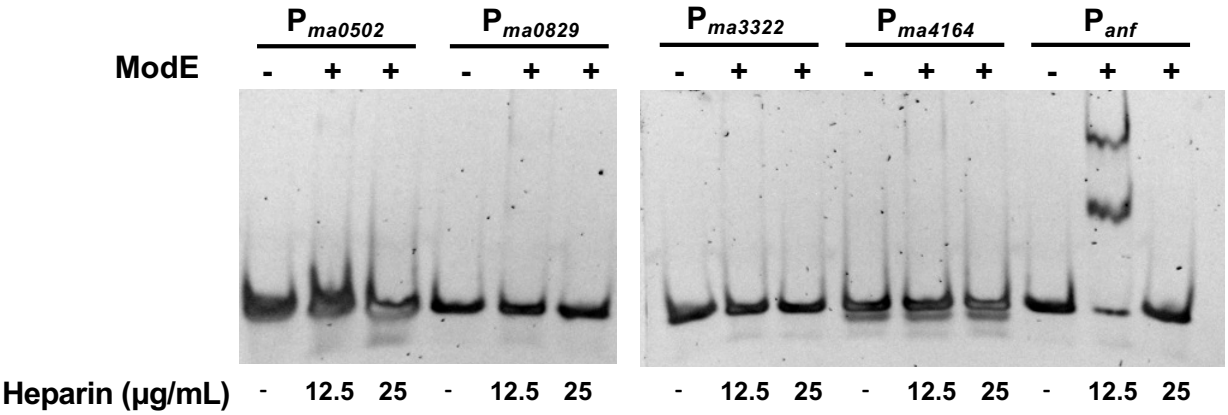

Figure 10. EMSAs demonstrating the specificity of ModE for P_{anf} compared to negative control oligos with different heparin concentrations.

A.

P_{anf} GGAACAAAATATG**GTTATGT**AATTCTAA**ACATAAC**GAATAATAACCATG

P_{anf*} GGAACAAAATATG**GTGGGGT**AATTCTAA**ACATAAC**GAATAATAACCATG

P_{anf-} GCCCTCTGGAACAAAATATG-------AATTCTAA**ACATAAC**GAATAATAACCATG

P_{anf--} GCCCTCTGGAACAAAATATG-------AATTCTAA-------GAATAATAACCATGAATTAAA

B.

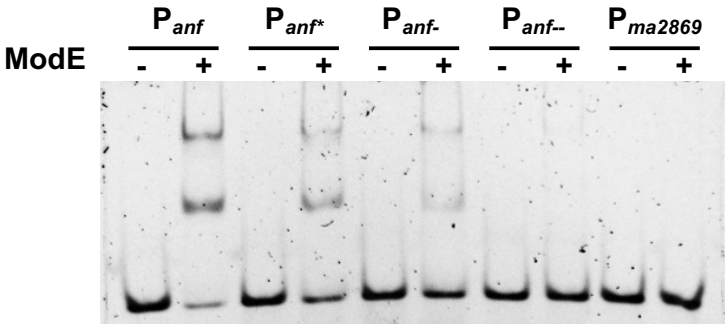

C.

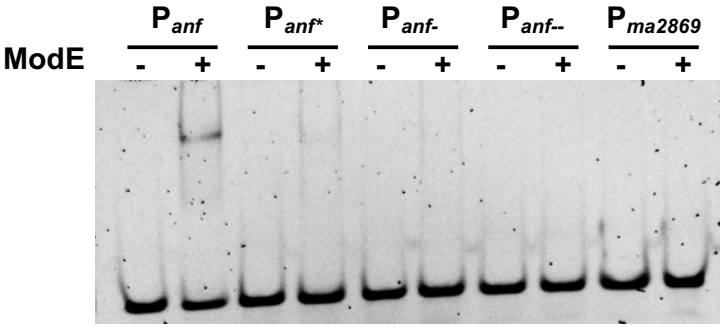

Figure 11. EMSAs demonstrating the affinity of ModE for $P_{anf,}$ its variants, and negative control P_{ma2869} (A) with 12.5 ug/mL heparin (B) and 25 ug/mL heparin (C). Predicted sites are underlined, mutations are red, partial sites are green.

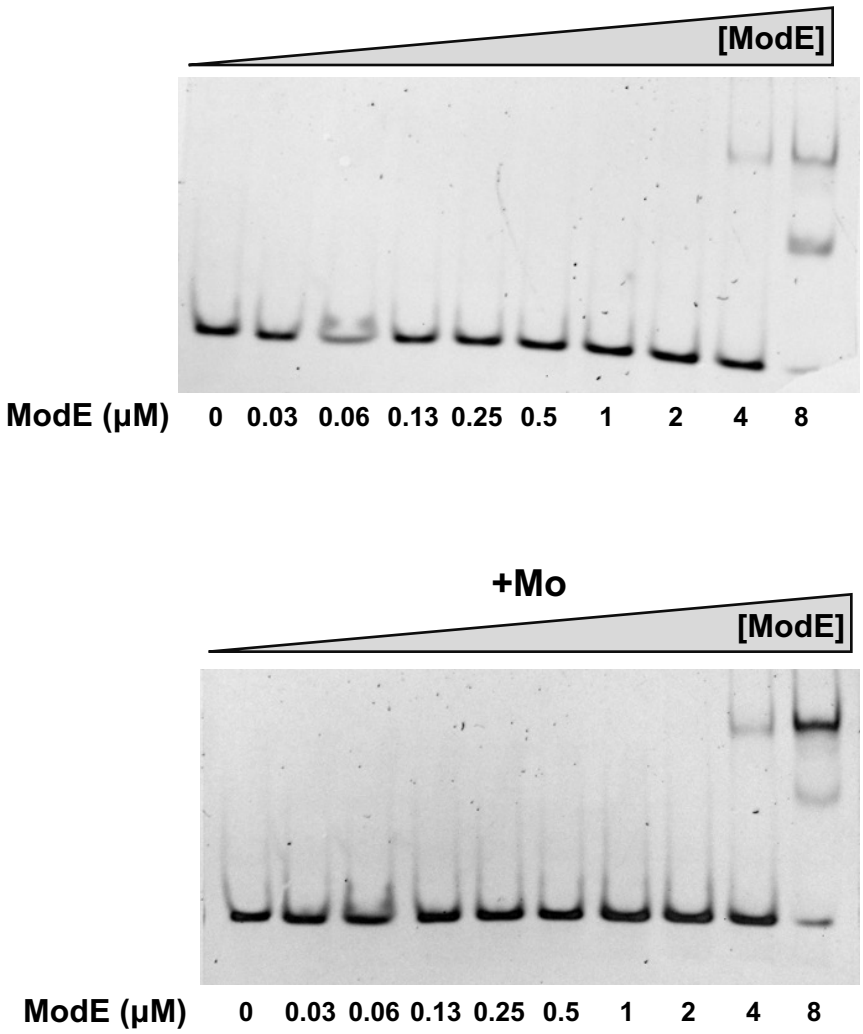

Figure 12. EMSAs demonstrating the affinity of ModE (0-8 uM) for P_{anf} with and without added Mo.

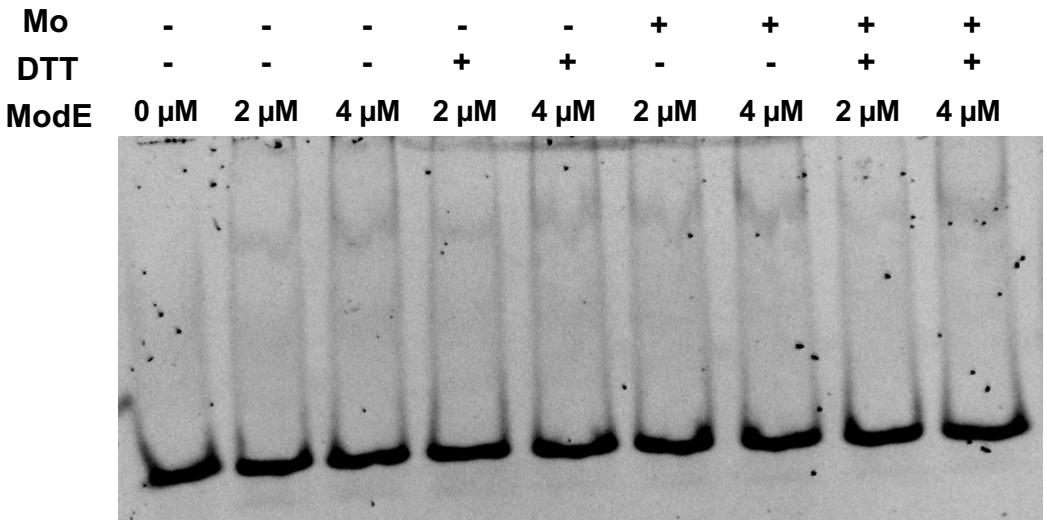

Figure 13. EMSA with ModE pre-incubated with Mo and/or DTT.

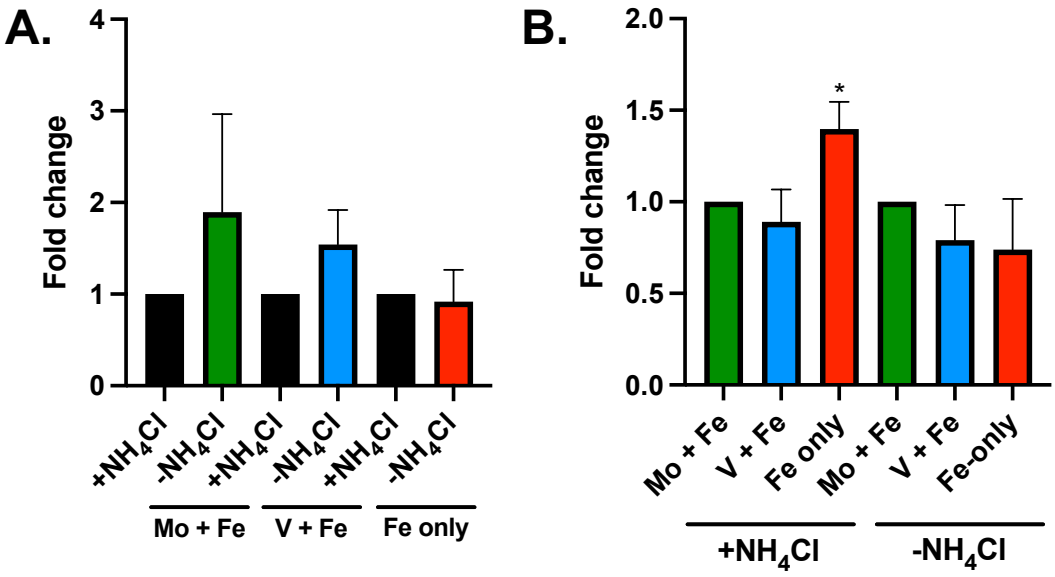

Figure 14. Expression of *modE* in *M. acetivorans* relative to (A) fixed nitrogen and (B) molybdate. * $p < 0.05$.

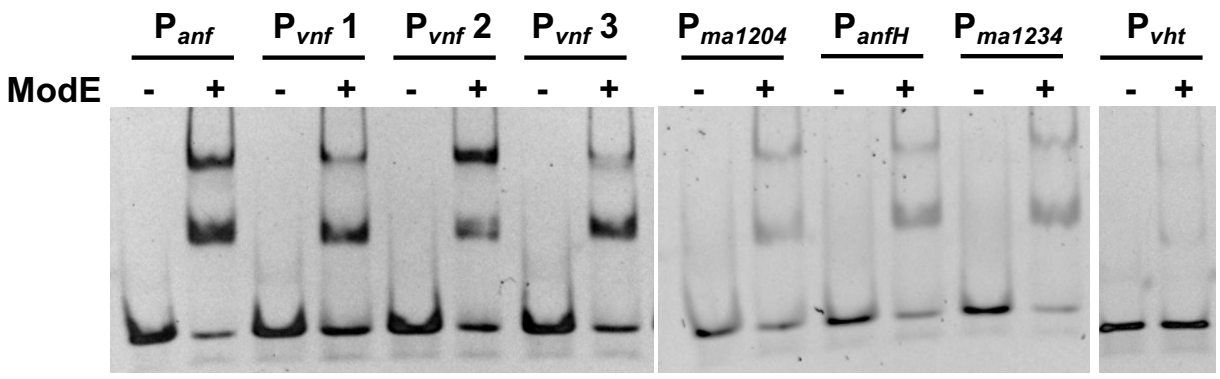

Figure 15. EMSAs demonstrating the affinity of ModE for DNA upstream of additional genes.

Table 4. List of gel shift oligos with ModE binding motifs bolded.

Oligo	Sequence
P_{anf}	GGAACAAAATATG**GTTATGT**AATTCTAA**ACATAAC**GAATAATAACCATG
P_{vnf1}	GAAACTTAAATCATT**GTTATGT**TTGAATAA**ACATAAT**ACAGATTAAACTA
P_{vnf2}	ATTGAAATAAAATA**GTTATGT**TTACTTAA**ACATAAC**AATATGCAATTCAC
P_{vnf3}	TTTCATGTGAGTTT**GTTATGT**TCAGTTAA**GCATAAC**CTGATGAGGTACTT
P_{anfH}	CTTAATATAAAGCTTA**GTTATGT**TTGATTAA**ACATAAC**ACTTTATGGTC
P_{ma1204}	GTTTTTTGGTTAATTT**ATTATGT**ATAACTGT**ACATAAC**CACGTGCATCTG
P_{ma1234}	CTATGTACATATCC**ATTATGT**TTATTTGA**ACATAAC**AACTATTATATAAT
P_{vht}	CATTATTGGTATATTTATATACACATTTATATAATTAATACGAATCTAAA
P_{anf*}	GGAACAAAATATG**GT**GGG**GT**AATTCTAA**ACATAAC**GAATAATAACCATG
P_{anf-}	GCCCTCTGGAACAAAATATGAATTCTAA**ACATAAC**GAATAATAACCATG
P_{anf--}	GCCCTCTGGAACAAAATATGAATTCTAAGAATAATAACCATGAATTAAA

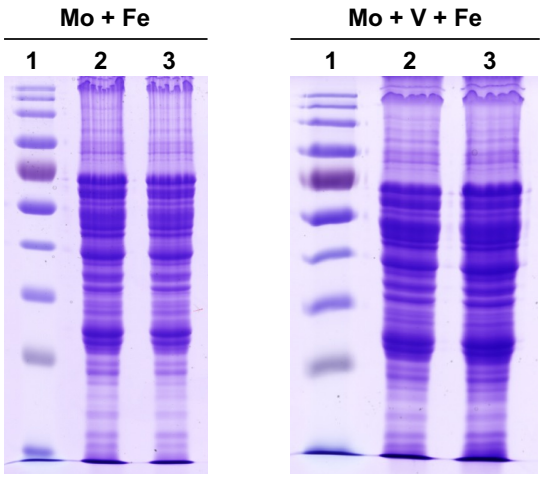

Supplemental Figure 1. SDS-PAGE gels showing normalization of protein loading for western blots in Fig. 5. 1) protein ladder; 2) lysates from control strain DJL72; 3) lysates from DJL89.

Chapter III

Initial genetic analysis of the role of nitrogenase-like proteins in *Methanosarcina acetivorans*

Melissa Chanderban

Cell and Molecular Biology Program, University of Arkansas,

Fayetteville AR, 72701, USA

Introduction

To mitigate nitrogen limitation, prokaryotes evolved three nitrogenase enzymes which convert dinitrogen gas into biologically available ammonia. The oldest extant nitrogenase—one using a molybdenum-containing catalytic cofactor—is predicted to have arisen in methane-producing archaea (methanogens) approximately 2 billion years ago.[1] From this molybdenum nitrogenase, an isozyme evolved to use vanadium (V) in place of molybdenum (Mo). The V-nitrogenase likely duplicated in the methanogen order Methanosarcinales to yield the iron-only nitrogenase, the cofactor of which contains iron (Fe) instead of Mo or V. Nitrogenases likely arose from a general reductase complex to be more specific to nitrogen fixation. Other nitrogenase-like enzymes may have diverged from this proto-nitrogenase as well, with active site differences conferring specificities to other substrates.[2]

While there are differences in substrate, cofactor, and oligomerization, nitrogenases and nitrogenase-like proteins all comprise a catalytic component that functions to reduce a substrate (e.g., N_2), and a reductase component that delivers electrons from host metabolism to the catalytic component. For example, the molybdenum nitrogenase complex includes the catalytic component dinitrogenase, also known as the MoFe protein, and dinitrogenase reductase, also known as the Fe protein. The MoFe protein is heterotetrameric, containing two subunits each of NifD and NifK. NifD and NifK are joined by a bridging [8Fe-7S] P-cluster, while NifD harbors the [7Fe-9S-C-Mo-homocitrate] catalytic cofactor, or M-cluster. Electrons to reduce dinitrogen are supplied by NifH, the Fe protein. NifH is a homodimer with a bridging [4Fe-4S] cluster and ATPase domains. A similar scheme follows for the V-nitrogenase (VnfHDK) and Fe-nitrogenase (AnfHDK), except these require an additional subunit (VnfG/AnfG).[3]

A few nitrogenase-like complexes have been characterized and shown to reduce substrates other than N_2. For example, the MarHDK complex was recently shown to reduce volatile organic sulfur compounds dimethylsulfide and (2-methylthio)ethanol to methane and ethylene in *Rhodospirillum rubrum*. MarDK contains residues that may bind a P-cluster. Interestingly, the presence of MarB, an analog to nitrogenase maturation protein NifB which generates the M-cluster precursor, indicates MarDK likely uses a unique catalytic cofactor.[4] All other nitrogenase-like proteins characterized to date—CfbCD, BchLNB, and BchXYZ—reduce tetrapyrroles which occupy the active site instead of a catalytic cofactor. CfbCD is used in the biosynthesis of coenzyme F430, the cofactor of methyl-CoM reductase (Mcr) which catalyzes the methane-releasing step of methanogenesis and is required in methanogens. The Fe protein CfbC donates electrons to CfbD, which is a homomer unlike all other NifDK-like proteins. CfbD also coordinates a [4Fe-4S] cluster instead of a P-cluster.[5,6] Similarly, nitrogenase-like Bch systems reduce precursors in the biosynthesis of chlorophyll and bacteriochlorophyll. BchL and BchX donate electrons to BchNB and BchYZ, respectively. Like CfbD, BchNB and BchYZ coordinate a [4Fe-4S] cluster instead of a P cluster, but the latter are heterotetramers.[7]

Nitrogenase-like proteins thus far play important roles in the global cycles of nitrogen (nitrogen fixation), carbon (methanogenesis, photosynthesis), and sulfur (reduction of volatile sulfur compounds). However, there are nitrogenase family proteins that have yet to be characterized. For example, in addition to containing Mo-, V-, and Fe-nitrogenases, the genome of *Methanosarcina acetivorans* encodes additional uncharacterized nitrogenase-like genes, the *ma1631-33* and *ma2032-33* gene clusters. The *ma1631-33* gene cluster encodes NifH and NifDK homologs. The *ma2032-33* gene cluster features fused NifH/NifD and NifK homologs. It is unclear if these proteins also function in nitrogen fixation and/or function to reduce some other

substrate (e.g., tetrapyrrole cofactor). To begin to understand the role of these genes, the CRISPRi-dCas9 system recently developed for *M. acetivorans* was used to test the importance of these genes to the physiology of *M. acetivorans*, including potential roles in nitrogen fixation and carbon source utilization.

Materials and Methods

Bioinformatics

To assess the distribution of nitrogenase-like proteins in methanogens, MA2032 and MA1631 sequences were used as queries for NCBI protein BLAST within Euryarchaeota with default parameters. The gene neighborhoods of MA1631-33 and MA2032-33 homologs were visually assessed for each hit. To determine conserved nitrogenase residues, MA2032-33 and MA1631-33 sequences were compared to those of characterized nitrogenases (NifHDK and VnfHDK) and nitrogenase-like proteins (CfbCD, NifEN).

Growth

M. acetivorans strains were grown in defined high salt medium with 125 mM methanol and 0.025% sodium sulfide added unless indicated otherwise.[8] Mutant strains were maintained with 2 μg/mL puromycin. For carbon source experiments, 100 mM sodium acetate or 50 mM trimethylamine were added instead of methanol. Cultures were adapted to each carbon source for several generations before experiments. During growth with acetate, Balch tubes were incubated on their sides. To evaluate nitrogen fixation phenotypes, *M. acetivorans* strains were grown in NH_4Cl-free, Mo-deplete, DTT-reduced medium with 1 mg/mL NH_4Cl, 1 μM Na_2MoO_4, or 1 μM Na_3VO_4 added as specified.

Construction of CRISPRi-dCas9 strains

Guide RNAs targeting dCas9 to *ma1631* and *ma2032* were designed using Geneious Prime (Fig. 1). Synthetic DNA oligos (IDT) were designed to encode gRNAs for assembly with the dCas9 plasmid pDL734.[9] Oligos and *Asc*I-digested pDL734 were assembled using Gibson Assembly Ultra Kit (Synthetic Genomics). The assembly mix was used to transform *Escherichia coli* strain WM4489. Colonies were screened using PCR, and the gRNA regions of plasmids were sequenced. Upon confirming the correct sequence, plasmids were used to transform *M. acetivorans* strain WWM73 using liposome-mediated methods.[10] Plasmid integration was screened using PCR. Dual knockdowns were generated similarly, except the IDT oligos used above were PCR amplified to modify the ends and allow overlap with pDL540 and pDL542 linearized with *Hpa*I, providing a second location for oligo insertion. See Table 1 for a list of strains used and Table 2 for a list of primers used.

qPCR

For cultures grown with methanol or TMA, 4 mL were harvested anaerobically at mid-log (OD ~0.4) and resuspended in 1 mL Trizol. For cultures grown with acetate, 8 mL were harvested at an OD ~0.25 and resuspended in 1 mL Trizol. RNA was extracted using Zymo Direct-zol kit and further purified with Invitrogen DNA-free DNA Removal kit. cDNA was generated using 300 ng RNA with iScript Select cDNA Synthesis kit (Bio-Rad). Diluted cDNA was then used in biological triplicate and technical duplicate qPCR reactions with SsoAdvanced Universal SYBR Green Supermix (Bio-Rad). Relative quantification was calculated using the $2^{-\Delta\Delta Ct}$ method, comparing expression of *ma1631* or *ma2032* between strains/conditions using reference gene 16S rRNA.

Results

M. acetivorans nitrogenase-like proteins contain conserved cofactor binding residues.

MA1631-33 and MA2032-33 both encode NifH and NifDK homologs. MA1631-33 and MA2032-33 sequences were compared to those of *M. acetivorans* nitrogenase family proteins NifHDK, NifEN, VnfHDK, VnfEN, AnfHDK, and CfbCD to identify conserved motifs which may indicate protein function, as summarized in Fig. 2. To better compare residue position, MA2032 was split into its N-terminal NifH-like domain ($MA2032^{N}$, residues 1-276) and C-terminal NifK-like domain ($MA2032^{C}$, residues 277-752 now labelled 1-476).

NifEN and VnfEN are the scaffolds upon which nitrogenase catalytic clusters are built for NifDK and VnfDGK, respectively. NifEN and VnfEN are homologous to NifDK and VnfDK.[11] NifEN/VnfEN bind a [4Fe-4S] cluster using 3 cysteines from NifE/VnfE and 1 cysteine from NifN/VnfN (Table 3).[12] MA1631 and MA1632 have these four [4Fe-4S]-binding residues while $MA2032^{C}$ and MA2033 do not. However, $MA2032^{C}$-33 could use other cysteines to bind a [4Fe-4S] cluster, like CfbD which coordinates its [4Fe-4S] through two cysteines per monomer.[11] Additionally, MA1631-32 and $MA2032^{C}$-33 contain 3 cysteines on each subunit that may coordinate a [8Fe-7S] P-cluster as in NifDK, VnfDGK, and AnfDGK.[13] MA1631 and $MA2032^{C}$ also encode a cysteine and histidine that could potentially bind a catalytic cluster (Table 4).

MA1633 and $MA2032^{N}$ have conserved residues in common with *M. acetivorans* Fe proteins NifH and VnfH/AnfH as well as CfbC, the Fe protein specific to NifD-like CfbD (Table 5). These residues include an ATP binding motif as well as two cysteines per monomer which bind a bridging [4Fe-4S] cluster.[14,15] Overall, conserved residues indicate MA1633 and $MA2032^{N}$ likely donate electrons to their partner proteins in an ATP-dependent manner via a

[4Fe-4S] cluster. MA1631-32 and MA2032^{C}-33 likely receive those electrons using either a [4Fe-4S] or P cluster which transfers electrons to the active site. However, whether that is an active site catalytic cofactor, a tetrapyrrolic substrate, or some other substrate is unclear.

Distribution and gene neighborhoods of *ma1631-33* and *ma2032-33*. The gene neighborhoods of MA1631-33 and MA2032-33 were examined in *M. acetivorans* and other methanogens to identify potential roles for these nitrogenase-like proteins. For example, CfbBC is located in an operon with other proteins involved in coenzyme F430 biosynthesis. Upstream of MA1631-33 are methyltransferases MtaCB3 (MA1616-1617) and MtaA2 (MA1615) which catalyze the first step in methanogenesis from methanol. MtaA2 is not required for methylotrophy, but a deletion strain produces less methane from methanol and demonstrates a longer generation time during growth on trimethylamine and dimethylamine.[16] A deletion of *mtaCB3* has a longer lag time transitioning from trimethylamine to methanol and acetate to methanol.[17] The proximity of MA1631-33 to these methyltransferase genes may indicate a role in growth using methylamines, perhaps reducing the corrinoid cofactor of MtaC.

Unlike MA1631-33, which only has homologs in *Methanocella paludicola* SANAE, MA2032-33 homologs are more widely distributed in methanogens, present in strains of *Methanosarcina barkeri* and *Methanosarcina mazei*, among others. In *M. mazei* and *Methanosarcina* sp. Kolksee, homologs of *ma2032-33* are next to genes encoding methyl-CoM reductase, the methane-releasing enzyme containing cofactor F430 which in turn requires nitrogenase-like CfbCD for its biosynthesis.[5] In *Methanosarcina* sp. WH1 and *Methanosarcina* sp. WWM596, MA2032-33 homologs are near MtbCB. MtbCB is a methyltransferase analogous to MtaCB but specific for dimethylamine.[17] Like MA1631-33, the localization of MA2032-33

homologs to methyltransferase-related genes suggests a potential role in methanogenesis such as the reduction of coenzyme F430 or the MtbC corrinoid.

Relative expression of nitrogenase-like genes with different carbon and nitrogen sources. While a role for *ma1631-33* and *ma2032-33* in nitrogen fixation was not expected, relative expression of *ma1631* and *ma2032* was examined in cells grown in the presence and absence of fixed nitrogen because these are nitrogenase-like genes. There is no difference in expression between these conditions (Fig. 3). To determine if MA1631-33 and MA2032-33 may be involved in methanogenesis with different carbon sources, relative expression of *ma1631* and *ma2032* was compared between cells grown with methanol (MeOH), trimethylamine (TMA), or acetate (NaOAc). Because growth with MeOH uses Mta methyltransferases located near *ma1631-33*, an increase in expression of *ma1631* was expected here. Similarly, an increase in expression was expected for *ma2032* during growth with TMA, which uses Mtb methyltransferases that cluster near *ma2032-33*. However, there is no difference in expression of *ma1631* and *ma2032* between cells grown with MeOH or TMA (Fig. 4). There is a ~3-fold increase of *ma1631* during growth with acetate compared to MeOH. Although there is also an increase in the relative abundance of *ma2032* transcript during growth with acetate, the increase is not statistically significant ($p=0.57$).

Generation of single and dual gRNA *ma1631* and *ma2032* knockdown strains. To assess the role(s) of MA1631-33 and MA2032-33, strains DJL121 and DJL123 were generated that contain a single gRNA that targets *ma1631* and *ma2032* for repression by dCas9, respectively. These gRNAs target the beginning of each gene's coding sequence as seen in Fig. 1. However, there is

no decrease in relative expression of *ma1631* and *ma2032* in DJL121 and DJL123 compared to control strain DJL72 (Fig. 4). To increase repression, plasmids were constructed that have a second gRNA targeting *ma2032* and *ma1631* ~200-400 bp downstream of the first (Fig. 1). Having both gRNAs successfully knocked down *ma2032* and *ma1631* ~25-fold (96%) and ~100-fold (99%) during standard growth conditions in DJL125 and DJL126, respectively (Fig. 5).

Repression of *ma2032-33* affects Mo-dependent diazotrophic growth. While *ma1631* and *ma2032* did not show changes in transcript abundance during nitrogen fixation, bona fide nitrogenase proteins are post-transcriptionally regulated as shown in chapters 1 and 2 and changes in protein abundance may not be reflected at the transcriptional level. Thus, the knockdown strains were grown in the presence and absence of fixed nitrogen and metal availabilities corresponding to requirement of each nitrogenase to examine potential phenotypes. While strain DJL126 has no growth phenotype in any of the conditions, strain DJL125 has a slight delay in growth during nitrogen fixation in the presence of Mo (Fig. 6). Strain DJL125 does not display this phenotype during diazotrophy in the absence of Mo. To determine if the delay in growth is due to a change in nitrogenase production, similar to a strain DJL89 growth defect coupled to Fe-nitrogenase production in chapter 3, strain sDJL125 cell lysates were probed for expression of each nitrogenase. However, there is no difference in the presence or absence of NifD, VnfD, or AnfD for strain DJL125 (Fig 7).

Repression of *ma1631-33* affects acetate utilization. Because *ma1631* was upregulated during acetate utilization, strains DJL125 and DJL126 were adapted to acetate from a culture grown with methanol. Unlike nitrogen fixation experiments wherein a nitrogen-replete inoculum

transitions to nitrogen fixation over several days, adapting to growth on acetate can take several weeks. The adaptation period was monitored for any potential phenotypes (Fig. 8). While one replicate of strain DJL125 began growing ~200 hours before the control, the other four replicates began growth ~350 hours after the control. There was no trend for strain DJL126 growth in comparison to the control.

One drawback of CRISPRi-dCas9 is the ability of a strain to overcome repression; if a gene is required for growth, mutations which alleviate repression could arise. To determine if *ma2032* and *ma1631* are still repressed after growth on acetate, cultures of DJL72, DJL125, and DJL126 from the adaptation experiment were used to inoculate cultures harvested for qPCR. While *ma2032* is still repressed ~33-fold (97%) in DJL125, *ma1631* is no longer repressed in strain DJL126 (Fig. 9). Thus, *ma1631* is likely required for growth using acetate and/or adaption to acetoclastic growth.

Discussion

MA1631-33 and MA2032-33 are nitrogenase family proteins of unknown function. Because these proteins are nitrogenase-like, one potential physiological role is during nitrogen fixation. Expression of *ma1631* and *ma2032* was compared between cells grown in the presence and absence of fixed nitrogen. There is no change in transcript abundance. However, genes involved in nitrogen fixation can be post-transcriptionally and post-translationally regulated, so change in transcript—or lack thereof—does not always correlate with protein production or activity. To further investigate the physiological role of these proteins, strains were constructed that used CRISPR interference and 2 gRNAs to repress *ma1631* (DJL126) and *ma2032* (DJL125). These strains were grown in the presence and absence of fixed nitrogen. Only strain

DJL125 has a phenotype, a decreased log phase during nitrogen fixation in the presence of Mo but not in the absence of Mo. There is no detectable change in nitrogenase production. Whether MA2032-33 plays a direct role in Mo-dependent nitrogen fixation is unclear and warrants further experimentation.

It is unsurprising that *ma1631-33* has no clear role in nitrogen fixation. Nitrogenase-like proteins have been characterized with functions separate from N_2 reduction, including in *M. acetivorans*— nitrogenase-like CfbCD is used for the biosynthesis of coenzyme F430 in methanogens and methanotrophic archaea. Nitrogenase-like proteins BchLNB and BchXYZ are also involved in chlorophyll and bacteriochlorophyll synthesis. MarBHDK in *Rhodospirillum rubrum* reduces volatile organic sulfur compounds.[7]

Based on proximity to methyltransferase genes, these nitrogenase-like proteins may have some role in the maturation of cofactors needed for methanogenesis with different carbon sources. Specifically, *ma1631-33* is located near *mta* genes involved in methanol utilization, while *ma2032-33* homologs are near methyl-CoM reductase as well as *mtb* genes involved in dimethylamine utilization. Mta and Mtb require a corrinoid cofactor, while methyl-CoM reductase uses coenzyme F430. These cofactors are potential substrates for MA1631-33 and MA2032-33 reduction, as in other nitrogenase-like proteins that reduce tetrapyrroles. To determine if MA1631-33 and MA2032-33 might be upregulated during growth using Mta and Mtb, *ma1631* and *ma2032* transcript abundance was compared between cells grown with methanol, trimethylamine, and acetate. There is no difference between MeOH and TMA, but *ma1631* is ~3-fold upregulated during growth with acetate. Similarly, proteome data showed MA1633 is expressed 2.7-fold higher during growth with acetate compared to CO.[18] To further explore the role of MA1631-33 during acetoclastic growth, strains DJL125 and DJL126 were

adapted to acetate from methanol. While *ma2032* remains repressed in acetate-adapted DJL125, *ma1631* is no longer repressed in acetate-adapted DJL126. Taken together with the upregulation of *ma1631*, this indicates MA1631-33 is required for acetate utilization or adaptation. The precise function of MA1631-33 during growth with acetate also remains unclear and warrants further investigation.

Based on homology to characterized nitrogenases and nitrogenase-like proteins, MA1633 and the N-terminal region of MA2032 are likely NifH-like proteins that donate electrons to NifDK-like MA1631-32 and MA2033 and the C-terminus of MA2032, respectively. MA1633 and MA2032 share ATP binding and [4Fe-4S] binding residues with the characterized *M. acetivorans* Fe proteins NifH, VnfH/AnfH, and CfbC. It is also likely that MA1631-32 and MA2032-33 coordinate either a simple [4Fe-4S] cluster or complex [8Fe-7S] P-cluster. Both sets of proteins encode 3 cysteines each needed for P-cluster binding. MA1631-32 also encodes 2 cysteines analogous to those in scaffolds NifEN/VnfEN which bind a [4Fe-4S] cluster. MA1631-32 and MA2032-33 may potentially bind a catalytic cofactor based on conserved cysteine and histidine residues that coordinate the M-cluster in NifDK/VnfDK/AnfDK. Biochemical studies are needed to determine the cofactors found in MA1631-33 and MA2032-33.

The NifHD domain architecture of MA2032 is unique. All other Fe proteins identified to date are separate. While CfbC, BchL, BchX, and MarH have not demonstrated functions other than electron donation during catalysis, nitrogenase Fe proteins also contribute to the formation of the P-cluster and M-cluster.[19] The fused Fe protein of MA2032 may suggest a limited role—one of only electron donation to its partner—compared to other Fe proteins. The fused Fe protein may also affect oligomerization. For nitrogenase, one Fe protein dimer interacts with a heterodimer of reductase subunits. Assuming MA2032 dimerizes at the Fe protein domain, it is

unclear how MA2032^{N} would interact with a MA2032^{C}-MA2033 dimer. Moreover, as nitrogenase Fe proteins associate and dissociate with their partners in an ATP-dependent manner to receive and donate electrons, MA2032 may follow a different scheme if the protein is fused *in vivo*.

Overall, results from these initial genetic studies indicate *M. acetivorans* nitrogenase-like proteins have potential roles in nitrogen fixation and acetate utilization. *ma1631-33* is upregulated during acetoclastic growth, and a *ma1631-33* repression strain overcomes repression when grown on acetate. While there is no change in *ma2032* expression during nitrogen fixation, repressing *ma2032-33* causes a negative growth phenotype during Mo-dependent diazotrophic growth. Future studies are needed to further define the role(s) of MA1631-33 and MA2032-33, including analysis of cofactor content and substrate specificity.

References

1. Boyd, E. S. *et al.* A late methanogen origin for molybdenum-dependent nitrogenase. *Geobiology* **9**, 221–232 (2011).

2. Boyd, E. S., Hamilton, T. L. & Peters, J. W. An Alternative Path for the Evolution of Biological Nitrogen Fixation. *Front. Microbiol.* **2**, (2011).

3. Jasniewski, A. J., Lee, C. C., Ribbe, M. W. & Hu, Y. Reactivity, Mechanism, and Assembly of the Alternative Nitrogenases. *Chem. Rev.* **120**, 5107–5157 (2020).

4. North, J. A. *et al.* A nitrogenase-like enzyme system catalyzes methionine, ethylene, and methane biogenesis. *Science* **369**, 1094–1098 (2020).

5. Zheng, K., Ngo, P. D., Owens, V. L., Yang, X. & Mansoorabadi, S. O. The biosynthetic pathway of coenzyme F430 in methanogenic and methanotrophic archaea. *Science* **354**, 339–342 (2016).

6. Moore, S. J. *et al.* Elucidation of the biosynthesis of the methane catalyst coenzyme F430. *Nature* **543**, 78–82 (2017).

7. Ghebreamlak, S. M. & Mansoorabadi, S. O. Divergent Members of the Nitrogenase Superfamily: Tetrapyrrole Biosynthesis and Beyond. *ChemBioChem* **21**, 1723–1728 (2020).

8. Metcalf, W. W., Zhang, J. K., Shi, X. & Wolfe, R. S. Molecular, genetic, and biochemical characterization of the *serC* gene of *Methanosarcina barkeri* Fusaro. *J. Bacteriol.* **178**, 5797–5802 (1996).

9. Dhamad, A. E. & Lessner, D. J. A CRISPRi-dCas9 System for Archaea and Its Use To Examine Gene Function during Nitrogen Fixation by *Methanosarcina acetivorans*. *Appl. Environ. Microbiol.* **86**, (2020).

10. Metcalf, W. W., Zhang, J. K., Apolinario, E., Sowers, K. R. & Wolfe, R. S. A genetic system for Archaea of the genus *Methanosarcina*: Liposome-mediated transformation and construction of shuttle vectors. *Proc. Natl. Acad. Sci.* **94**, 2626–2631 (1997).

11. Hu, Y. & Ribbe, M. W. Nitrogenase and homologs. *JBIC J. Biol. Inorg. Chem.* **20**, 435–445 (2015).

12. Kaiser, J. T., Hu, Y., Wiig, J. A., Rees, D. C. & Ribbe, M. W. Structure of Precursor-Bound NifEN: A Nitrogenase FeMo Cofactor Maturase/Insertase. *Science* **331**, 91–94 (2011).

13. Hu, Y. & Ribbe, M. W. Biosynthesis of the Metalloclusters of Nitrogenases. *Annu. Rev. Biochem.* **85**, 455–483 (2016).

14. Layer, G., Krausze, J. & Moser, J. Reduction of Chemically Stable Multibonds: Nitrogenase-Like Biosynthesis of Tetrapyrroles. in *Protein Reviews: Volume 17* (ed. Atassi, M. Z.) 147–161 (Springer, 2017). doi:10.1007/5584_2016_175.

15. Rettberg, L. A. *et al.* Structural Analysis of a Nitrogenase Iron Protein from *Methanosarcina acetivorans*: Implications for CO_2 Capture by a Surface-Exposed $[Fe_4S_4]$ Cluster. *mBio* **10**, e01497-19 (2019).

16. Bose, A., Pritchett, M. A. & Metcalf, W. W. Genetic Analysis of the Methanol- and Methylamine-Specific Methyltransferase 2 Genes of *Methanosarcina acetivorans* C2A. *J. Bacteriol.* **190**, 4017–4026 (2008).

17. Pritchett, M. A. & Metcalf, W. W. Genetic, physiological and biochemical characterization of multiple methanol methyltransferase isozymes in *Methanosarcina acetivorans* C2A. *Mol. Microbiol.* **56**, 1183–1194 (2005).

18. Lessner, D. J. *et al.* An unconventional pathway for reduction of CO_2 to methane in CO-grown *Methanosarcina acetivorans* revealed by proteomics. *Proc. Natl. Acad. Sci.* **103**, 17921–17926 (2006).

19. Jasniewski, A. J., Sickerman, N. S., Hu, Y. & Ribbe, M. W. The Fe Protein: An Unsung Hero of Nitrogenase. *Inorganics* **6**, 25 (2018).

Figures and Tables

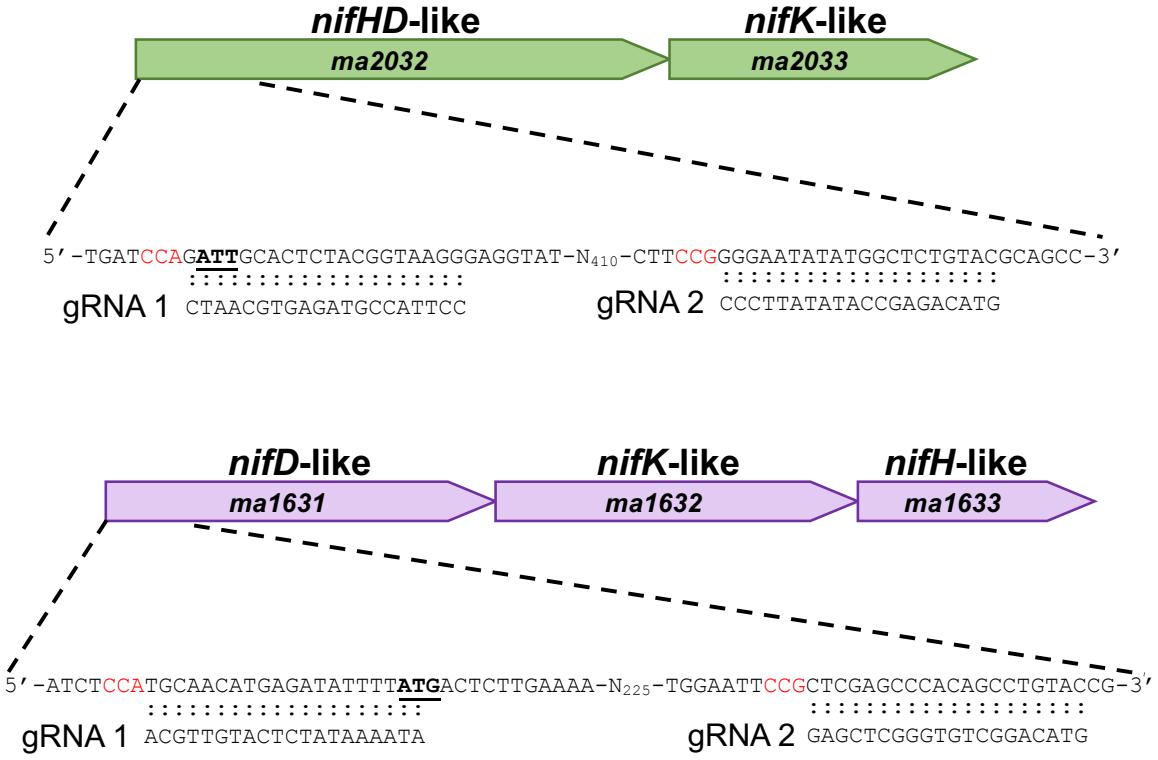

Figure 1. Location of gRNA targets for *ma2032-33* and *ma1631-33* gene clusters. Start codons are bolded and underlined, while PAM sequences are red.

Table 1. List of primers used.

Primer	Sequence	Description
hpa.Promoter.F	GACAAAATACCTGGTTACCCAGGCCGTGCCGGCACGTTAACAACAACATCAGTCACCTA	Forward primer to amplify gBlocks for assembly with the *Hpa*I site of dCas9 plasmids
hpa.Terminator.R	CTCGACAGCGACACACTTGCATCGGATGCAGCCCGGTTAACTACATGAGGGCTGAAAAGC	Reverse primer to amplify gBlocks for assembly with the *Hpa*I site of dCas9 plasmids
ma2032_qPCR_For	CTCGGTGACCTTGAGCTTGA	Forward qPCR primer to amplify *ma2032* transcript
ma2032_qPCR_Rev	GCAGAGGGAACAGAGCTCC	Reverse qPCR primer to amplify *ma2032* transcript
ma1631_qPCR_For	CGCCCTCAACGAAAGCCA	Forward qPCR primer to amplify *ma1631* transcript
ma1631_qPCR_Rev	CCGGAACAGCAGCAAGAAAG	Reverse qPCR primer to amplify *ma1631* transcript
16sRNA.qPCR.F	GGTACGGGTTGTGAGAGCAA	Forward qPCR primer to amplify 16S rRNA transcript
16sRNA.qPCR.R	CTCGGTGTCCCCTTATCACG	Reverse qPCR primer to amplify 16S rRNA transcript

Table 2. List of methanogen strains.

Strain	Plasmid	Description
WWM73	n/a	Pseudo wild-type *M. acetivorans*
DJL72	pDL734	*M. acetivorans* expressing dCas9 with no gRNA (control)
DJL121	pDL540	*M. acetivorans* expressing dCas9 with one gRNA targeting *ma1631*
DJL123	pDL542	*M. acetivorans* expressing dCas9 with one gRNA targeting *ma2032*
DJL125	pDL544	*M. acetivorans* expressing dCas9 with two gRNAs targeting *ma2032*
DJL126	pDL545	*M. acetivorans* expressing dCas9 with two gRNAs targeting *ma1631*

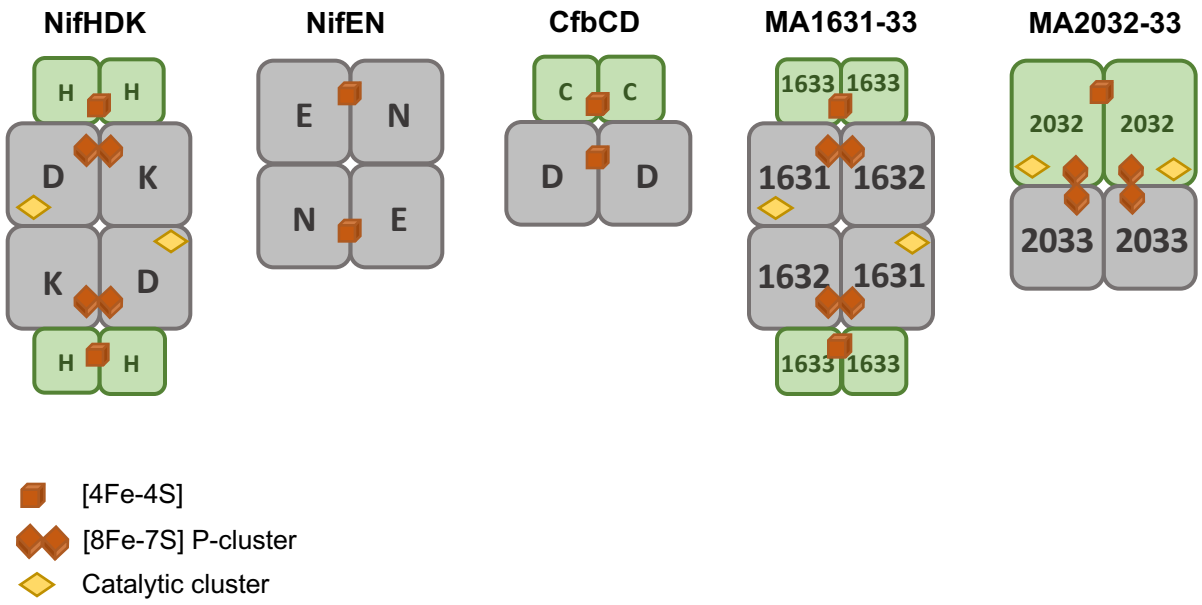

Figure 2. Predicted cofactor binding and oligomerization of MA1631-33 and MA2032-33 compared to *M. acetivorans* NifHDK, NifEN, and CfbCD.

Table 3. Conserved [4Fe-4S] cluster binding residues of M-cluster scaffolds and nitrogenase-like proteins.

Protein	[4Fe-4S] cluster binding*	Residue(s)
NifE	RACVY – IGCAG – STCIV	46, 71, 132
NifN	QGCST	40
VnfE	RPCKF – SGCAF – TSCAT	39, 64, 127
VnfN	QGCSS	45
MA1631	PMCKF – TGCPL – LSCCC	38, 63, 126
MA1632	QGCEY	44
CfbD	PGCSF – GTCAS	39, 94

*Based on homology to *Azotobacter vinelandii* NifEN.

Table 4. Conserved P-cluster and M-cluster binding residues in putative and known catalytic components.

Protein	P-cluster binding*	Residues	M-cluster binding*	Residues
NifD	RGCAF - IGCAY - ATCPV	58, 84, 149	CHRS - QIHSY	267, 485
VnfD	RGCSY - VGCAY - QTCAS	49, 75, 138	CARS - NGHAY	257, 423
AnfD	RGCAY - VGCTY - QTCAS	49, 75, 138	CARS - NIHGY	257, 423
MA2032[C]	YGCAF - RSCTH - STCPG	338, 363, 431	CFRL - GVHYD	253, 436
MA1631	TGCPL - TACTA - IGCRV	63, 89, 149	CFDW - NVHPY	247, 355
NifK	KICQP - QGCLS - TTCVA	23, 48, 106		
VnfK	YTCQP - QGCSM - TTCST	20, 45, 104		
AnfK	FTCQP - QGCVM - TTCST	20, 45, 104		
MA1632	LRCAF - QGCEY - SACGP	19, 44, 103		
MA2033	TGCKL - VPCTC - DRCFV	31, 67, 126		

*Based on homology to *Clostridium pasteurianum* NifDK and *A. vinelandii* VnfDK.

Table 5. Conserved ATP-binding and [4Fe-4S] cluster binding residues in putative and known Fe proteins.

Protein	ATP binding*	Residues	[4Fe-4S] binding*	Residues
NifH	IAIYGKGGIGKSTT	7-14	VGCAGRGI - VVCGG	95, 98 - 130
VnfH/AnfH	IAFYGKGGIGKSTT	8-15	VGCAGRGV - VVCGG	97, 100 - 132
MA1633	IAIYGKGGIGKSTI	7-14	IGCAGRGV - VVCGG	100, 103 - 136
MA2032^{N}	MALYGKGGIGKSTV	4-11	IGCAGRGI - VVCGG	92, 95 - 127
CfbC	VAIYGKGGIGKSST	10-17	IGCAGRGI - IVCGG	96, 99 - 132

*Based on homology to *M. acetivorans* NifH.

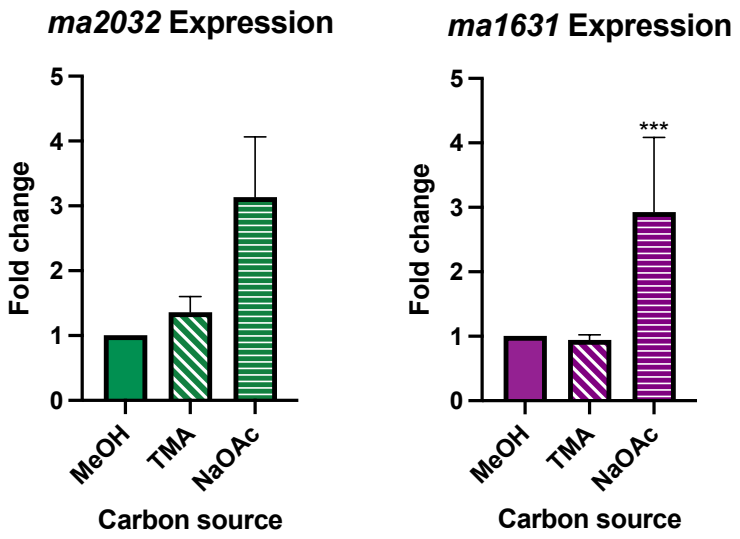

Figure 3. Relative expression of *ma2032* and *ma1631* during diazotrophic growth compared to non-diazotrophic growth in wild-type *M. acetivorans*.

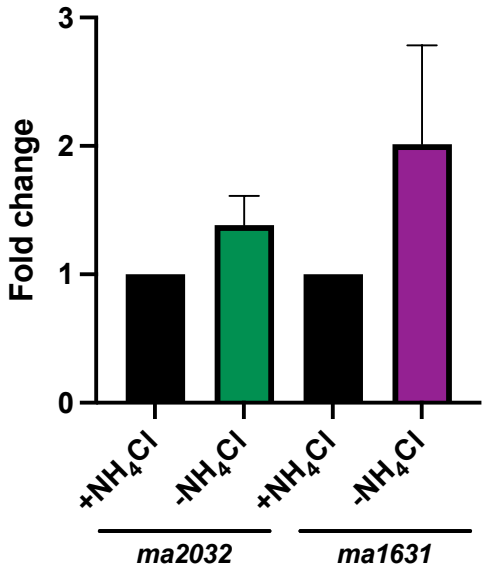

Figure 4. Relative expression of *ma2032* and *ma1631* in wild-type *M. acetivorans* grown with different carbon sources. Expression during growth with acetate (NaOAc) and trimethylamine (TMA) is compared to that during growth with methanol (MeOH).
*** $p<0.001$.

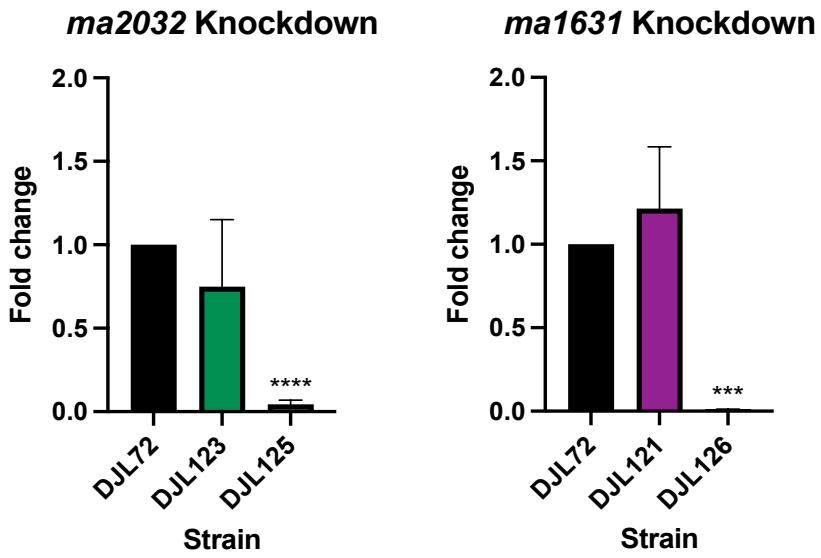

Figure 5. Relative expression of *ma2032* and *ma1631* in strains with one gRNA (DJL123, DJL121) or two gRNAs (DJL125, DJL126) compared to gRNA-free control DJL72.
*** $p<0.001$, **** $p<0.0001$

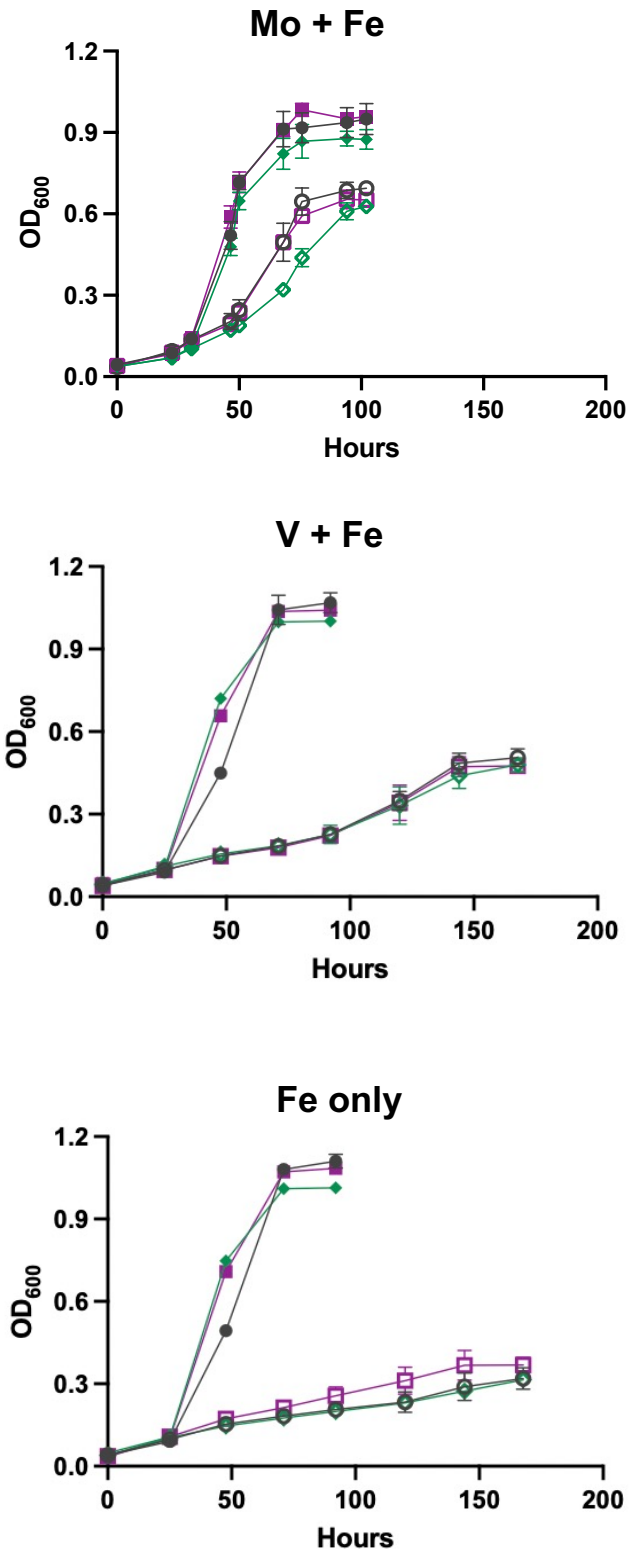

Figure 6. Growth of DJL125 (green diamonds) and DJL126 (purple squares) strains compared to control DJL72 (gray circles) with and without fixed nitrogen (closed shapes and open shapes, respectively) with different metal availabilities.

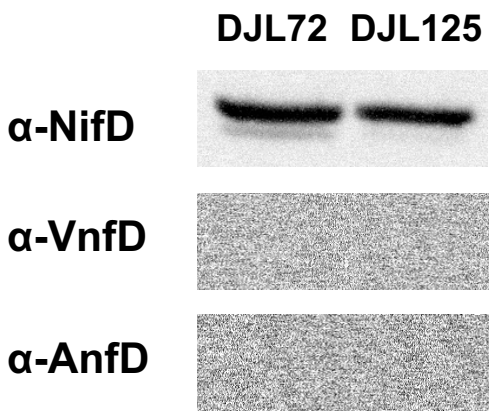

Figure 7. Western blot probing for NifD, VnfD, and AnfD in diazotrophic DJL72 and DJL125. Data are representative of three biological replicates. The SDS-PAGE gel showing protein normalization is located in Supplemental Fig. 1.

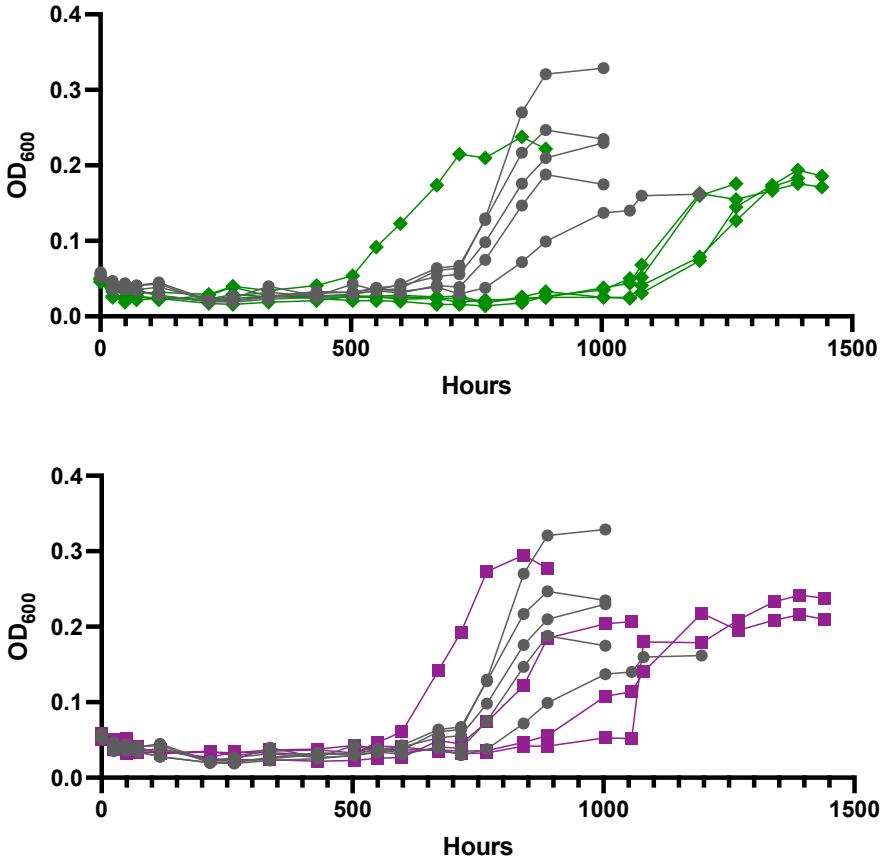

Figure 8. Growth of at least 4 biological replicates of DJL125 (green diamonds) and DJL126 (purple squares) strains compared to DJL72 (gray circles) during adaptation from methanol to acetate.

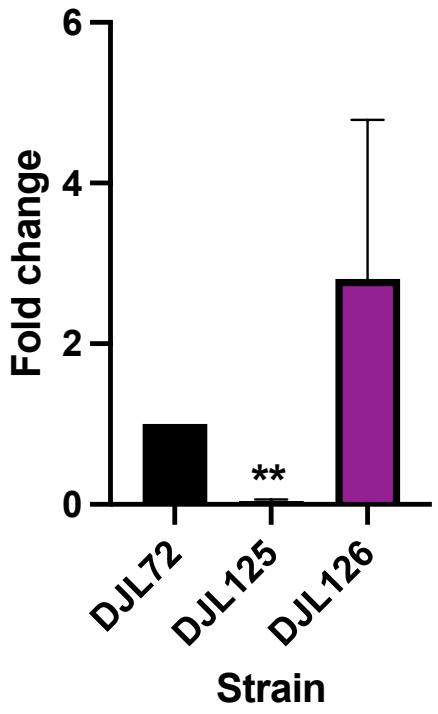

Figure 9. Relative expression of *ma2032* in DJL125 and *ma1631* in DJL126 after adaptation to acetate. ** $p<0.01$

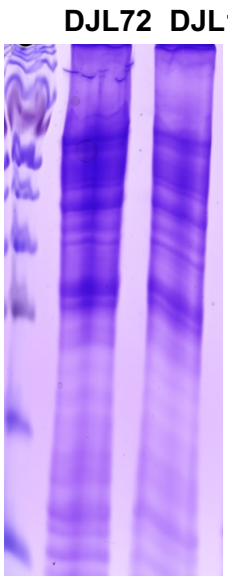

Supplemental Figure 1. SDS-PAGE gel showing loading normalization for Fig. 7.

Conclusion

Nitrogenase proteins have shaped life as we know it by catalyzing the production of bioavailable nitrogen. Reduction of dinitrogen to ammonia by nitrogenase in early bacteria and methanogenic archaea (methanogens) is how life on Earth received most of its usable nitrogen for billions of years. “Nitrogenase-like” proteins, similar in structure but different in mechanism, are used to synthesize chlorophyll independent of light in photosynthetic organisms. Another nitrogenase-like complex in methanogens is necessary for cofactor maturation in the enzyme which releases methane. Thus, nitrogenase family proteins are critical to nitrogen and carbon cycles. Despite the importance of nitrogenase and related enzymes to methanogens, the regulation and properties of nitrogenases remained underexplored. This dissertation investigated nitrogenase family proteins in the model methanogen *Methanosarcina acetivorans*. *M. acetivorans* encodes six sets of nitrogenase family proteins: three bona fide nitrogenases, one nitrogenase-like protein complex to produce the methanogenesis cofactor described above, and two uncharacterized nitrogenase-like gene clusters.

In comparison to their bacterial counterparts, methanogen nitrogenase-related proteins are easier to express recombinantly, conferring benefits for agricultural and biotechnological applications. Of the three nitrogenases—molybdenum, vanadium, and iron types, named for the metal present in their catalytic cofactor— vanadium and iron nitrogenases offer additional advantages for biofuel production compared to the molybdenum nitrogenase. While there is much to be learned about nitrogen fixation in methanogens, V- and Fe-nitrogenases have been minimally investigated in methanogens.

Characterizing nitrogenases requires nitrogenase production, which is tightly regulated at transcriptional, post-transcriptional, and post-translational levels. The first chapter of this

dissertation explored nitrogenase expression and function in *M. acetivorans*. In bacteria with three nitrogenases, nitrogenase production is dependent on the absence of fixed nitrogen and the presence of the corresponding metal (Mo, V, or Fe only). As in bacteria, *M. acetivorans* nitrogenase production requires absence of fixed nitrogen. But unexpectedly, all three nitrogenases are produced in the absence of Mo and are not affected by the presence of V. This is the first demonstration of such regulation in a diazotroph.

To determine which nitrogenases are used, and why all three might be produced at once, *M. acetivorans* strains were constructed with each nitrogenase repressed using CRISPR interference. These strains revealed that the Mo-nitrogenase is required for expression of both V- and Fe-nitrogenases. The reason for this requirement is currently unknown and warrants further investigation. In contrast, a lack of Mo-nitrogenase in bacteria alleviates metal-dependent repression of V- and Fe-nitrogenases. The Fe-nitrogenase in *M. acetivorans* can also be used in the presence of V. How *M. acetivorans* coordinates multiple nitrogenases at once and ensures metal specificity will be the focus of future experimentation.

The second chapter of this dissertation explored ModE, a putative repressor of expression of the V- and Fe-nitrogenases. ModE as characterized in bacteria regulates transcription in a Mo-dependent manner, and there are predicted ModE binding sites upstream of the V- and Fe-nitrogenases. Repressing *modE* leads to production of the Fe-nitrogenase even when Mo is present. Transcription of the V-nitrogenase is upregulated when *modE* is repressed, but the protein is not made, suggesting Mo-dependent post-transcriptional regulation. Recombinant ModE specifically binds the promoters of the operons encoding the V- and Fe-nitrogenases, as well as other genes likely involved in nitrogen fixation, but binding *in vitro* is independent of Mo availability. How Mo is sensed *in vivo* by ModE will require additional investigation.

The third and final chapter examined the physiological role of nitrogenase-like proteins *ma1631-33* and *ma2032-33* with potential roles in carbon source utilization and/or nitrogen fixation. Neither *ma1631* nor *ma2032* are differentially expressed in the presence or absence of fixed nitrogen. However, *ma2032-33* repression causes a slight negative growth phenotype during nitrogen fixation in the presence of Mo, but there is no difference in nitrogenase production. *ma1631* is 3-fold upregulated during growth with acetate compared to methanol and may be required during acetoclastic growth. MA2032-33 and MA1631-33 have conserved residues that may bind nitrogenase cofactors, but potential substrates are unknown.

Overall, the results within this dissertation provide a basis for understanding the regulation and physiological roles of *M. acetivorans* nitrogenases and nitrogenase-like proteins. This knowledge provides a foundation that will aid in attempts to exploit the use of methanogen nitrogenases in biotechnological applications.